TRIBOPOLYMERIZATION : CERAMIC LUBRICATION UNDER HIGH LOADS AND HIGH SPEEDS

by

Benjamin R. Tritt

Thesis submitted to the Faculty of

Virginia Polytechnic and State University

in partial fulfillment of the requirements for the degree of

MASTER OF SCIENCE

in

Mechanical Engineering

APPROVED:

Michael J. Furey, Chairman

Norman S. Eiss, Jr.

Brian Vick

January 1995

Blacksburg, Virginia

TRIBOPOLYMERIZATION : CERAMIC LUBRICATION UNDER HIGH LOADS AND HIGH SPEEDS

by
Benjamin R. Tritt
Michael J. Furey, Chairman
Mechanical Engineering Department

(ABSTRACT)

An experimental study of ceramic lubrication by tribopolymerization at high loads and high speeds is presented. One condensation monomer -- C_{36} dimer acid/ethylene glycol monoester -- and five addition monomers, i.e., diallyl phthalate, lauryl methacrylate, vinyl acetate, methyl-2-acrylamido-2-methoxy acetate, and vinyl octadecyl ether, were used at 1 wt. % concentrations in hexadecane with alumina on alumina pin-on-disk testing. A two by two matrix of load and speed conditions was used to determine the effects of load and speed on wear reduction.

At low speeds, the monomers showed significant wear reductions, from 37 percent up to 98 percent, compared to pure hexadecane lubrication. Changes in load at low speed had mixed effects dependent on the monomer. At high speeds, the monomers did not decrease wear; in some cases wear increased.

ESEM surface studies show a relationship between the anti-wear effectiveness and the consistency of a formed wear debris layer on the alumina surface. The surface films of wear debris and the formed polymeric products may reduce wear by providing protection to the sliding surfaces.

Proposed wear mechanisms and a discussion of possible speed-wear interactions are presented with recommendations for continued tribological testing.

ACKNOWLEDGEMENTS

The completion of this research would not be possible without the help of many other people. I would like to thank everyone who has helped me in this task. Special thanks goes to my advisor Dr. Michael J. Furey for his guidance, support and helpful suggestions. Thanks to my committee members Dr. Norman Eiss and Dr. Brian Vick for their insight and contributions in focusing this research.

The services of the Mechanical Engineering machine shop and electrical shop have proven invaluable in providing well made parts and service; special thanks are given to Mr. Jerry Lucas for his time and help.

My understanding of the chemistry of tribopolymerization and the use and interpretation of FTIR are attributed to the knowledge and help given to me by Dr. Czeslaw Kajdas and Dr. Roman Kempinski. Without the help of Dr. Bhawani Tripathy, I would not have been able to complete the research. His patience and thoughtfulness are greatly appreciated.

I would also like to thank several others: Ms. Erica Ergenbright for her assistance, especially in profilometry and photomacroscopy; Mr. Chris Smith for his assistance in the start of this research; Gang Cheng, Ph.D, manager of the Materials Characterization Laboratory for use of and instruction on the ESEM; and Dr. R.J. Bodnar and Mr. Frank Harrison of the Virginia Tech Geology Department for the use of the FTIR microscope used for analysis in this research.

I also thank the tribology graduate students Mr. Ed Lee, Mr. Matt Schroeder, Mr. Mark Freeman and Mr. Doug Patterson for their support and friendship.

Finally, I would like to thank God, my parents and my fiancée, Ms. Michele Smith, for their love, support and encouragement which help me make it through each day.

TABLE OF CONTENTS

LIST OF FIGURES

LIST OF TABLES

CHAPTER 1

INTRODUCTION

1.1 RATIONALE

The use of ceramics as engineering materials has grown considerably in the last decade. Desirable ceramic properties include hardness, inertness, use at high temperatures, corrosion resistance, and resistance to erosion and abrasion. Some ceramics are less dense than the more commonly used steels. Tribological applications of ceramics include automotive engine components, higher temperature automotive engines, machining tools for difficult alloys, propulsion systems, ceramic heads for magnetic recording, advanced high-temperature bearings, artificial joints and any high-temperature corrosive or abrasive tribological condition [1]. Ceramics for such applications include alumina, silicon nitride, silicon carbide and partially stabilized zirconia.

The use of ceramics for industrial purposes could result in tremendous monetary savings. For example, Katz [2] has determined that the annual fuel savings from the use of ceramics in adiabatic diesel engines could be as much as $ 5 billion in the U.S. alone.

A most difficult regime of lubrication is that of 'boundary lubrication'. Severe sliding conditions result from a thin film of liquid lubricant and the contact of asperity tips. When a hydrodynamic film breaks down due to lower viscosity, lower sliding speeds or higher loads, the boundary lubrication regime is characterized by increased friction, high wear and possible surface damage.

Surface chemistry is extremely important in boundary lubrication due to the mixed contact of solids and liquids. Success in boundary lubrication depends on the total environment of the solids, surfaces, surface layers and lubricants.

The lubrication of ceramic surfaces in tribological contact requires methods different from traditional metal lubrication schemes. Current methods of ceramic lubrication are limited to four main categories [1]:

- Incorporating other materials (e.g., graphite) into the ceramic
- Surface treatments or coatings
- Fluids containing dispersed solid lubricants (e.g., graphite, MoS_2)
- Conventional lubricants

The current methods have limitations or disadvantages which demonstrate the need for an effective method of ceramic lubrication. Changes to the ceramic could change the mechanical and material properties, possibly eliminating the advantages of the ceramic in the first place. Surface treatments will eventually wear off and the lubrication will be gone. Solid materials added to a liquid lubricant require high concentrations and result in high costs. Conventional lubrication oils for metals do not work well with ceramics because the anti-wear additives which react with metals to form a surface film cannot be expected to react with ceramic surfaces.

A new method for effective ceramic lubrication is tribopolymerization. Tribopolymerization is defined as the planned and intentional formation of protective polymeric films directly and continuously on surfaces in tribological contact to reduce damage and wear by the use of minor concentrations of selected compounds capable of forming polymeric films *in situ* [3]. Although

tribopolymerization is not fully understood, it offers a possibility for effective ceramic lubrication under conditions where other methods of lubrication are not effective. As a boundary lubrication mechanism, the tribopolymer films are formed on the surfaces of the ceramics in the contact region where needed. The concept is shown schematically in Figure 1.1.

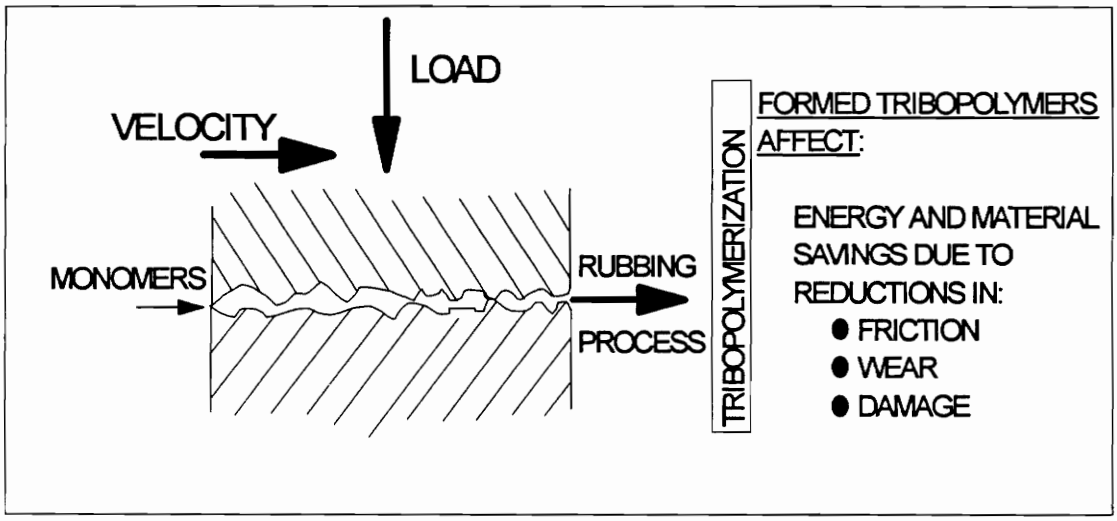

Figure 1.1 Tribopolymerization as a Mechanism of Boundary Lubrication [4].

The mechanism of tribopolymerization may depend on temperature, load, sliding speed, frictional heat generation, and exoelectron emission [4]. Reactions may also be initiated by the energy from frictional heat generation released during sliding.

Previous research in the Virginia Tech tribology laboratory on tribopolymerization has chiefly been under low frictional heat generation conditions. The rate of frictional energy generation is the product of sliding speed and friction force.

$\dot{Q} = \mu W V = F V$

$\dot{Q}$: frictional heat generation (J / sec or Watts)

μ : coefficient of friction

W : normal load (N)

V : sliding velocity (m / s)

F : friction force (N)

The commonly used test conditions (shown in Table 1.1) of a 20 N normal load and 0.25 m/s sliding speed result in a frictional heat generation of 0.5 Watts (for an assumed average coefficient of friction of μ = 0.1). More practical applications of tribopolymerization may involve much higher frictional energy generation.

Table 1.1 Previous Liquid Lubrication Pin-on-Disk Test Conditions

System:	Material I on Material II
Geometry:	Sphere (Ball) on Rotating Flat (Disk)
Specimen Size:	3.2 mm (1/8 ") ball, 25 mm (1") Diameter Disk
Lubricants:	Hexadecane Plus Selected Monomers
Applied Normal Load:	5 to 40 N (20 N typical)
Sliding Velocity:	0.25 m/s
Sliding Distance:	500 m
Ambient Temperature:	19 to 23 °C
Relative Humidity:	Uncontrolled Atmospheric Conditions (35% to 45%)

Higher loads, higher speeds or higher friction coefficients are likely in many possible tribological systems. The question to be answered is: Will

tribopolymerization be effective in reducing ceramic wear at higher loads and speeds than used in our previous studies?

1.2 OBJECTIVES

Previous tribopolymerization tests have been limited to speeds of 0.25 m/s and loads from 5 to 40 N, with 20 N being the most common. Tests have been conducted in two regimes of lubrication, i.e., boundary lubrication with liquid lubricants and vapor-phase lubrication using heated monomers in a nitrogen carrier gas. Loads and speeds in tribopolymerization experiments were increased in this study. Test speeds were 0.25 m/s and 1.0 m/s while loads were extended to 40 N and 160 N. Boundary lubrication of alumina surfaces continued to be the lubrication testing regime.

The objectives of this study are:

1) To determine the effectiveness of selected monomers capable of forming polymers under high loadand high speed conditions in ceramic pin-on-disk experiments.

2) To determine the effects on ceramic wear of varying the normal load and varying the sliding speed.

3) To identify and characterize surface films formed during pin-on-disk tribological experiments.

Information on the influences of normal load, sliding speed, temperature, pressure and frictional heat generation can help in the understanding of

tribopolymerization. Figure 1.2 shows the components involved in the study of tribopolymerization at high speeds and high loads.

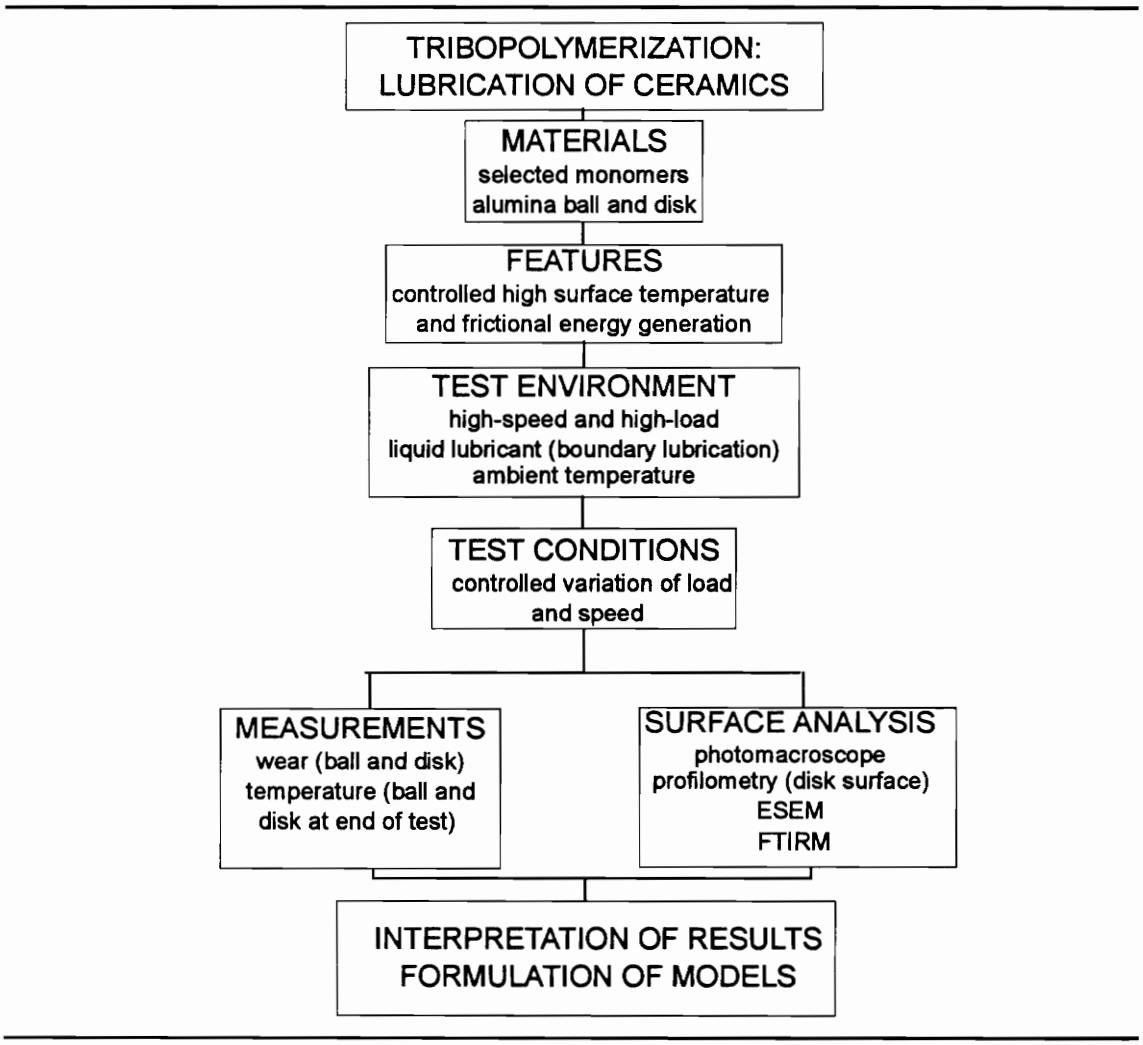

Figure 1.2 Components of High Speed High Load Pin-On-Disk Experiments

CHAPTER 2

LITERATURE REVIEW

Literature on ceramic lubrication, mechanisms of ceramic wear, and tribopolymerization has been reviewed. Information relevant to the present high speed and high load tribopolymerization study is presented below.

2.1 CERAMIC LUBRICATION

The following compilation of material discusses the general nature of ceramic lubrication.

Although ceramics are inert in the general chemical sense, tribochemical reactions with the ceramic surface are extremely important in the magnitude of ceramic wear and friction [5]. Chemical reactions involving lubricants, surfaces and surface films may affect either friction or wear or both.

Ceramics are different from metals in both mechanical properties and in tribological response. Ceramics react differently to lubricants than do traditional metals. For example, Studt [6] showed that the highly effective anti-wear additive for metals, ZDDP (zinc dialkyldithiophosphate) does not lubricate α--alumina surfaces. Several studies [7-15] have shown only small or no wear reduction effects for conventional lubricants used on ceramics.

Operating environments of ceramics may also be different from metals. Compared to the 700 °F diesel operating temperature of metals, ceramics can withstand temperatures up to 1200 °F [16]. Unlike metals that can usually plastically deform, size and distribution of material flaws determine the strength

of a ceramic [17]. Brittle fracture of ceramics is the dominant means of material failure and unlike many metals, significant ductile yielding does not occur.

Four distinct lubrication regimes should be mentioned when discussing ceramic lubrication. Dry sliding, vapor phase lubrication, boundary lubrication and elastohydrodynamic lubrication are all different conditions distinguished by the lack of or presence of a liquid lubricant, the load and speed conditions, and the lubricant viscosity.

The simplest sliding condition is dry sliding and is defined as the intentional lack of a lubricant between contacting surfaces. Only surface films or ambient air conditions separate sliding ceramics.

Lubrication in the vapor phase is a severe form of sliding in which an intentional film may be deposited on the rubbing surfaces from a gaseous source. Carrier gas, temperature and any vaporized compounds in the gas are highly significant in the vapor phase regime. Vapor phase lubrication of ceramics may add to the knowledge of ceramic lubrication.

Boundary lubrication is the ill-defined area between dry-sliding and elastohydrodynamic lubrication (EHL); there is a liquid film present but contact between asperities still occurs [18]. Oils intended for boundary lubrication usually contain additives that are meant to form protective surface films.

Elastohydrodynamic lubrication occurs when either speeds or viscosities are high enough or loads are low enough such that complete separation of the sliding surfaces occurs due to the presence of a liquid 'wedge'. The lack of contact means that wear can occur only by the stresses occurring due to the pressure in the liquid wedge. Elastohydrodynamic lubrication is characterized by the elastic deformation of the contacting members.

For vapor phase lubrication, Lauer and Dwyer [19] found that a very low friction coefficient ($\mu = 0.02$) was obtainable by supplying a continuous source of a hydrocarbon gas (ethylene, benzene or 1-propanol) at 700 °C in a nitrogen carrier gas. The gas resulted in deposits of graphitic carbonaceous material. High temperatures and the presence of a catalyst such as nickel or nickel alloy help to dissociate the hydrocarbon compounds. This requirement of a catalyst surface is a problem for uncoated ceramics. A nickel coating on a ceramic will serve as a catalyst, but may be lost over time due to wear. Although pure silicon nitride and silicon carbide surfaces did experience low wear and low friction, the process needed a run-in period during which high wear and high coefficients of friction resulted.

Lepage et al. [20] report that friction reductions resulted from preventing adhesion of pure ceramics by the presence of a surface film. Friction is reduced whether the surface film is caused by adsorbed gases, water vapor, surface layers or oxides.

Klaus and Graham et al. [21-24] have used tricresyl phosphate (TCP) for vapor phase ceramic lubrication at high temperatures. Research suggests that the decomposition products of TCP polymerized during tribological contact. Previous work suggested that a liquid-like polymer film resulted in the low wear. Some type of metal film (e.g., Fe_2O_3) needs to be precoated on ceramic surfaces for the TCP vapor to react and form a "lubricant film". Less chemically reactive surfaces such as ceramics, resulted in flaky deposits that were easily blown off the substrate. High temperatures are needed for the chemisorption process; otherwise the surface layer is formed by physisorption.

Boundary lubrication regime experiments were conducted with various lubricants and coatings for ceramic materials. In experiments by Jahanmir and Fischer [9], the coefficient of friction for lubricated silicon nitride was reduced due to tribochemical reactions between silicon nitride and water. Experiments with hexadecane and hexadecane plus stearic acid resulted in higher coefficients of friction than pure water, hexadecane plus water and humid air experiments.

Humidity of surrounding air in ceramic tribological contact plays an important role in the friction and wear behavior of ceramics. Fischer and Tomizawa [25] found that water on the surface of silicon nitride results in lower wear rates compared to silicon nitride in dry gases. The presence of liquid water or water vapor decreases the wear rate of silicon nitride [9,10]. For zirconia [26] and alumina [27] the wear rates under sliding contact increase in the presence of liquid water.

Gee [28] found that humidity has a large effect on friction in experiments with alumina. Aluminum hydroxide was formed by tribochemical reactions. As the humidity decreased in these experiments, the coefficient of friction was found to increase.

Applied surface films on ceramics are another method of ceramic lubrication. Erdemir et al [29,30] of Argonne National Laboratory give a classic example of applied surface layers which improve wear and frictional behavior while intact, but offer no protection when the applied layer is worn off. In their experiments, an ion-assisted deposited layer of silver was applied to ceramics in order to reduce friction and wear during tribological testing.

2.2 MECHANISMS OF CERAMIC WEAR

The process of material removal from ceramic tribological systems is not fully understood. In general ceramic wear is largely due to brittle fracture, although some plastic deformation may precede brittle failure. In order to understand the anti-wear action of monomers used for tribopolymerization, the process of ceramic wear must be examined. Relevant literature on the wear mechanisms of ceramics is highlighted below.

Kato identified four regimes of ceramic wear [5]: plastic deformation and ploughing, powder formation, flake formation, and steady sliding and ploughing. In all cases wear particles resulted from crack propagation, with most of the wear occurring by flake formation. The transition between wear modes depends on the characteristics of the load and the material properties. Hokkirigawa defined a severity of contact parameter that predicts the ceramic wear mode and transition points [31]. Crack propagation is thought to cause flake formation while powder formation is caused by microcracks.

Braza et al. [17] also discussed the brittle nature of ceramics. Mode I (tensile) failure of ceramics is probably the most common failure path, but a small plastic deformation caused by shear loading or frictional heating may precede brittle failure. Three basic modes of ceramic wear are chipping, spalling or grain pull-out.

According to Braza et al., ceramic wear is linked directly to the stresses at asperities and pores and to stresses caused by thermal gradients. Pores cause surface pits which can act as flaws to initiate crack growth. Temperature gradients can cause large compressive stresses parallel to the ceramic surface.

A subsurface crack under thermal stress can cause localized buckling, creating a spall as cracks grow to the surface.

Wear resistance of a ceramic is dependent on materials, ambient temperature, atmosphere, surface preparation, loading and sliding [17]. Aspects of wear are either related to mechanical effects or tribochemical effects. Cracking can occur in a transgranular (through a grain) or intergranular (between grains) manner. Ceramic cracks are generally transgranular due to tiny flaws present in the ceramic before wear began.

Deckman et al. conducted experiments with α-alumina lubricated with paraffin oil [32]. SEM showed intergranular fracture to be the main wear mechanism.

Buckley et al. report that ceramic fracture under sliding conditions is similar to metals but little or no plastic deformation occurs [33]. Cracks in ceramics can grow quickly under shearing loads. Ceramics may also be directional sensitive due to anisotropic behavior. The crystal structure may cause friction and wear to be dependent on sliding direction.

Buckley et al. mention two general types of ceramic wear, adhesive and abrasive, with adhesive wear being much smaller. The importance of surface chemistry was emphasized due to the large effects on tribological wear during ceramic sliding.

Generally it is agreed that brittle failure is largely responsible for ceramic wear. Unlike metals, no gross plastic deformation occurs in the wear of ceramics. Microcracks initially form at the surface or in the solid ceramic. These cracks propagate due to fluctuations in normal, frictional, and thermal stresses until failure occurs by the formation of a wear particle.

The critical crack size for ceramics tends to be small due to the generally brittle nature of ceramics. This creates small wear particles which may stay in a wear track. *Wear debris trapped in the contact region* may be very important in determining the continued wear and frictional characteristics of ceramic surfaces.

Jahanmir and Fischer report that a layer of very fine wear particles was found in the wear scar of silicon nitride under dry and lubricated sliding conditions [9,10]. Evidence of tribochemical reactions in this wear layer was also found.

A study by Gee [28] of the formation of aluminum hydroxide formed during alumina sliding proposed that wear debris stayed in the wear track by filling in the valleys between asperities. Water from the ambient humid air reacts with the wear debris to form this layer of aluminum monohydroxides.

Dry sliding tests by Hogmark et al. [34] of alumina, silicon carbide and Sialon resulted in a third-body layer formed in between the worn surfaces. The layer involved compacted wear fragments resulting from chemical reactions, plastic deformation and brittle fracture of the surface layer.

In tests with zirconia ceramics, Stachowiak et al. [35] found a formed tribolayer of fine wear debris compacted and deposited on the ceramic surface. A smooth wear layer was also visible.

Either dry or lubricated sliding systems could result in the formation of wear particles. In all cases, wear to the surfaces is reduced due to the protection of the formed tribolayer. A more strongly attached film would provide better protection under more severe environments.

2.3 TRIBOPOLYMERIZATION

Tribopolymerization is a designed approach to boundary lubrication in which protective films are formed directly on the rubbing surfaces by means of chemical reactions. Tribopolymerization comes from the combination of the Greek word "tribo", which means 'to rub' [36], and the polymerization of the monomers. The concept was conceived by Furey [3] and later updated by Furey and Kajdas [37-40]. Most early testing was with metal sliding systems. Highlights of early findings are taken from a review article in *Wear* by Furey [42] and presented here.

The compounds which form polymers by a polycondensation process are best represented by a monoester compound made from C36 dimer acid and ethylene glycol. The reaction mechanism in the formation of polyester films is :

$$HOOC{-}R{-}COO{-}C_2H_4OH \xrightarrow{\text{rubbing surfaces}} HO[{-}OC{-}R{-}COO{-}C_2H_4O]_n{-}H + H_2O$$

In Ryder Gear Tests, this monoester dramatically increased the anti-scuff rating of four fuels (jet, turbo, JP-4 and xylene) at 0.1 wt. % concentration [3]. For example, the JP-4 fuel anti-scuff rating increased from 350 N/cm to 5200 N/cm. Field tests of the monoester resulted in a large reduction of jet fuel pump wear.

Valve train wear tests in a V-8 automotive engine with radioactive valve lifters were used to accurately determine valve lifter wear [42]. A 1 wt. % addition of C_{36} dimer acid/ethylene glycol monoester to a mineral base oil reduced valve lifter wear by over 90 %. This reduction in wear is approximately

equal to the effects of ZDDP (zinc dialkyldithiophosphate) additives. ZDDP is widely used in automotive engine oils as an anti-wear additive.

An important observation was that the C36 dimer acid/ethylene glycol monoester was most effective in wear reduction when strictly in monomer form. Any polymerization before use as a lubricant to a diester or tetraester reduced the percentage wear reduction. This finding supports the "in-situ" idea by which the monomer polymerizes only where needed. Polymers simply added to the lubricant did not reduce the wear nearly as effectively as the monomers.

The monoester also provided a carry over effect of low wear rates for 3 to 6 hours in non-additive mineral oils. Similar valve train testing did not result in a carry over effect with the ZDDP, the dimer acid nor the glycol.

In more recent works, Marin-LaFleche, Furey and Kajdas [43,44] continued research on the monoester with experiments of oscillating metallic contact. Styrene and methyl methacrylate were added to include addition type monomers. Although the monoester was not very effective, both styrene and methyl methacrylate caused wear reductions up to 65 %. The FTIRM (Fourier Transform Infrared Microspectroscopy) examination of wear products confirmed the formation of polystyrene and chemical reactions between the monomers and metals. The research suggested that surface temperature was important for tribopolymerization of condensation monomers while exoelectron emission helps to initiate the addition monomer polymerization.

Monoester and other compounds are extremely effective in reducing wear in ceramic pin-on-disk experiments. A study by Furey and Kajdas [1] examined the feasibility of using monomers in a designed approach to ceramic lubrication. Initial pin-on-disk experiments with a number of ceramic systems (including

alumina, sapphire, zirconia, and silicon nitride) and compounds resulted in striking reductions in wear (40-80 %) for over 40 of the compounds. Ten of the compounds were most effective, with wear reductions over 70 % at concentrations of 1 wt. % or less.

Compounds with identical chemical formulas but different structures resulted in different wear reductions. Compounds with functional groups located in a position expected to aid in polymerization were more successful in reducing wear. Those compounds with functional groups in a position less conducive to polymerization were not effective in reducing wear.

Experiments with selected oxygen containing monomers on ceramics by Furey et al. [45] resulted in significant reductions in wear. For the monoester monomer, an anti-wear mechanism was proposed which involved a chemical reaction of the monoester with the alumina substrate and the formation of oligomer/polymer chains growing outward from the ceramic surface.

Exploratory studies of vapor phase tribopolymerization by Smith [46] found that delivering monomers in a nitrogen carrier gas at elevated temperatures significantly reduced the wear rates of alumina on alumina. As monomer temperature increased, the effectiveness of wear reduction also increased, with the optimum delivery temperature being close to the monomer's boiling point. Monomer temperature was more important in wear reduction than the monomer concentration. Friction was also reduced by as much as half at elevated bulk temperatures. FTIRM analysis provided evidence of polymerization for the diallyl phthalate monomer. The possibility of tribopolymerization was not ruled out by FTIRM for the other monomers. Diallyl phthalate and vinyl octadecyl ether resulted in over a 90 % reduction in ball wear

at elevated temperatures. In this high temperature severe environment, the cationic and free radical mechanisms were equally effective.

Results of pin-on-disk experiments with vinyl monomers on ceramics were presented at the 1994 Annual Meeting of the Society of Tribologists and Lubrication Engineers [47]. Wear evidence supported the NIRAM (negative-ion radical action mechanism) and exoelectron hypothesis of tribopolymerization initiation. Exoelectrons emitted by the rubbing surfaces initiated tribopolymerization for vinyl monomers capable of polymerizing by anionic or radical mechanisms. The vinyl monomer -- alumina tribological process involved a chemical reaction with the surface and the formation of tribopolymers. FTIRM spectra supported the surface reaction for all monomers and the polymerization for two of the monomers and did not rule out polymerization for the other monomers.

More recently, Tripathy [48] conducted pin-on-disk experiments with selected monomers in a 1 % wt. mixture with hexadecane. The condensation monoester compound reduced alumina wear by over 40 %. Four of the five addition-type monomers showed significant reductions in alumina wear. Lauryl methacrylate, diallyl phthalate, vinyl acetate, and methyl-2-acrylamido-2-methoxy acetate reduced wear by 63 %, 80 %, 57 %, and 56 % respectively. Vinyl octadecyl ether was only slightly effective with an average reduction of only 9 %. The effectiveness of the vinyl monomers was interesting in that the monomers which polymerized by free radical or anionic mechanisms were effective in reducing wear, but the cationic monomer (vinyl octadecyl ether) was only marginally effective. Friction was not significantly affected by the addition of any monomer to hexadecane.

FTIRM analysis of wear scars supported both a polymerization reaction and a reaction with the alumina surface. The polymerization of addition monomers is believed to be related to the negative-ion radical action mechanism (NIRAM).

Most recently, Tripathy et al. proposed a somewhat different mechanism of ceramic wear reduction via tribopolymerization [49]. Fine wear debris created by sliding contact reattaches to both the surface and itself by means of the binding action of the tribochemicals. This debris layer formed from tribochemicals and wear products could be responsible for the wear reduction of tribopolymerization.

SEM analysis was used extensively in Tripathy's study and yielded the following conclusions [49]. A compacted and reattached wear debris layer exists on all lubricated wear scars. The wear layer for pure hexadecane tests was removed by ultrasonically cleaning the disks in acetone. Debris layers formed in the presence of monomers remained intact after the acetone ultrasonic wash. A more effective monomer (in terms of wear reduction) produced a layer more strongly attached to the surface.

Evidence strongly supports the *in situ* proposal of tribopolymerization as an effective form of ceramic lubrication. However questions remain regarding the factors that influence the effectiveness of the tribopolymerization process. Surface chemistry, wear debris, surface temperature, pressure, loads and sliding speeds may affect the anti-wear mechanism of tribopolymerization.

CHAPTER 3

EXPERIMENTAL TECHNIQUE

3.1 HIGH-SPEED HIGH-LOAD CAPABILITY PIN-ON-DISK DEVICE

All tribological tests in this study were run on a pin-on-disk machine shown schematically in Figure 3.1. This machine consists of ball and disk holders, a milling machine, a force transducer and a pneumatic cylinder for normal load application. This machine was originally designed and developed by Smith [46]. Modifications made during this study to the high speed high load pin-on-disk machine are detailed in Appendix A.

The disk holder is attached to the rotating chuck of the milling machine. The rotational speed settings of the milling machine were used as a speed control. The alumina disks used in the tests were supported by a Teflon backing piece to allow both sides of a disk to be used for tests. Only one wear track on each side of the disk was possible due to the width of the 1/4" ball wear scar. The back of the Teflon disk holder was supported by the mill chuck piece. The ball holder and lubricated cup were supported by a linear motion ball-spline shaft and loaded by a pneumatic pancake cylinder. The ball-spline shaft provided an exceptionally smooth normal load application.

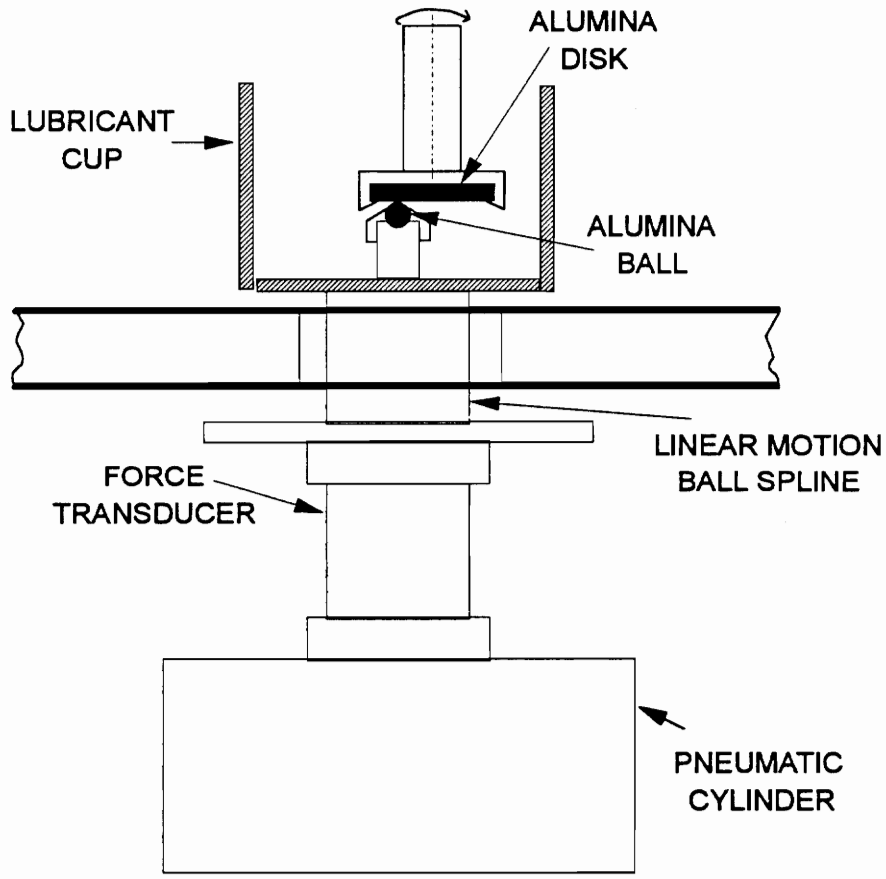

Figure 3.1 Schematic of High Speed High Load Pin-on-Disk Device.

Milling machine gear adjustments allow control of rotational speed and a x-y-z positioning table on the milling machine allows precise placement of the ball relative to the disk radius. The normal load is controlled by pressure adjustments to the pneumatic cylinder to obtain a desired strain indicator output. Strain gages attached to a thin wall aluminum cylinder act as a force transducer to monitor the normal force in the pin-on-disk system.

The high speed, high load system is capable of rather severe conditions. As an indication of severity, the applied load of 40 N results in a mean Hertzian pressure of 1.3 GPa for the alumina on alumina system and the 160 N load results in a mean Hertz pressure of 2 GPa. These values are greater than the severe environment of a highly loaded cam nose in a typical V-8 automotive engine valve train, which has a calculated mean Hertz pressure of about 1 GPa.

3.2 CERAMIC MATERIALS

Alumina disks were supplied by LSP Industrial Ceramics and were cut from a 99.5% pure isostatically pressed alumina rod. The disks were 25 mm (1 inch) in diameter, 3.2 mm thick and ground to an average surface roughness of 0.5-0.65 μm (CLA). Alumina balls were obtained from Sapphire Engineering, Inc. Also 99.5% pure, the Grade 25 balls were 6.35 mm (1/4 inch) in diameter.

3.3 MONOMERS

Table 3.1 gives characteristics of the six monomers used in this study. Each monomer was mixed at 1% by weight solution with a hydrocarbon carrier fluid. Five of the monomers were of the addition type and one was condensation. The condensation monomer, C_{36} dimer acid / ethylene glycol monoester was synthesized while the diallyl phthalate, methyl-2-acrylamido-2-methoxy acetate, lauryl methacrylate, vinyl acetate and vinyl octadecyl ether were obtained from chemical suppliers. The hydrocarbon carrier fluid was hexadecane (minimum 99% pure) supplied by Fisher Chemical and Sigma Chemical Company.

Table 3.1 Monomer Characteristics

Monomer Name	Type	Polymerization Mechanism	Molecular Weight	Functional Groups per Molecule	Supplier
Diallyl Phthalate	Addition	Radical	246.3	2	Aldrich Chemical
Monoester	Condensation	----------	605	2	Synthesized
MAMA	Addition	Hydrogen Transfer Anionic	173.2	1	Aldrich Chemical
Lauryl Methacrylate	Addition	Anionic and Radical	254.4	1	Aldrich Chemical
Vinyl Acetate	Addition	Radical	56.1	1	Aldrich Chemical
Vinyl Octadecyl Ether	Addition	Cationic	296.5	1	Polyscience

The MAMA compound is not 100 % soluble at 1 wt. % in hexadecane at room temperature. Based on previous tests by Tripathy [48], the compound was added to hexadecane in the proper mass proportions to result in a 1 wt. % solution. The insoluble portion of MAMA which settled on the bottom of the glass container was not used in the actual experiments. Therefore the concentration of MAMA in hexadecane was less than 1 wt. %, but still saturated.

Due to differences in chemical structures (as shown in Figure 3.2), the polymerization mechanism and number of functional groups per molecule vary among the monomers. A functional group is the part of the compound where chemical reactions can occur in the polymerization process. For example, diallyl phthalate and the monoester each have two functional groups per molecule.

Two locations on the molecule could be directly involved in the polymerization reaction with other monomer units.

1. DIALLYL PHTHALATE

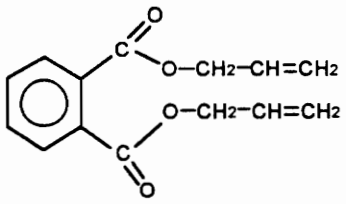

2. C36 Dimer Acid/Ethylene Glycol Monoester

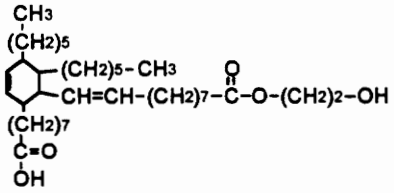

3. Methyl-2-Acrylamido-2-Methoxy Acetate

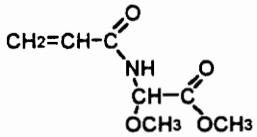

4. Lauryl Methacrylate

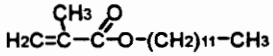

5. Vinyl Acetate

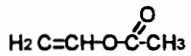

6. Vinyl Octadecyl Ether

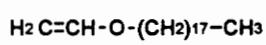

Figure 3.2. Chemical Structure Of Monomers In High Speed High Load Tests.

Diallyl phthalate has 2 carbon-carbon double bonds while the monoester has 2 C-O-H chain endings. The double carbon bonds can be broken open and changed to single bonds in two molecules. The formation of carbon-carbon

single bonds between molecules allows these monomers to add together in the addition reaction. In the condensation reaction, two C-O-H endings can react to form a C-O-C bond in the new molecule and a condensate of H_2O. Unlike the addition monomer, condensation monomers must have at least two functional groups per molecule in order to polymerize. The other addition monomers all have one functional group of a carbon-carbon double bond.

3.4 PROCEDURE FOR HIGH SPEED HIGH LOAD PIN-ON-DISK TESTS

A block diagram, shown in Figure 3.3, of the exact procedure involved in the high speed high load tests was developed to ensure exact repetition and repeatability of testing.

Ceramic test specimens were ultrasonically cleaned in baths of hexane, methanol and de-ionized water for 20 minutes per liquid. Specimens were then dried in a vacuum oven at 150 °C for 2 hours to evaporate the water. Disks and balls were stored in a desiccator until needed for testing.

At the beginning of a test, the strain indicator was turned on to allow stabilization of the output. The radius of contact was set using the **x** positioning table on the milling machine according to precalibrated marks on the table. The rotational speed was set using the Head-Spindle Rotational RPM shift levers. Next , the air supply to the pneumatic cylinder was connected and pressurized. The power to the milling machine, the air cylinder control power supply and the digital pressure indicator were all turned on.

Block Diagram of Testing Procedure for High-Speed High Load Testing

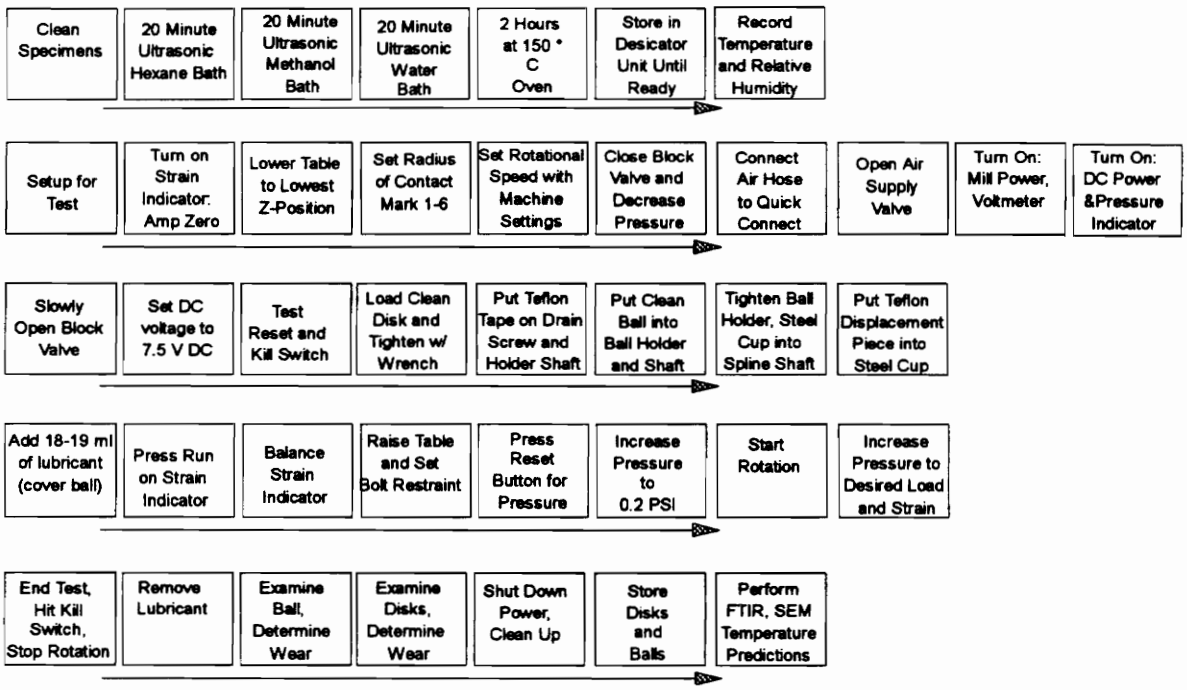

Figure 3.3 Block Diagram of Testing Procedure

After loading a clean disk in the Teflon backing piece, the disk and stainless steel housing were screwed on the steel disk-backing piece in the mill chuck. A clean ball was then put into the ball holder and the lubricant holder piece threaded into the ball spline opening. The Teflon lubricant displacement piece and the splash guard were put into place before adding sufficient lubricant to cover the top of the ball.

Before the test began, the strain indicator was balanced to produce a zero reading. Speeds and loads were set according to the testing matrix shown in Figure 3.4. This matrix of loads and speeds was chosen to help determine the effects on speeds and loads on the effectiveness of tribopolymerization. Normal load was controlled by the pneumatic cylinder pressure. Appendix F examines the normal load stability during experiments. Friction force was not measured during the tests due to machine limitations. However in previous pin-on-disk experiments [48], the change in coefficient of friction for monomers compared to pure hexadecane was insignificant.

Sliding Speed:	Load: 40 N	Load: 160 N
0.25 m/s	Low Load and Low Speed	High Load and Low Speed
1.0 m/s	Low Load and High Speed	High Load and High Speed

SLIDING DISTANCE IS 250 m PER TEST.

Figure 3.4. Load and Speed Matrix for High Speed High Load Tests.

After setting the vertical position of the milling table, the milling machine rotation was started and the air pressure increased to the proper load. The test was stopped after 250 m of sliding distance. Ball wear and disk wear were

measured with a photomacroscope and Taylor-Hobson Talysurf profilometer respectively.

The photomacroscope was used to measure the major and minor diameters of the ball wear scar. Using the average diameter of the spherical segment removed during a test, the volumetric wear was calculated using a simple geometric relationship.

The profilometer trace of the disk wear scar was taken at 4 locations on the disk, 90° apart. From these traces, an average cross-sectional area of the wear scar was in the difference between the trace and the original zero plane surface of the disk. The volume of disk wear was calculated from the cross-sectional area of the worn track multiplied by the track circumference. After measuring the ball wear scar diameter and taking a profilometer trace of the disk wear scar, specimens were stored for later analysis. A summary of test conditions is given in Table 3.2.

Table 3.2 Test Conditions For High Load - High Speed Testing.

System:	Alumina On Alumina
Geometry:	Sphere (Ball) On Rotating Flat (Disk)
Specimen Size:	6.4 mm (1/4 ") Ball, 25 mm (1") Diameter Disk
Lubricants:	Hexadecane Plus Selected Monomers
Applied Normal Load:	40 N, 160 N
Sliding Velocity:	0.25 m/s, 1.0 m/s
Sliding Distance:	250 m
Ambient Temperature:	19 to 22 °C
Relative Humidity:	Uncontrolled Atmospheric Conditions (35% to 45%)

3.5 SAMPLE ANALYSIS

The ball wear scar was examined using a Leitz-Wild Photomacroscope. By measuring the major and minor diameters of the ball wear scar, an average wear scar diameter was determined and used in the calculation of wear based on the volume of a spherical segment.

Disk wear was examined by using a profilometer trace taken with a Taylor-Hobson Talysurf profilometer. The cross sectional area of the wear scar was determined by the difference between the original unworn zero plane of the disk and the wear scar profile. The volume of material worn away was calculated from the average of four cross-sectional areas multiplied by the wear track circumference.

A Nicolet 740 FT-IR Spectrometer was used to analyze the disk wear tracks from selected tests. One of two methods was used to analyze wear tracks. The first method used the edge of a glass microscope slide to scrape surface films from the disk wear tracks and then to deposit the film on a gold coated mirror. The other method was to collect the washings of MEK (methyl ethyl ketone) applied to the wear track. Wear track sample was deposited on a gold mirror by evaporating the collected MEK-sample mixture. Using the reflectance mode on the Nicolet Fourier Transform Infrared Microscope, adsorption spectra were taken and saved for later examination.

The MEK washings method was chosen because direct scraping of the disk surface did not result in any useful spectrum. When applying the MEK washings solution to the gold mirror, the MEK evaporates leaving behind a visible film. When pure MEK was placed on a gold mirror and allowed to

evaporate, the solvent evaporated completely leaving no visible film. FTIR spectra of the evaporated pure MEK was different from MEK solutions.

The principle of FTIRM (Fourier Transfer Infrared Microspectroscopy) is the adsorption of infrared radiation at frequencies which correspond to the natural modes of molecular vibration. Different types of bonds and different atoms vibrate at different frequencies. By looking at the adsorption spectra, peaks can be matched to different chemical structures in the process of identifying the chemical make-up of the surface films.

Visual inspection of surfaces was conducted using a Electroscan Environmental Scanning Electron Microscope (ESEM) and a Wild Heerbrugg Photomacroscope. ESEM offers the advantage of 3-D images in focus, unlike photomacroscopy which can focus only on one level. ESEM was used to examine the worn surfaces of selected tests. A vacuum treatment was applied to the specimens at room temperature for 24 hours to remove any liquid hexadecane. Photomacroscope pictures of all testing conditions were also taken at various magnifications and lighting conditions for balls and disks.

CHAPTER 4

RESULTS

Ball wear, disk wear, total wear, photomacrographs, ESEM findings and FTIRM spectra are presented for hexadecane and the six monomers tested in the matrix of loads and speeds. Wear data are presented for the four load-speed conditions, followed by each monomer's wear results. Photomacroscope pictures which help to show wear and surface differences are also included. ESEM photographs which show differences in wear scar surfaces are presented for selected monomers. Absorbance spectrum from FTIR analysis of selected wear scars are also presented. Finally the calculated surface temperature rises due to frictional heat generation are presented.

4.1 BALL, DISK AND TOTAL WEAR

Reductions in ball wear, disk wear and total wear are generally similar for all cases of load, speed and monomer. Exceptions to this general observation are highlighted as necessary. Appendix B lists the wear volumes for each test of all monomers at all loads and speeds. Statistical analysis of wear results is detailed in Appendix D. Results of the Analysis of Variance statistics are summarized where appropriate in each load-speed section.

4.1.1 Overview

The wear volumes for (a) low load and low speed, (b) low load and high speed, (c) high load and low speed, and (d) high load and high speed test

conditions are presented by bar graphs of average wear (mm^3) for each monomer. The average wear volume is the average of two tests for a given load, speed and monomer.

4.1.1.1 Low Load - Low Speed Results.

Testing at conditions of 40 N normal load and 0.25 m/s sliding speed lasted 16 minutes, 40 seconds (1000 seconds) for a resulting sliding distance of 250 m. Under these conditions, ball wear, disk wear and total wear were significantly reduced for all monomers except MAMA. The MAMA compound resulted in significant reductions in disk and total wear, but ball wear was only reduced by 18 %, which is not statistically different from hexadecane. The average wear volumes (mm^3) for the 40 N load and 0.25 m/s sliding speed are shown in Figures 4.1, 4.2 and 4.3 for ball, disk and total wear respectively.

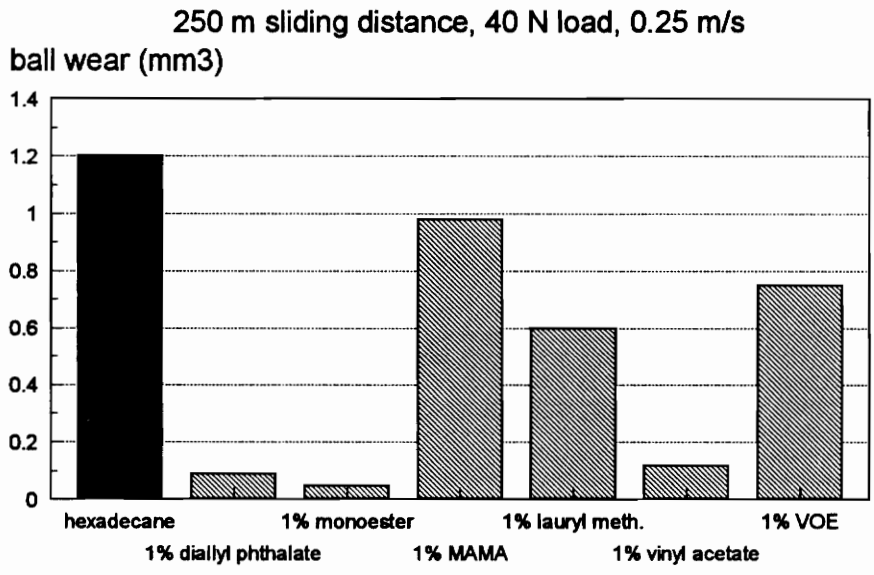

Figure 4.1 Ball Wear For Low Load and Low Speed Conditions.

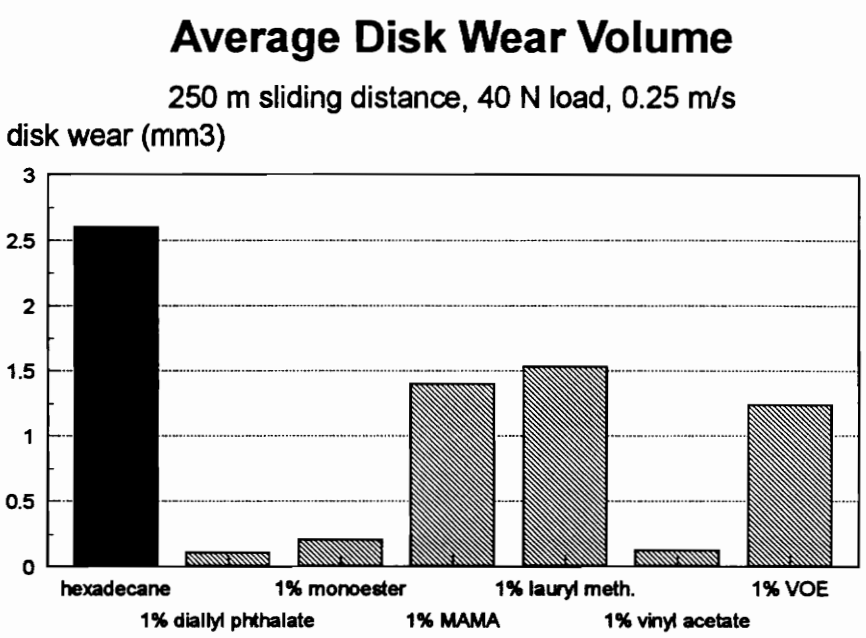

Figure 4.2 Disk Wear For Low Load and Low Speed Conditions.

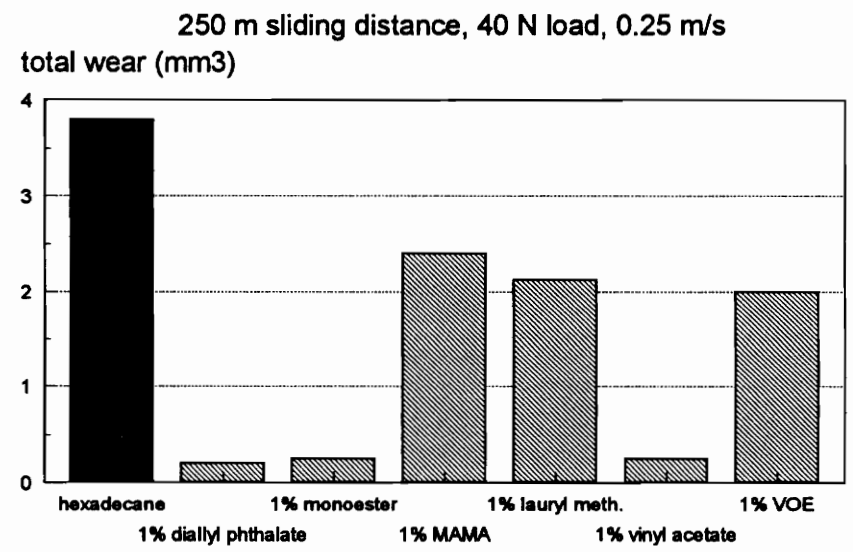

Figure 4.3 Total Wear For Low Load and Low Speed Conditions.

As shown in Figures 4.1 - 4.3, two levels of wear are observed for the monomers. Three monomers (diallyl phthalate, the monoester and vinyl acetate) resulted in extremely large wear reductions, greater than 90 percent. Lauryl methacrylate and vinyl octadecyl ether resulted in significant wear reductions, 44 and 48 % respectively. The MAMA compound was borderline in terms of wear reduction significance. The total wear reduction for MAMA is 37 percent.

4.1.1.2 Low Load - High Speed Results

Tests at 40 N normal load and 1.0 m/s sliding speed lasted 4 minutes, 10 seconds (250 seconds) for a resulting sliding distance of 250 m. The average volumetric wear (mm^3) is shown in Figures 4.4, 4.5 and 4.6 for ball, disk and total wear respectively.

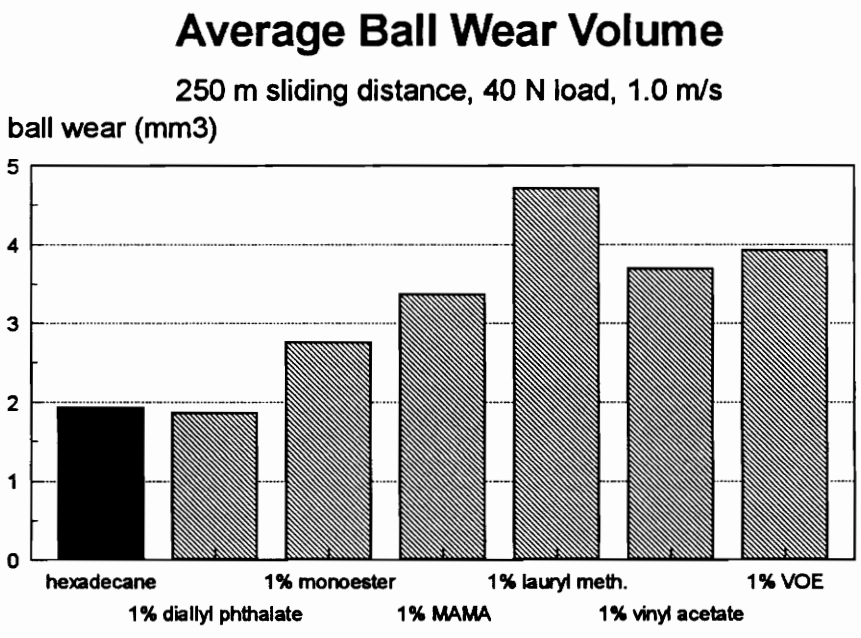

Figure 4.4 Ball Wear For Low Load and High Speed Conditions.

The addition of monomers to the hexadecane carrier fluid generally increased alumina wear. However, diallyl phthalate and hexadecane wear volumes were not statistically different at the 90 percent confidence level. The increase in wear for the other five monomers is a surprising finding.

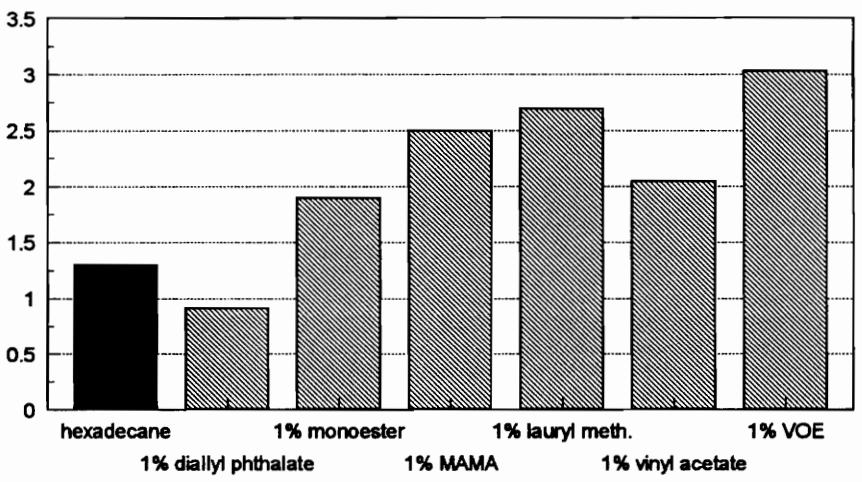

Figure 4.5 Disk Wear For Low Load and High Speed Conditions.

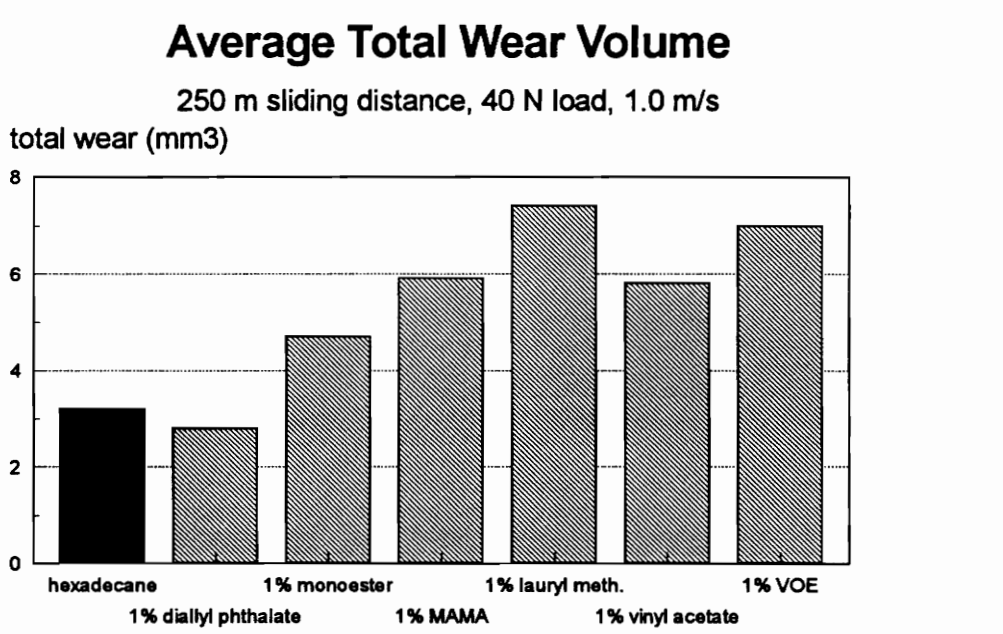

Figure 4.6 Total Wear For Low Load and High Speed Conditions.

4.1.1.3 High Load - Low Speed Results

Testing at 160 N normal load and 0.25 m/s sliding speed lasted 16 minutes, 40 seconds (1000 seconds) for a resulting sliding distance of 250 m. However the pure hexadecane and the MAMA tests resulted in excessive wear which prevented the tests from being completed. Pure hexadecane and MAMA tests lasted an average of 54 m sliding distance before reaching the maximum ball wear, as determined by a mechanical safety stop on the pin-on-disk machine.

Ball wear, disk wear and total wear were significantly reduced for all monomers except MAMA under the high load and low speed condition. Unlike other load-speed conditions, wear reduction percentages for high load and low speed are based on the incomplete wear tests run with the carrier fluid. Any

monomer which allowed a test under these conditions to be completed (for 250 m sliding distance) with the same wear as hexadecane increases the useful life by a factor of five. Not only did the effective monomers allow the tests to be completed, but they actually decreased wear compared to the incomplete pure hexadecane tests. Figures 4.7, 4.8 and 4.9 show the wear volumes (mm^3) of all tests at 160 N and 0.25 m/s for ball, disk and total wear respectively.

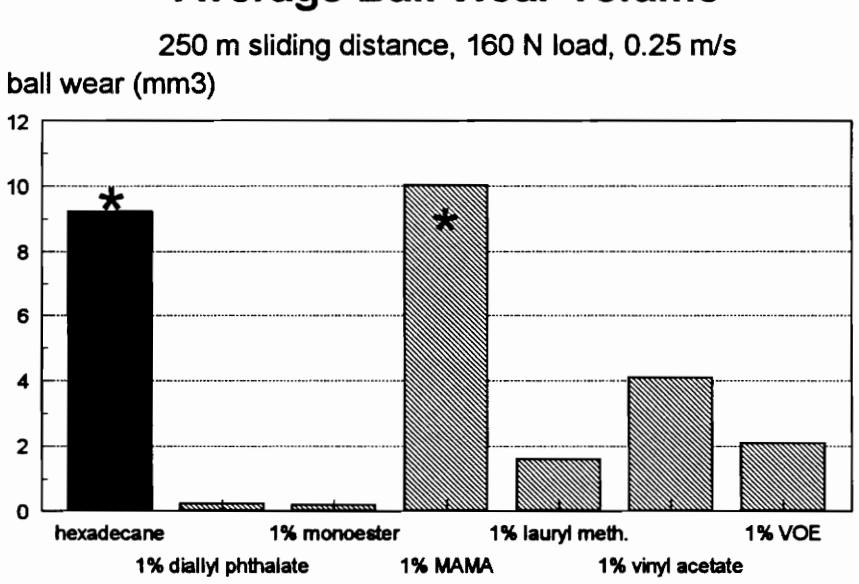

Figure 4.7 Ball Wear For High Load and Low Speed Conditions.

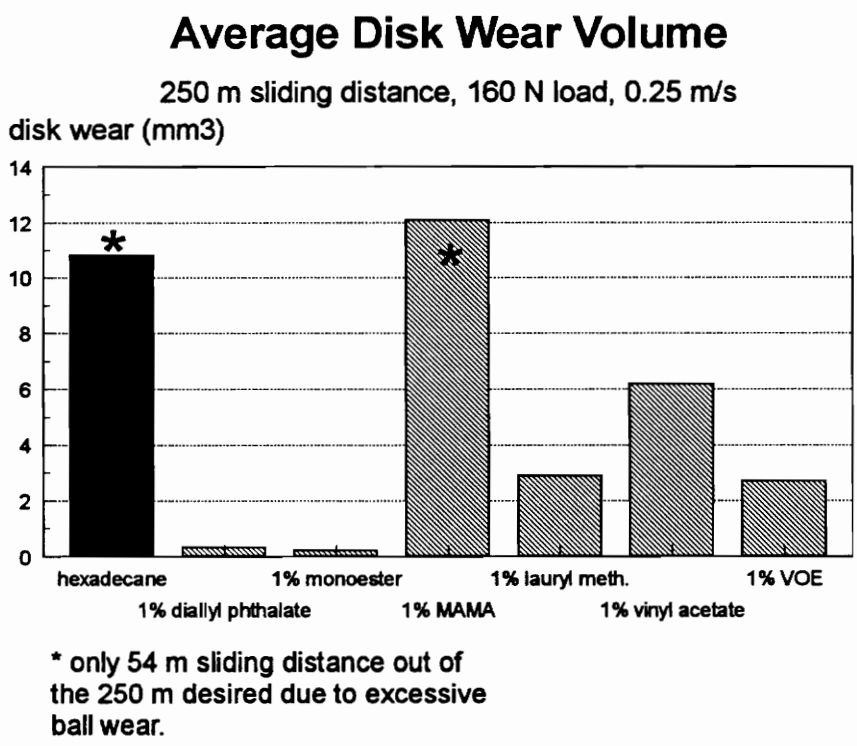

Figure 4.8 Disk Wear For High Load and Low Speed Conditions.

Three levels of wear result at 160 N load and 0.25 m/s speed. Diallyl phthalate and the monoester were extremely effective, resulting in at least 97 % total wear reduction. Lauryl methacrylate, vinyl acetate and vinyl octadecyl ether resulted in significant wear reductions, between 49 and 78 percent. Again, these percentages are based on the incomplete test wear volumes of hexadecane. MAMA wear and hexadecane wear were not statistically different.

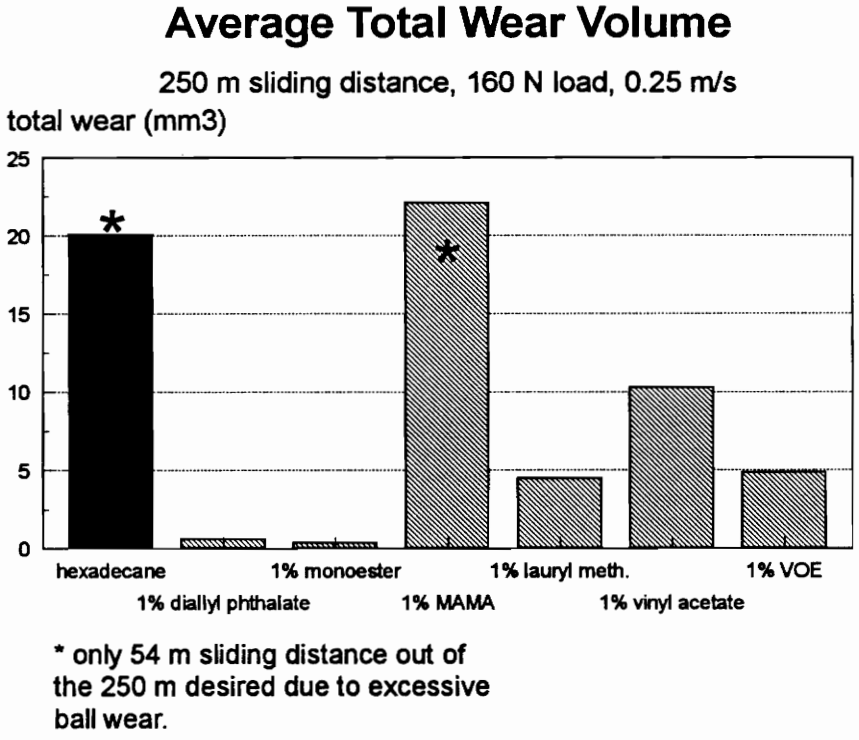

Figure 4.9 Total Wear For High Load and Low Speed Conditions.

4.1.1.4 High Load - High Speed Results

Experiments at 160 N normal load and 1.0 m/s sliding speed lasted 4 minutes, 10 seconds (250 seconds) for a resulting sliding distance of 250 m. Under these conditions, none of the six monomers reduced alumina wear. Figures 4.10, 4.11 and 4.12 show the wear volumes (mm^3) of all tests at 160 N normal load and 1.0 m/s sliding speed for ball, disk and total wear respectively.

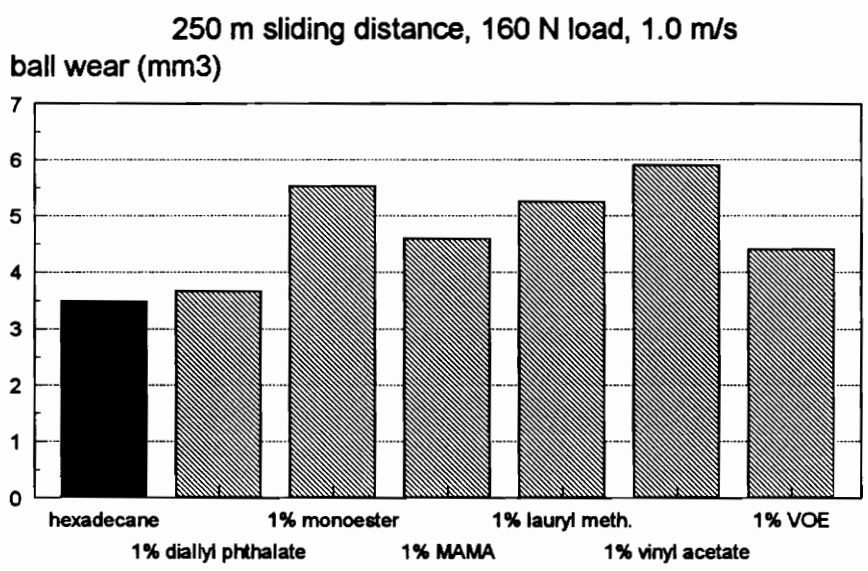

Figure 4.10 Ball Wear For High Load and High Speed Conditions.

High speed and high load tests caused cracks to appear in the disk for every test. However the cracks did not cause the test to fail as disks usually remained intact until removed from the Teflon backing piece. A distinct 'click' sound could be heard at about 45-60 seconds into the 250 second test. Cracks were visible after the test as thin lines randomly spread across the disk surface.

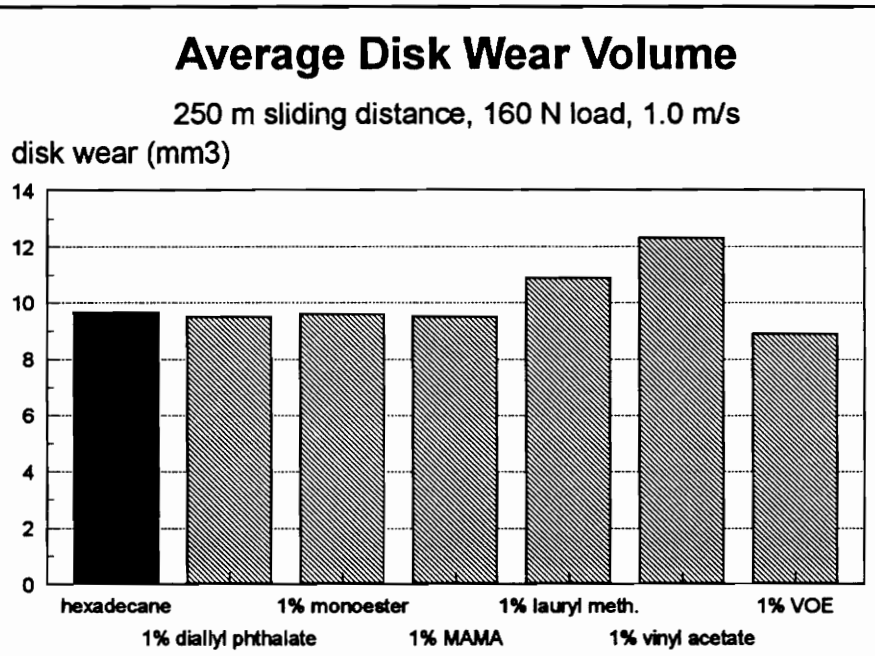

Figure 4.11 Disk Wear For High Load and High Speed Conditions.

The total wear of diallyl phthalate, the monoester, MAMA and VOE were not statistically different from hexadecane wear. However lauryl methacrylate and vinyl acetate increased total wear under the high load and high speed conditions.

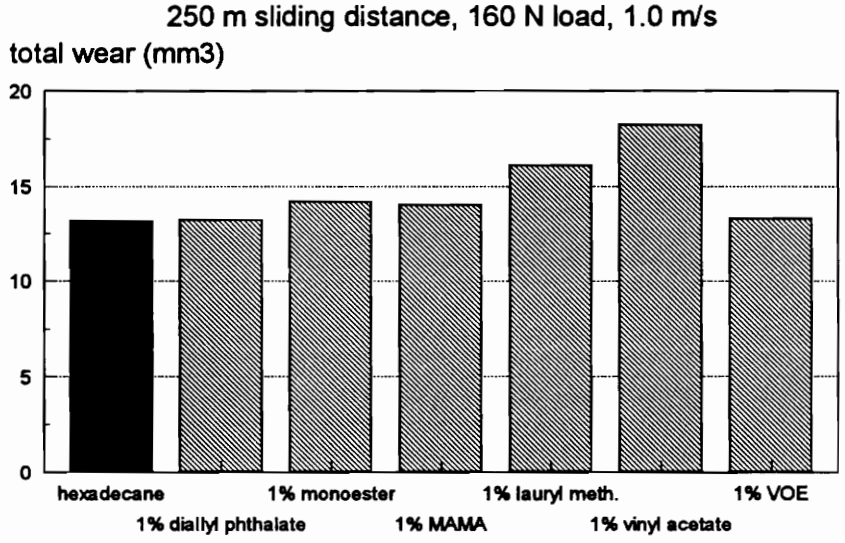

Figure 4.12 Total Wear For High Load and High Speed Conditions.

4.1.2 Monomer Effects

4.1.2.1 Diallyl Phthalate

Regardless of normal load, diallyl phthalate was effective in reducing wear at the low speed conditions, but not at the high speed conditions. This monomer has been proven to be very effective in reducing alumina wear in previous tests by Smith [46] and Tripathy [48].

Figure 4.13 compares total wear (ball + disk) for pure hexadecane and 1 wt. % diallyl phthalate in hexadecane for all test conditions. Total wear is representative of either ball or disk wear, since the changes in wear were usually similar for both ball and disk for a given monomer.

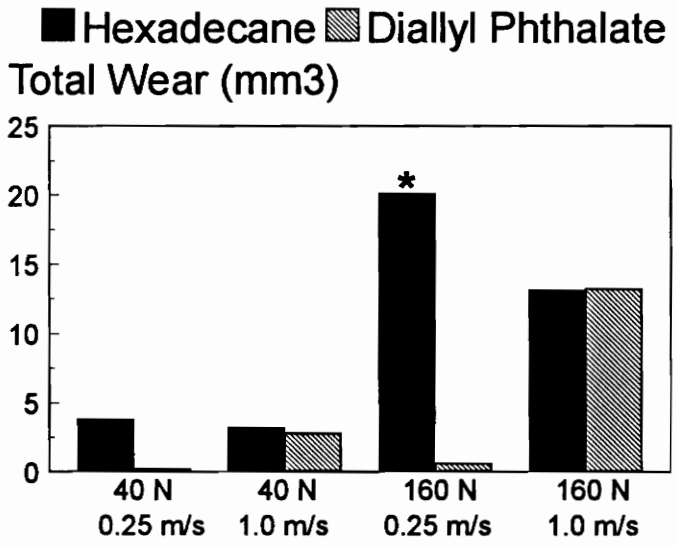

250 m total sliding distance unless *
* indicates 54 m average sliding distance

Figure 4.13 Effects of Diallyl Phthalate, Load and Speed on Total Wear.

For low load and low speed test conditions, the reduction in wear for diallyl phthalate is one of the highest among all the monomers. Ball wear, disk wear and total wear were reduced by 93 %, 96 % and 95 % respectively at low load and low speed.

At low speeds, the effect of load on alumina wear is very high for pure hexadecane. The average total wear for pure hexadecane increases from 3.8 mm^3 at 40 N, to 20.1 mm^3 at 160 N, with the 160 N test only completing 54 m compared to the 250 m distance for the 40 N test. However the addition of diallyl phthalate almost eliminates the effect of load on wear. The average total wear for 1 wt. % diallyl phthalate increased from 0.2 mm^3 at 40 N to 0.59 mm^3 at 160 N, at 0.25 m/s sliding speed. This increase is very small compared to that of pure hexadecane.

At the higher 160 N load and 0.25 m/s sliding speed, diallyl phthalate is very effective in reducing wear, showing at least a 97 % reduction. The increase in speed at 160 N eliminates the beneficial effect of diallyl phthalate. Diallyl phthalate had no effect on wear at the 1.0 m/s sliding speed.

4.1.2.2 C36 Dimer Acid/Ethylene Glycol Monoester

Under low speed test conditions, 1 wt. % monoester in hexadecane resulted in striking alumina wear reductions for both low and high loads. At high speeds, the monoester increased wear somewhat at low loads and had no effect at high loads. Figure 4.14 compares total wear of monoester and pure hexadecane for all load and speed conditions.

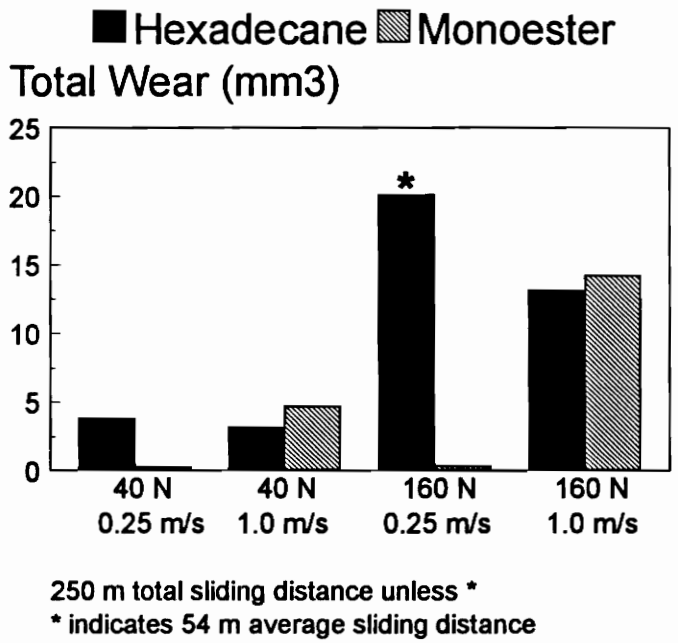

Figure 4.14 Effect of Monoester, Load and Speed on Total Wear.

Like diallyl phthalate, the effect of load on wear depends on the speed for the monoester. Increasing the load at the 0.25 m/s sliding speed results in a very small increase in wear for the monoester. At high speeds, increasing the load greatly increases the wear for the monoester.

4.1.2.3 Methyl-2-Acrylamido-2-Methoxy Acetate

The general effect of the MAMA solution was a small reduction in wear at the low load and low speed condition, and no reduction or an increase in wear for the other three conditions. Figure 4.15 compares wear results of a 1 wt. % MAMA mixture with pure hexadecane at all test conditions.

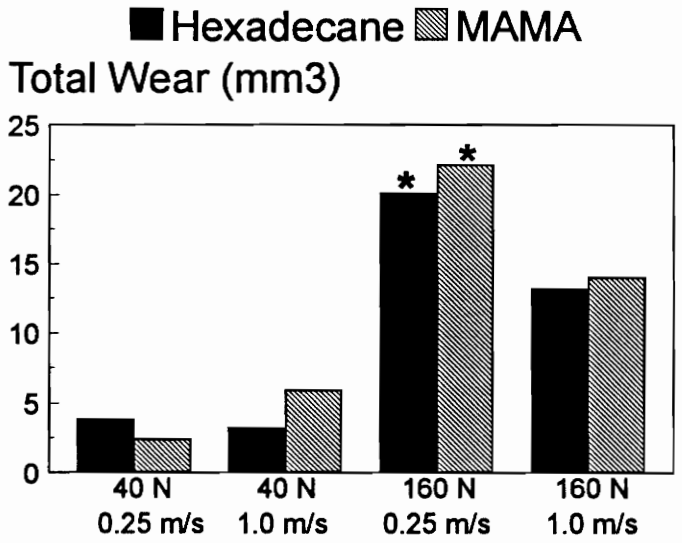

250 m total sliding distance unless *
* indicates 54 m average sliding distance

Figure 4.15 Effect of MAMA, Load and Speed on Total Wear.

The effect of load on total wear for MAMA is dependent on the sliding speed. An increase in load at the low speed also results in an increase in total wear. However at the high speed, an increase in load results in a decrease in wear. The interaction of the load and speed factors is apparent from Figure 4.15 and supported by the analysis of variance statistical method (see Appendix D).

4.1.2.4 Lauryl Methacrylate

Under the low load and low speed test conditions, lauryl methacrylate resulted in a modest wear reduction. For high load and low speed conditions, a very large reduction in wear occurred. Wear increased for lauryl methacrylate at the 1.0 m/s sliding speeds, at both loads. Figure 4.16 compares average total wear of lauryl methacrylate and pure hexadecane for all load and speed conditions.

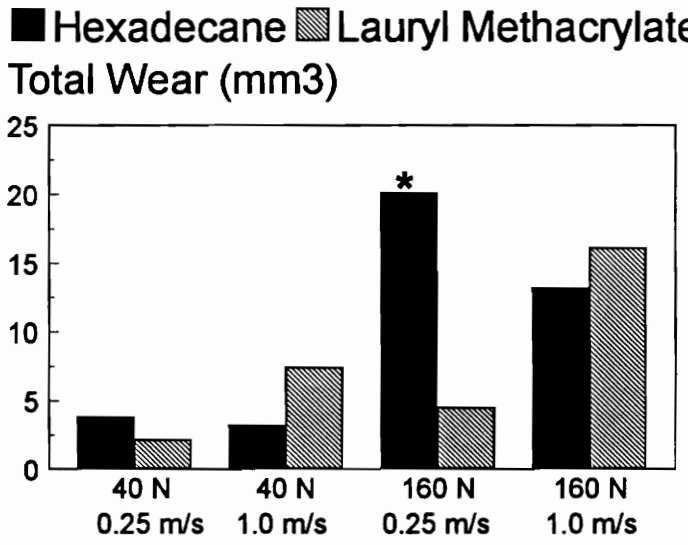

Figure 4.16 Effect of Lauryl Methacrylate, Load and Speed on Total Wear.

4.1.2.5 Vinyl Acetate

Figure 4.17 compares average wear of vinyl acetate and pure hexadecane for all testing conditions. Vinyl acetate was most effective at the low load and low speed condition, resulting in a 93 % total wear reduction. At high load and low speed conditions, vinyl acetate was still effective (at least 49 % total wear reduction) in reducing wear. High speed conditions increased alumina wear.

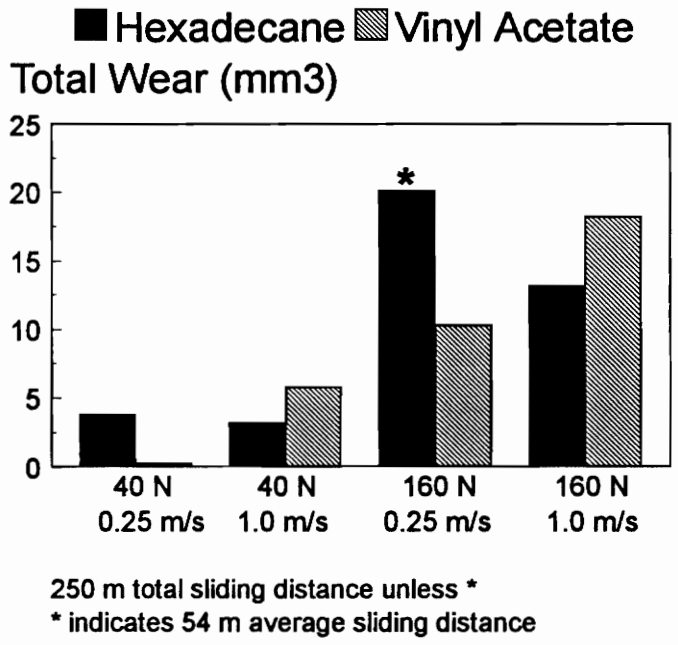

Figure 4.17 Effect of Vinyl Acetate, Load and Speed on Total Wear.

4.1.2.6 Vinyl Octadecyl Ether

Figure 4.18 compares average wear of vinyl octadecyl ether and pure hexadecane for all testing conditions. At low load and low speed, total wear decreased by 48 percent. A larger wear decrease occurred at the high load and low speed condition, a 76 percent reduction. Total wear increased at low load and high speed. No change in wear occurred at the high load and high speed condition.

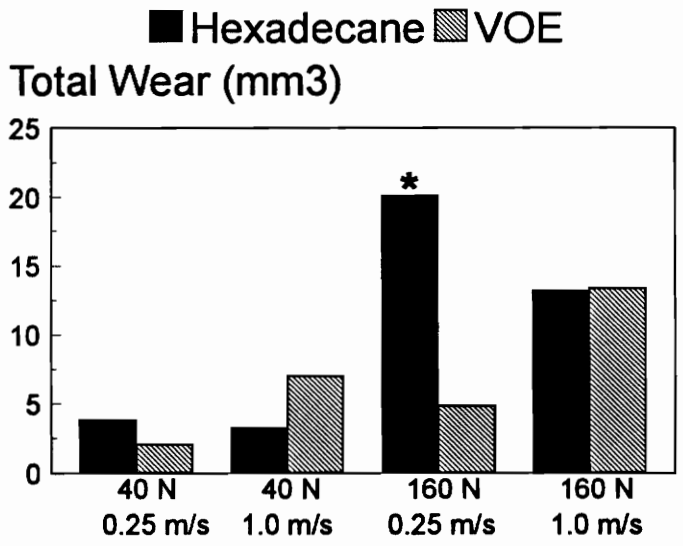

Figure 4.18 Effect of Vinyl Octadecyl Ether, Load and Speed on Total Wear.

4.2 PHOTOMACROGRAPHS

Visual inspection of disk and ball surfaces was performed using the Wild-Heerbrugg photomacroscope. Photomacrographs that show certain surface features, or are representative of many of the test specimens, are included here. Although all test specimens were examined using the photomacroscope, not all specimens were photographed. Surfaces with smooth wear tracks and little wear debris (at the macroscopic level, 16.25**X** magnification) did not result in useful pictures. *All photomacrographs have a section of the disk wear scar oriented on the page such that the outer portion of the wear scar is at the top of the picture.* The entire wear scar can be seen for low load conditions, however high load wear scars may be too large to fit within the picture.

A photomacrograph of the low load and low speed disk wear track for pure hexadecane lubrication is shown in Figure 4.19.

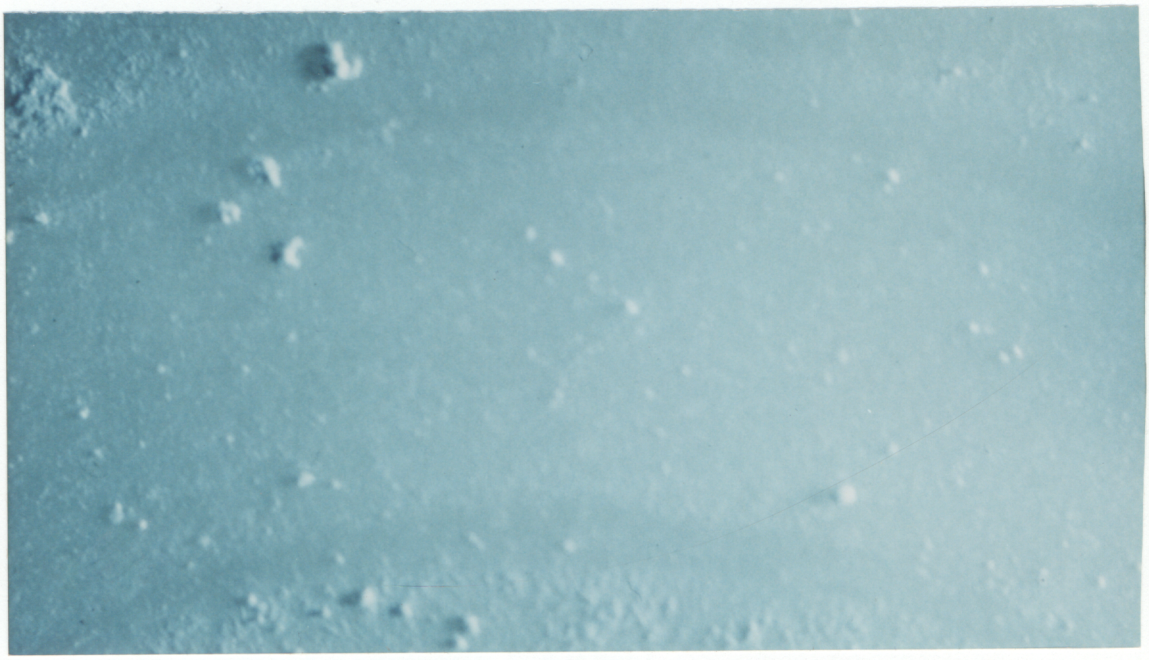

Figure 4.19 Photomacrograph of Hexadecane Lubricated Disk Wear Scar for 40 N Load and 0.25 m/s Sliding Speed. (16.25X magnification)

The darker patches in the wear scar in Figure 4.20 are smooth reflective patches on the alumina wear track. The disk surface is from a 160 N load and 1.0 m/s sliding speed, hexadecane lubricated test.

Figure 4.20 Photomacrograph of Hexadecane Lubricated Disk Wear Scar for 160 N Load and 1.0 m/s Sliding Speed. (16.25X magnification)

Photomacroscope pictures taken with a direct overhead light, perpendicular to the disk surface, result in bright areas where the disk surface is very reflective and surface characteristics are not visible. A photographic light source shining at a low angle relative to the disk surface was necessary for pictures which enhance surface characteristics, while not showing the mirror-like reflection from the dark patches.

Comparing the diallyl phthalate wear scar in Figure 4.21 to the hexadecane wear scar in Figure 4.19, the photomacroscope pictures show

obvious differences in wear scar sizes for the two lubricants at the low load and low speed condition. The diallyl phthalate wear scar is much smaller, darker and more consistent in appearance, suggesting a smooth surface. The unworn disk surface appearance can be seen inside the wear scar, at the bottom of the picture. The surface of the diallyl phthalate wear scar is most similar to the vinyl acetate wear scar surface at 40 N and 0.25 m/s.

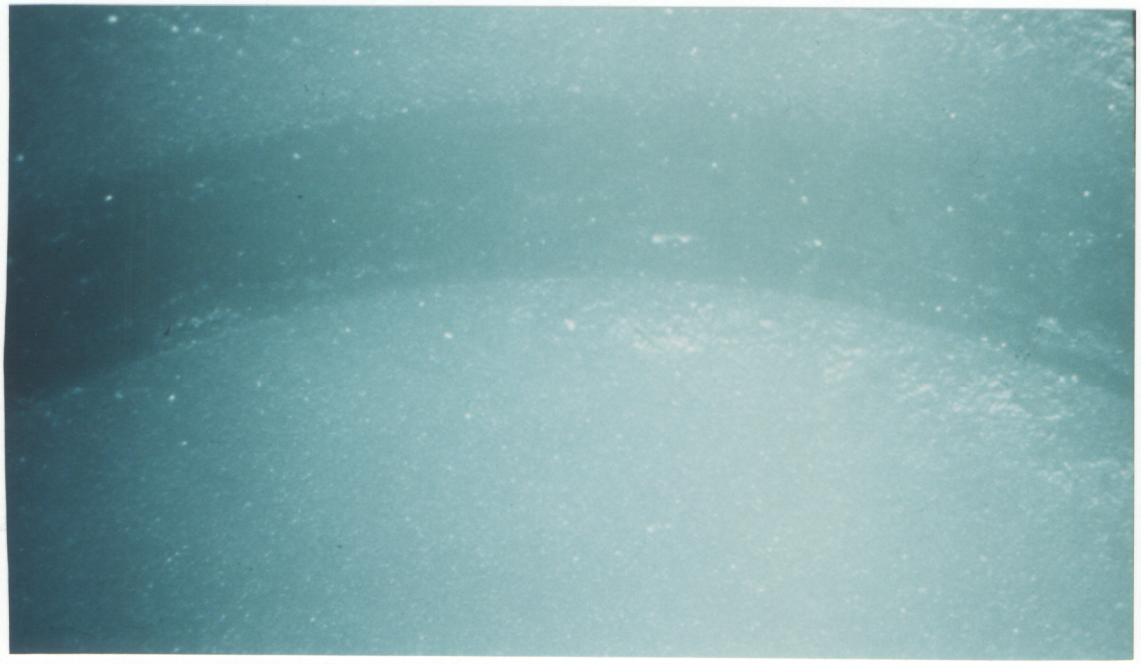

Figure 4.21 Photomacrograph of 40 N Load and 0.25 m/s Speed Diallyl Phthalate Disk Wear Scar. (16.25X magnification)

Figure 4.22 shows a photomacroscope picture of the high speed and high load surface at 16.25X magnification. The diagonal crack is an example of the cracks which occurred in every high load and high speed test. The diallyl phthalate wear scar has more clumps of wear debris than the hexadecane wear scar shown in Figure 4.20.

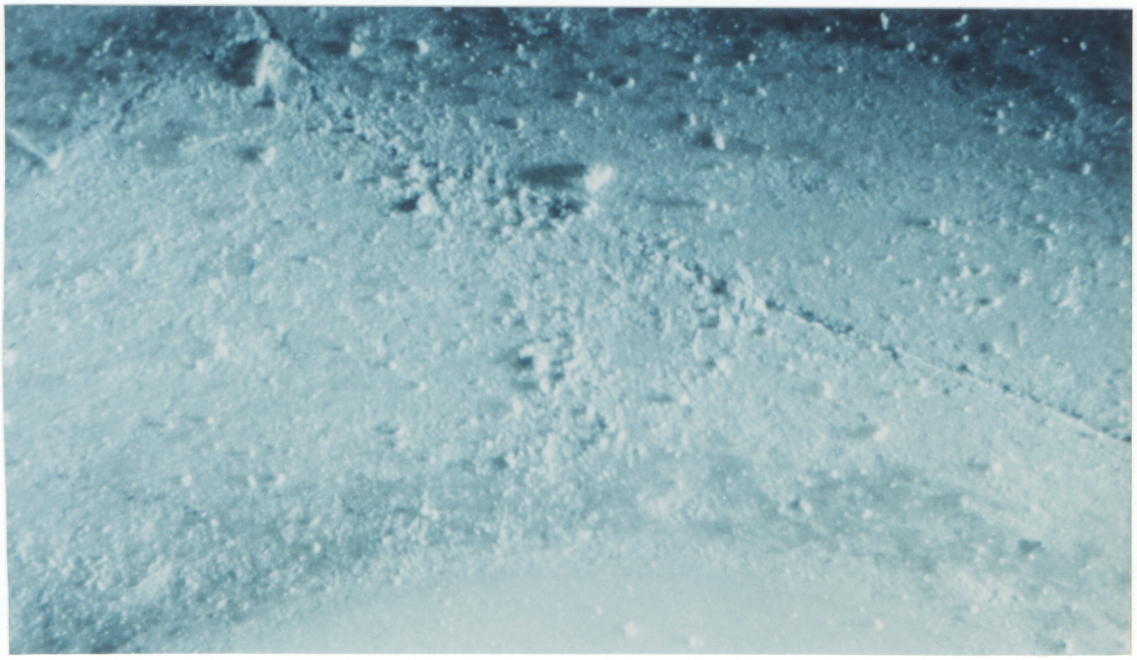

Figure 4.22 Photomacrograph of 160 N Load and 1.0 m/s Speed Diallyl Phthalate Disk Wear Scar. (16.25X magnification)

Photomacroscope pictures of monoester lubricated samples are not very useful as most surface features were not apparent under any light conditions. However the photomacrograph in Figure 4.23 shows the surface of the monoester lubricated disk wear scar for 160 N load and 1.0 m/s sliding speed. Like the hexadecane wear scar in Figure 4.20, the surface shows two regimes: the dark highly reflective patches mixed in with lighter more powdery areas. The monoester wear scar appears to have a more consistent surface than the hexadecane. Grainy pockets on the hexadecane surface are not present on the monoester surface.

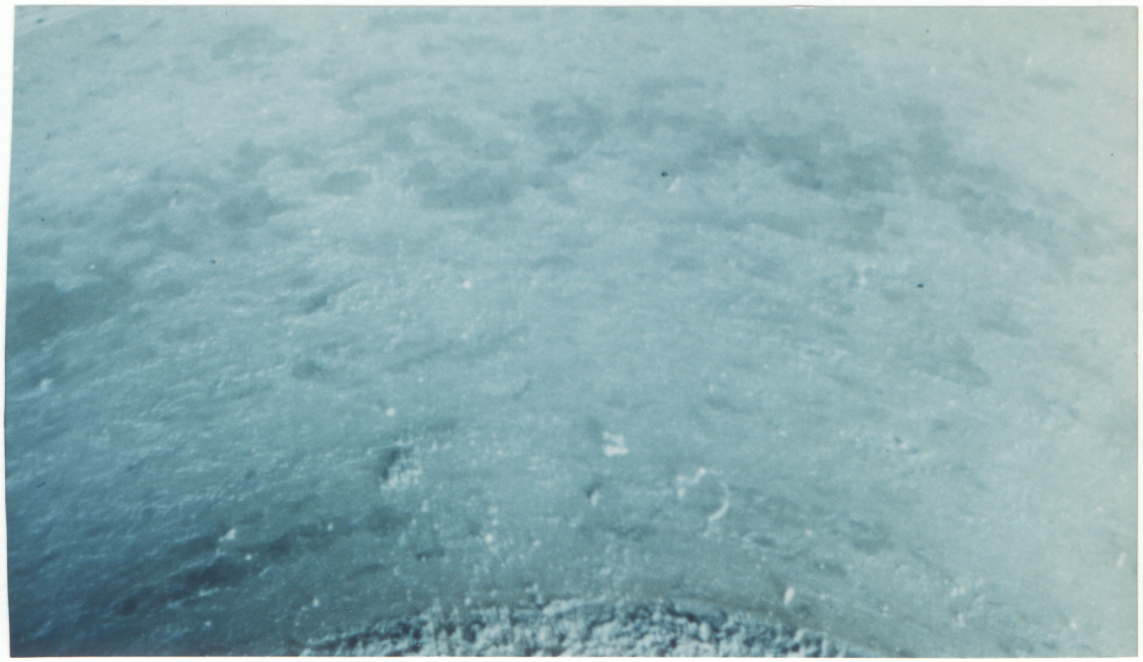

Figure 4.23 Photomacrograph of Monoester Lubricated Disk Wear Scar at 160 N and 1.0 m/s. (16.25X Magnification)

The photomacroscope picture in Figure 4.24 offers the MAMA disk wear scar at 160 N load and 0.25 m/s sliding speed. The worn surface has consistent features, no reflective patches exist.

Figure 4.24 Photomacrograph of MAMA Lubricated Disk Wear Scar at 160 N and 0.25 m/s. (16.25X Magnification)

The photomacrograph in Figure 4.25 of the 160 N and 1.0 m/s MAMA disk wear scar shows the highly reflective areas along with more powdery and grainy surfaces. In this photograph, the lighting is a mixture of side and overhead lighting, which tends to illuminate the dark patches and partially demonstrate their reflectiveness, while still showing surface features.

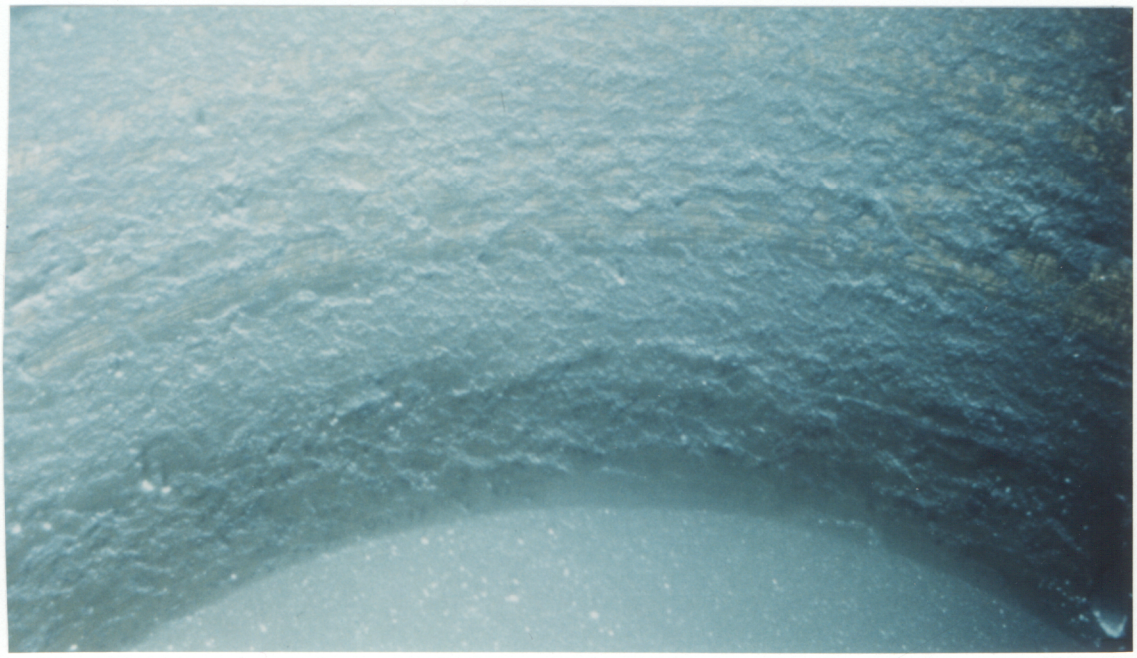

Figure 4.25 Photomacrograph of MAMA Lubricated Disk Wear Scar at 160 N Load and 1.0 m/s Sliding Speed (16.25X Magnification).

As an example of the mirror-like surface which forms at high speeds, a photomacroscope picture using only the top light is included in Figure 4.26, for vinyl acetate at 160 N and 1.0 m/s.

Figure 4.26 Photomacrograph of Vinyl Acetate Lubricated Disk Wear Scar for 160 N Load and 1.0 m/s Speed (16.25X Magnification).

The definite contrast between worn and unworn disk surface can be seen in Figure 4.27, a photomacrograph of the disk wear scar surface at 160 N load and 1.0 m/s sliding speed for the vinyl octadecyl ether monomer. The worn surface is clearly much rougher than the smooth unworn surface at the bottom of the picture.

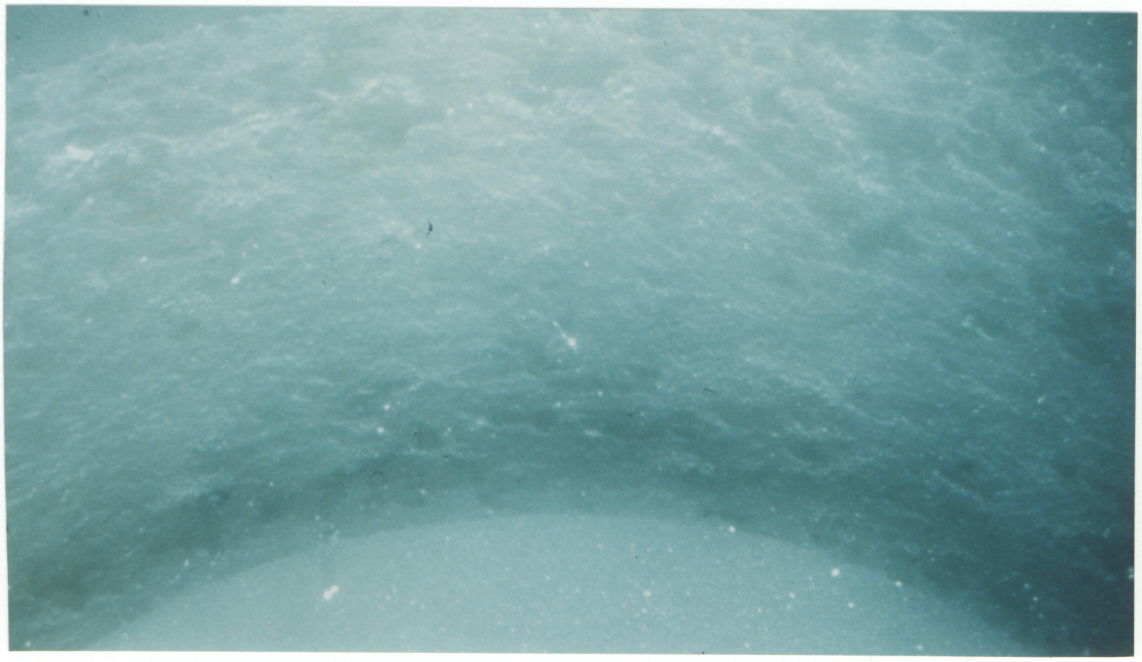

Figure 4.27 Photomacrograph of Vinyl Octadecyl Ether Lubricated Disk Wear Scar for 160 N Load and 1.0 m/s Sliding Speed (16.25X Magnification).

4.3 ESEM PHOTOGRAPHS

Environmental Scanning Electron Microscopy (ESEM) may be used to give more detailed information on surface features. ESEM photographs at 400**X** magnification were useful for comparison of surface characteristics. Not every specimen was examined using ESEM. However selected specimens are included here to show certain surface features. One highly effective monomer (the monoester), one effective monomer (vinyl octadecyl ether), one ineffective monomer (MAMA) and pure hexadecane were chosen for ESEM disk wear scar examination.

Figure 4.28 shows the unworn alumina surface of a disk. Sharp grains are visible and no wear debris or fine ceramic particles are visible.

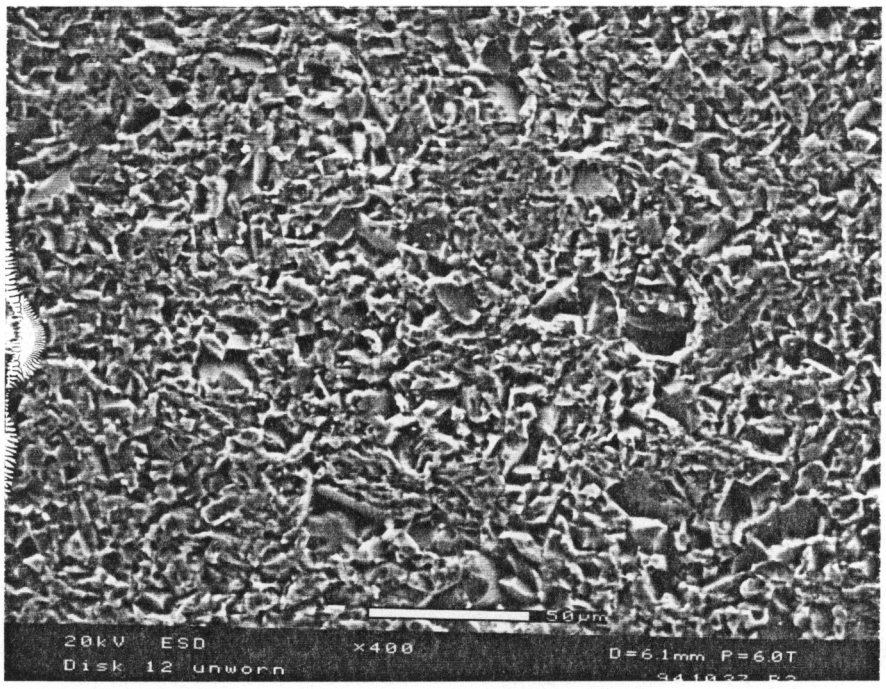

Figure 4.28 ESEM of Unworn Disk Surface.

Low Load and Low Speed

The ESEM photograph in Figure 4.29 of the pure hexadecane lubricated disk wear scar shows a clear difference from the 1 wt. % monoester lubricated disk surface in Figure 4.30, for 40 N load and 0.25 m/s speed. The surface of the pure hexadecane wear scar is much rougher due to the visibility of actual ceramic grains. The monoester wear scar does not have as many surface irregularities and appears to be a generally smooth surface.

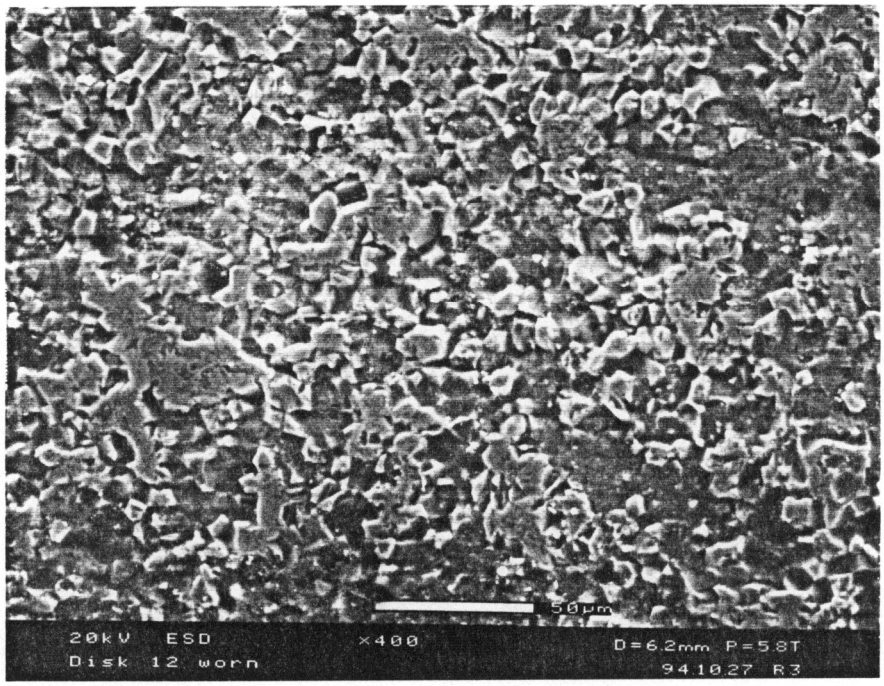

Figure 4.29 ESEM of Hexadecane Lubricated Disk Wear Scar for 40 N Load and 0.25 m/s Sliding Speed.

The worn surface in Figure 4.29 is also clearly different from the unworn surface shown in Figure 4.28. Ceramic grains are still visible in the worn surface, along with wear debris in between the grains.

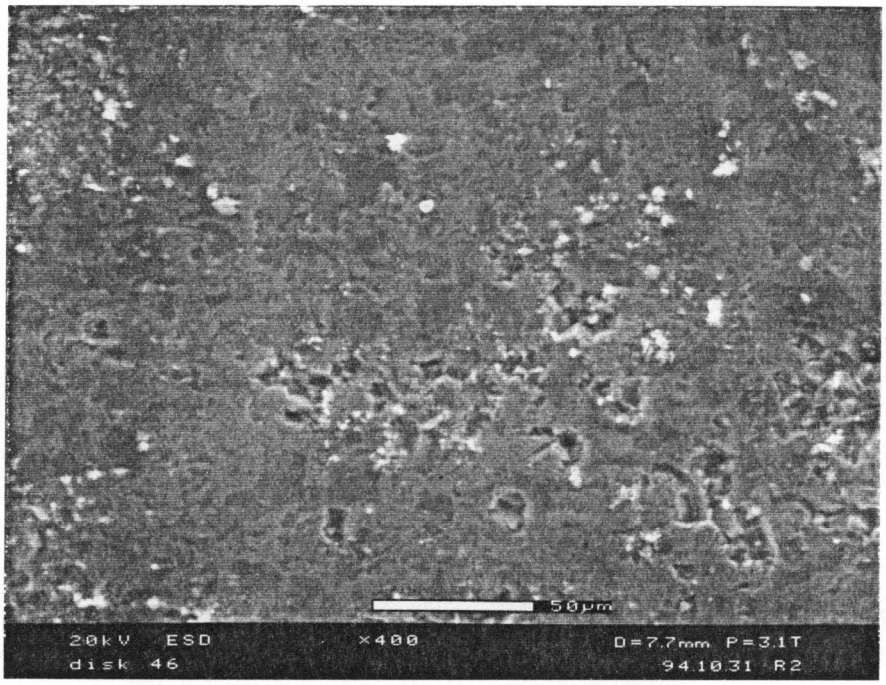

Figure 4.30 ESEM of Monoester Lubricated Disk Wear Scar for 40 N Load and 0.25 m/s Sliding Speed.

The ESEM photograph in Figure 4.31 of the 1 wt. % MAMA lubricated disk surface in the wear scar is very similar to the pure hexadecane lubricated disk surface in Figure 4.29. The surfaces of the pure hexadecane and the MAMA wear scars have visible ceramic grains and lack a smooth wear debris layer. Unlike diallyl phthalate and monoester, the wear debris particles did not attach to the alumina surface and to each other to form a smooth wear debris layer.

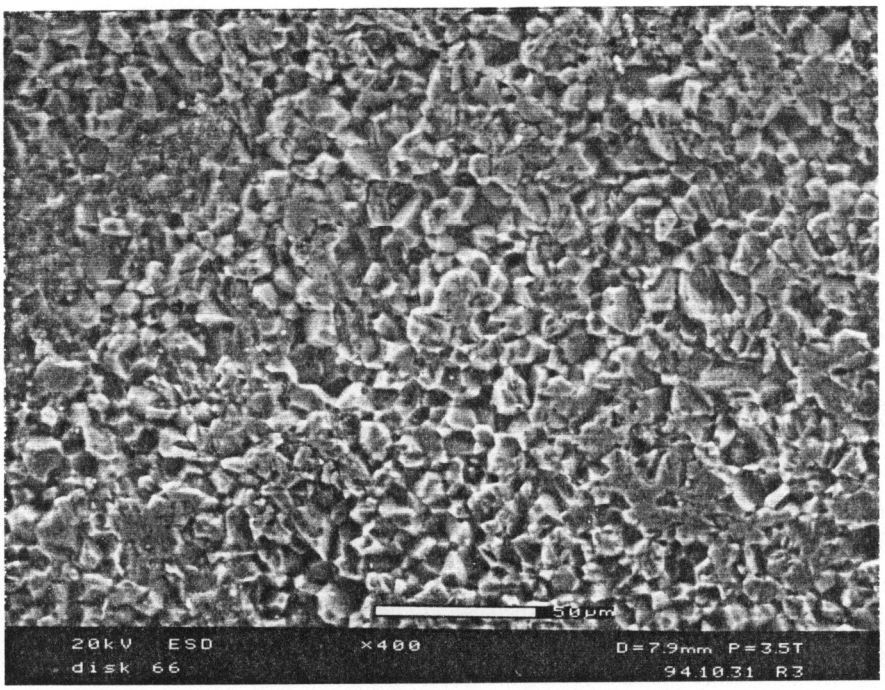

Figure 4.31 ESEM of MAMA Lubricated Disk Wear Scar for 40 N Load and 0.25 m/s Sliding Speed.

The ESEM photograph in Figure 4.32 of the 1 wt. % vinyl octadecyl ether lubricated wear scar surface is different from the pure hexadecane lubricated disk surface in Figure 4.29. The surface of the pure hexadecane wear scar is much rougher due to the visibility of actual ceramic grains. The vinyl octadecyl ether wear scar does not have as many surface irregularities due to more of the compacted wear debris layer, although it does not appear as smooth as the monoester lubricated surface.

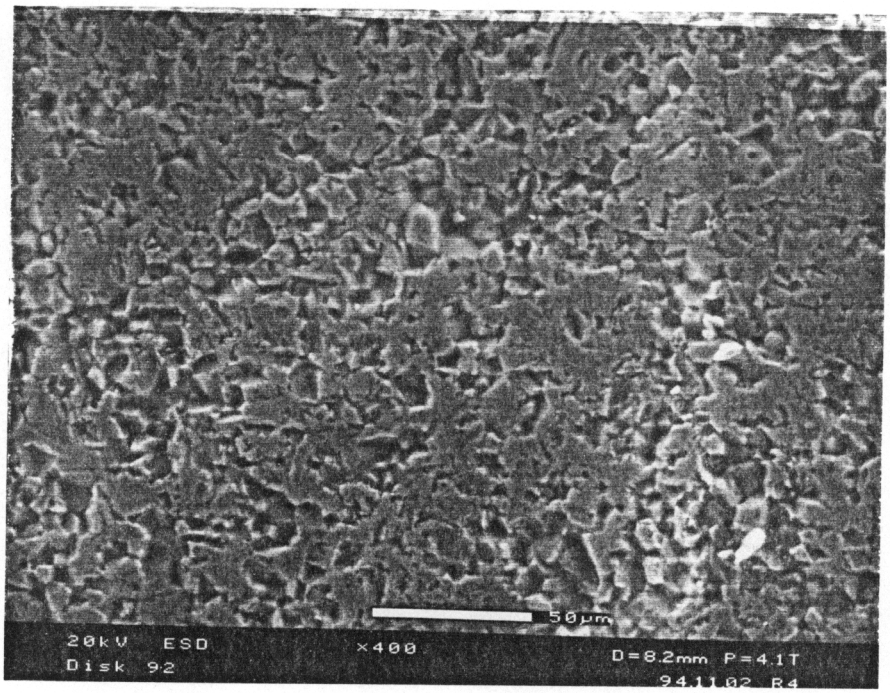

Figure 4.32 ESEM of Vinyl Octadecyl Ether Lubricated Disk Surface for 40 N Load and 0.25 m/s Sliding Speed.

High Load and Low Speed

The disk wear track surface for the 160 N load and 0.25 m/s sliding speed with hexadecane lubrication is shown in Figure 4.33. Compared to the monoester surface in Figure 4.34, the monoester surface is smooth with more of the surface texture filled in with a compacted debris layer. Although not as smooth as the 40 N monoester surface, the 160 N monoester surface has most of the sharp grains covered by a debris layer.

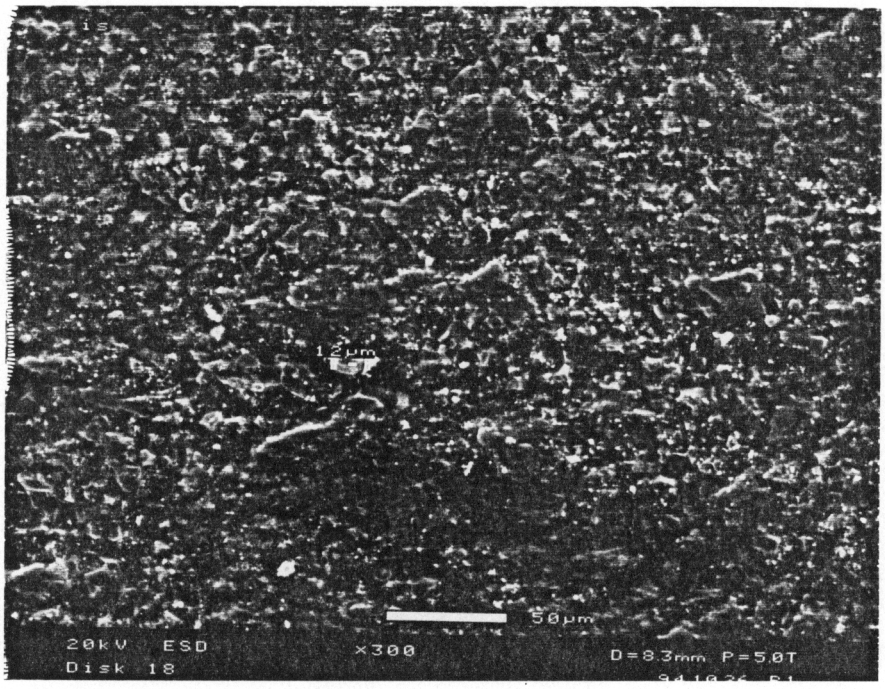

Figure 4.33 ESEM of Hexadecane Lubricated Disk Wear Scar for 160 N Load and 0.25 m/s Sliding Speed.

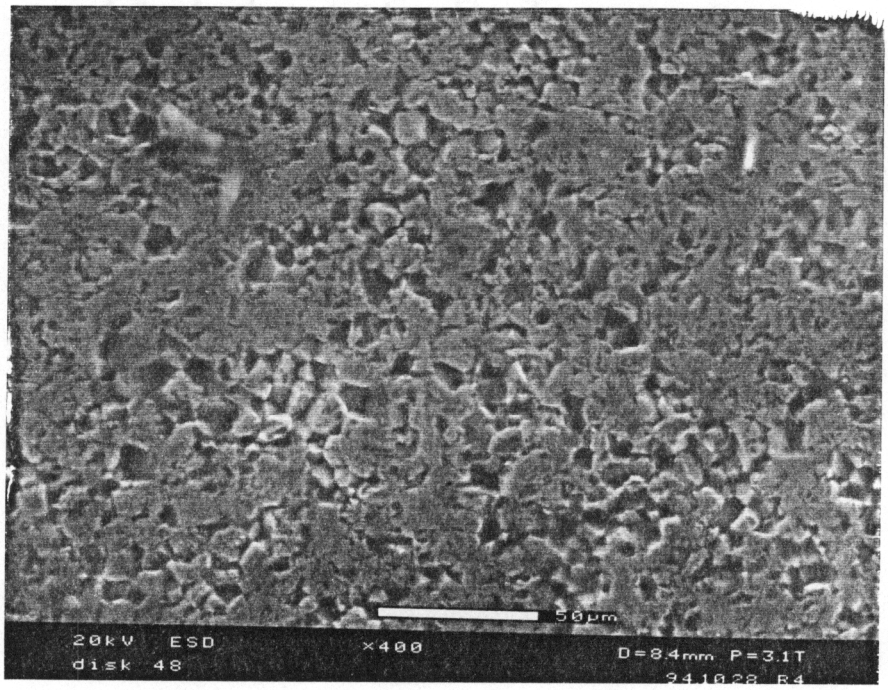

Figure 4.34 ESEM of Monoester Lubricated Disk Wear Scar for 160 N Load and 0.25 m/s Sliding Speed. (300**X** magnification)

Figure 4.35 is an ESEM picture of the hexadecane lubricated disk wear scar for 160 N load and 0.25 m/s sliding speed at a higher (3050**X**) magnification. Alumina grains are clearly visible, as are the fine wear particles spread over the surface. Some of the fine particles appear to be flake-like in shape.

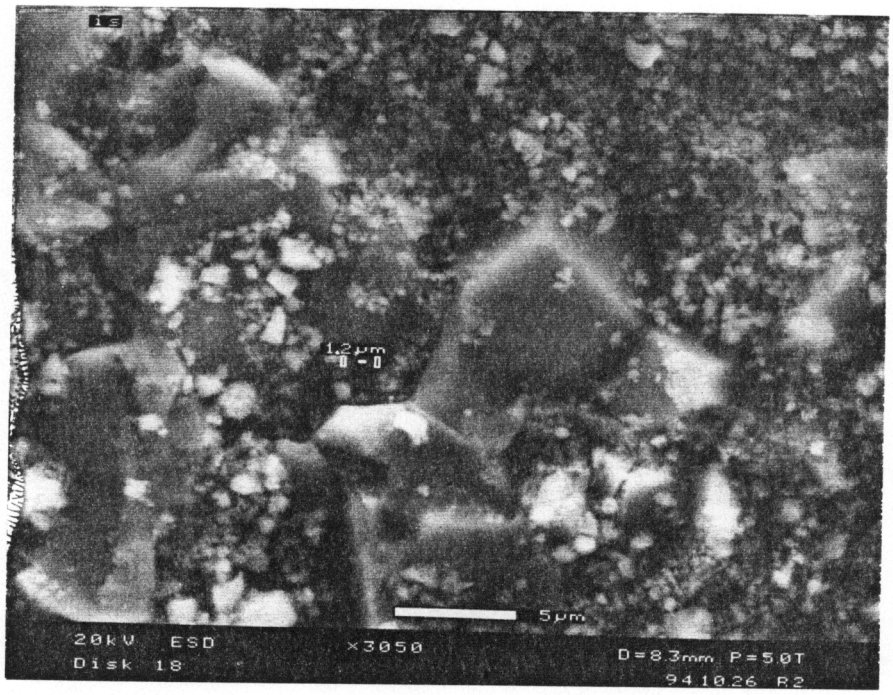

Figure 4.35 ESEM of Pure Hexadecane Lubricated Disk Wear Scar for 160 N Load and 0.25 m/s Sliding Speed at 3050**X** magnification.

At high load and low speed, the MAMA wear scar surface is different from that obtained with hexadecane, although wear volumes are statistically equal. The MAMA surface shown in Figure 4.36 has more smooth areas of compacted wear debris compared to hexadecane in Figure 4.35.

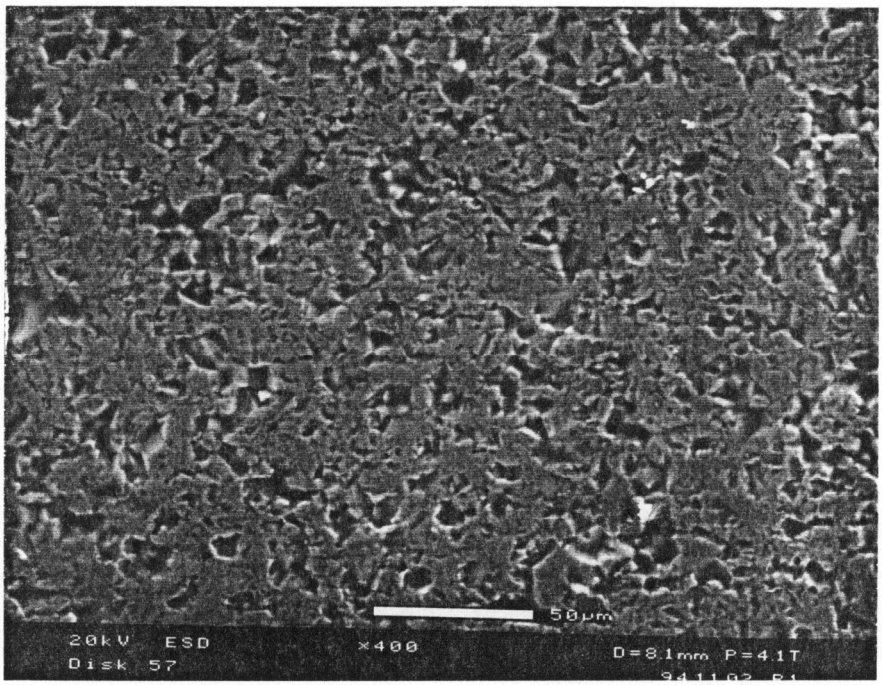

Figure 4.36 ESEM of MAMA Lubricated Disk Wear Scar for 160 N Load and 0.25 m/s Sliding Speed.

The ESEM picture in Figure 4.37 of vinyl octadecyl ether disk wear scar shows the mixture of wear debris layer and open grains. Areas of craters without wear debris could have occurred during sliding when the debris layer flaked away.

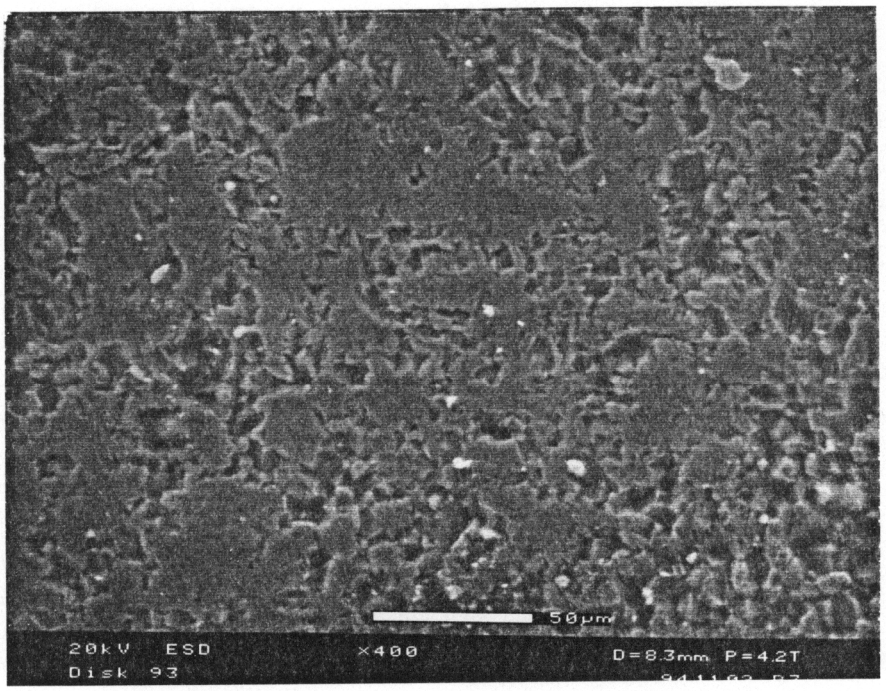

Figure 4.37 ESEM of Vinyl Octadecyl Ether Lubricated Disk Surface for 160 N Load and 0.25 m/s Sliding Speed.

Low Load and High Speed

The disk wear track ESEM photograph is shown in Figure 4.38 for low load and high speed with hexadecane lubrication. Although the light contrast is different, the surface features are similar to the monoester surface for the same test conditions in Figure 4.39.

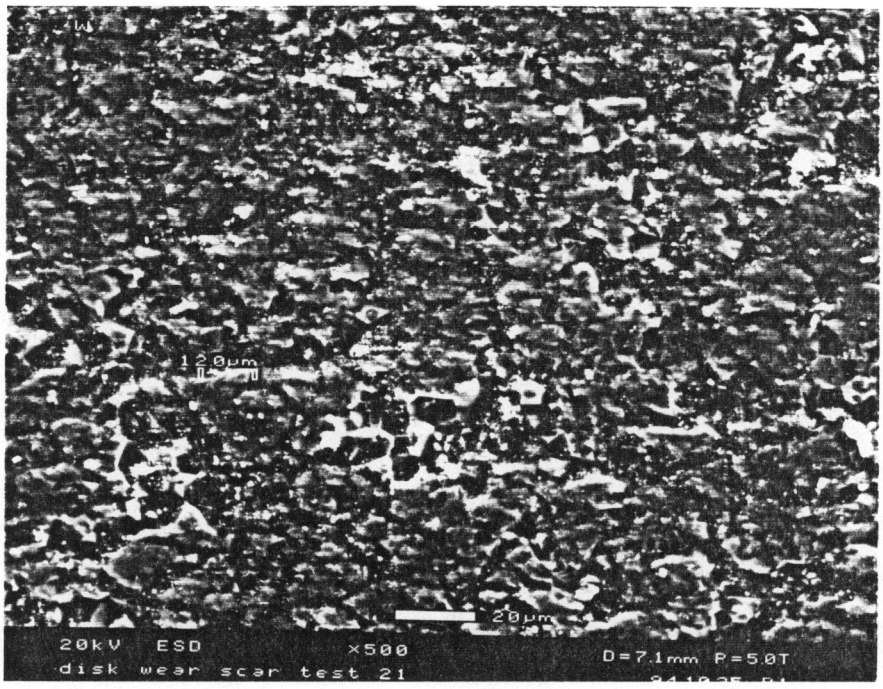

Figure 4.38 ESEM of Hexadecane Lubricated Disk Wear Scar for 40 N Load and 1.0 m/s Sliding Speed.

The monoester and pure hexadecane wear scar surfaces are consistent. No large patches of either compacted wear debris or open sharp grains exist. The surface has fine wear particles spread over the surface, but a smooth surface does not exist.

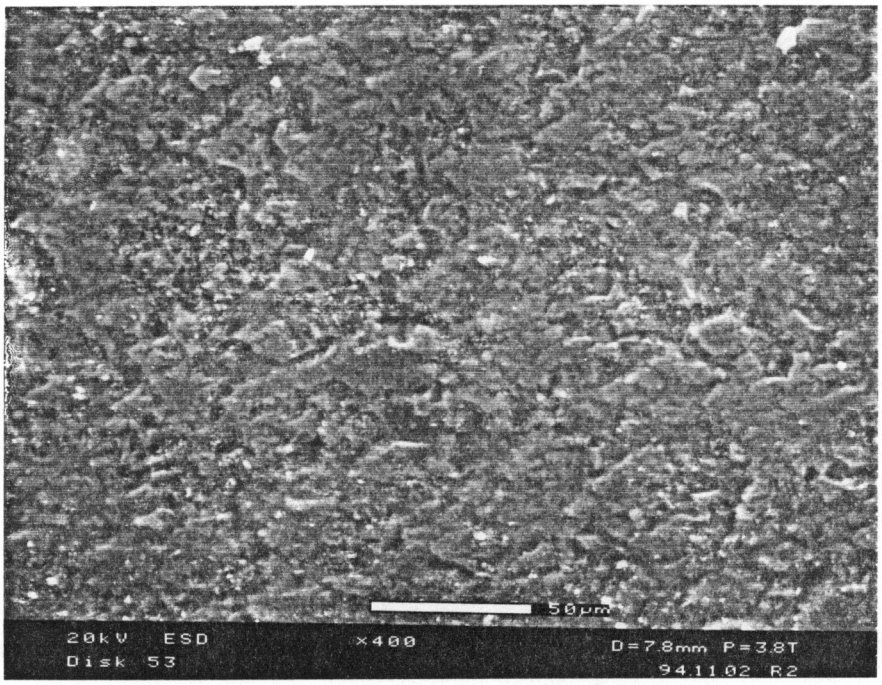

Figure 4.39 ESEM of Monoester Lubricated Disk Wear Scar for 40 N Load and 1.0 m/s Sliding Speed. (500**X** magnification)

High Load and High Speed

Figures 4.40 and 4.41 show wear track surfaces for pure hexadecane and monoester tests respectively at high load and high speed. Some areas are filled in with wear debris while others are open and sharp grain edges are clearly visible. The rough areas in the monoester wear scar have more fine wear particles than the hexadecane wear scar, making the hexadecane grains clearer.

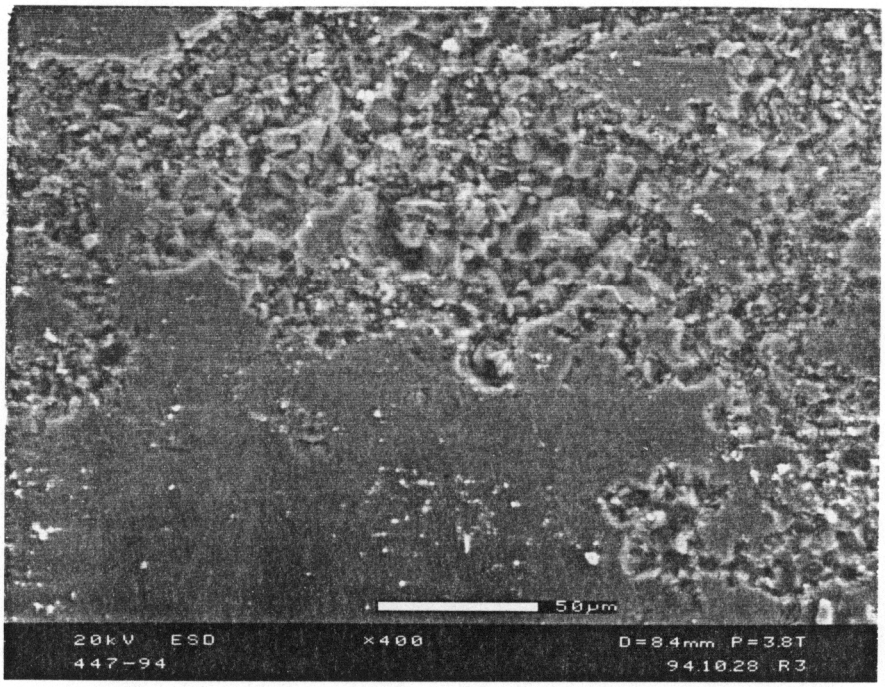

Figure 4.40 ESEM of Hexadecane Lubricated Disk Wear Scar for 160 N Load and 1.0 m/s Sliding Speed.

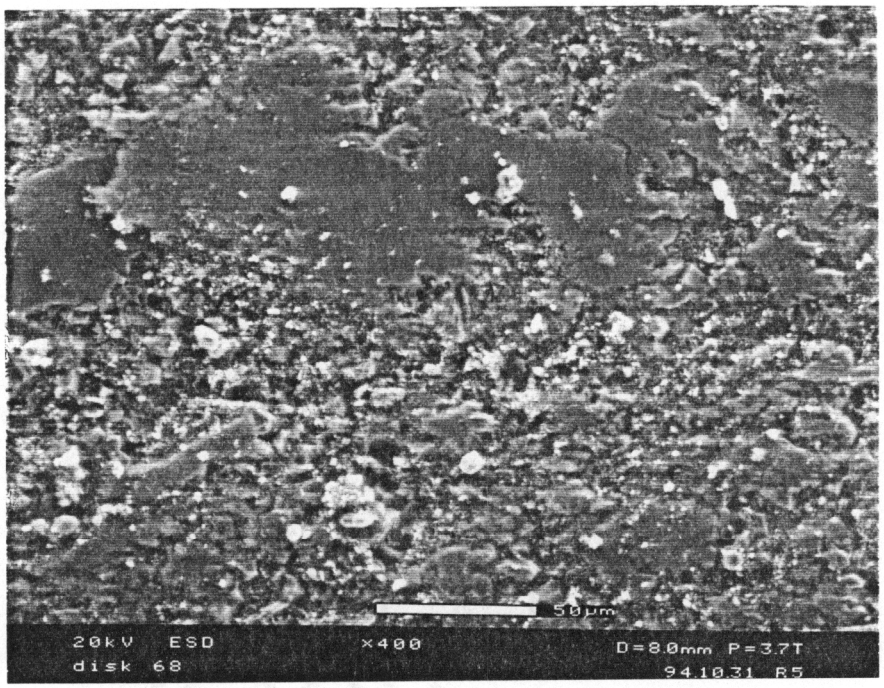

Figure 4.41 ESEM of Monoester Lubricated Disk Wear Scar for 160 N Load and 1.0 m/s Sliding Speed.

The MAMA lubricated disk wear scar surface from the high load and high speed condition is shown in Figure 4.42. The surface is very similar to the pure hexadecane surface of Figure 4.40. Both surfaces have areas of smooth wear debris and sharp alumina grains.

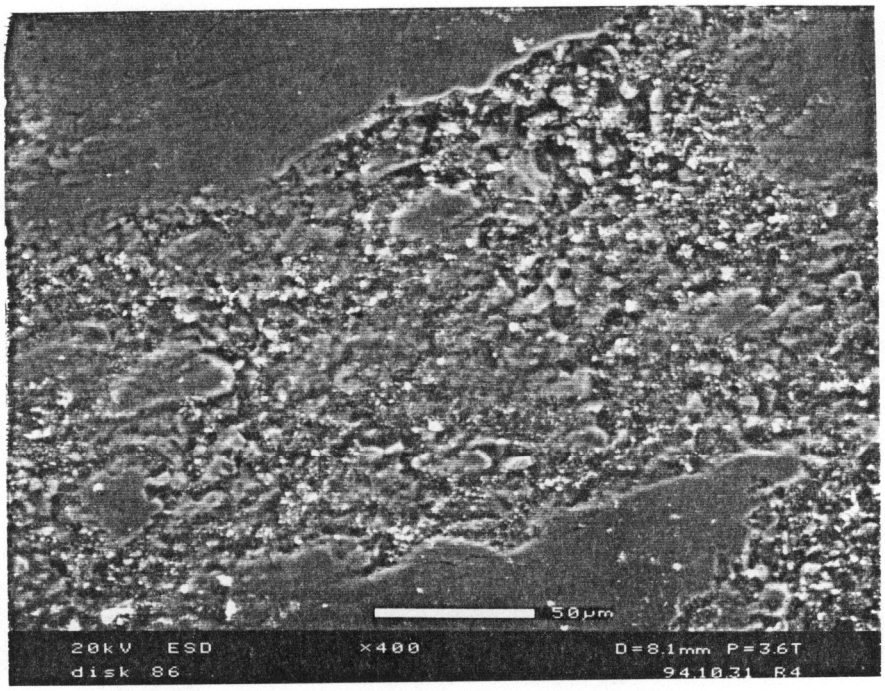

Figure 4.42 ESEM of MAMA Lubricated Disk Wear Scar for 160 N Load and 1.0 m/s Sliding Speed.

4.4 FTIR SPECTRA

After the completion of all testing, films formed during tribological experiments were analyzed using Fourier Transform Infra-Red Spectroscopy (FTIR). Chemical changes that occur during a tribological test may be detected by FTIR spectroscopy. Chemical bonds vibrate at a frequency determined by the mass of the atoms in the bond, the type of bond, and surrounding bonds and atoms. This vibrational frequency can be detected by infrared light. Different bonds have characteristic vibrations given by the wave number (cm^{-1}). Bonds will absorb infrared light at their characteristic frequency, causing a peak in the spectrum corresponding to that bond's natural vibration.

The procedure of FTIR analysis involves first scanning the clean gold mirror in the *scan background mode* to obtain a background signal. An example FTIR scan of the gold background is shown in Figure 4.43.

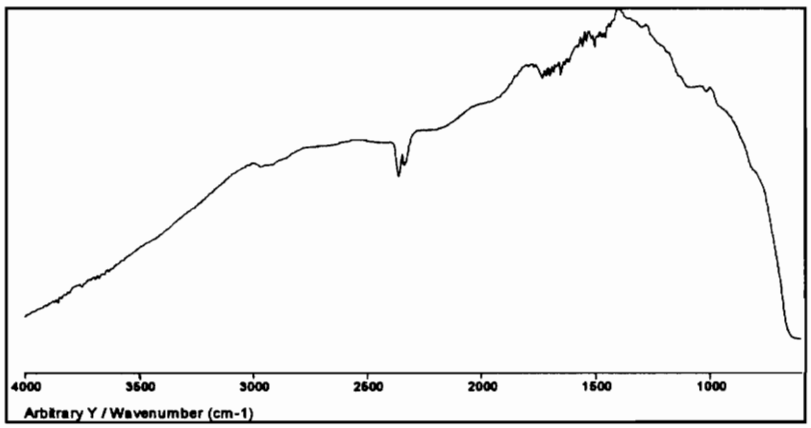

Figure 4.43 FTIR Spectrum of Gold Mirror Background.

Liquids involved in the lubrication (hexadecane) or cleaning (hexane or MEK) process were also analyzed individually. Figures 4.44, 4.45 and 4.46 are FTIR absorbance spectra of the hexadecane, hexane and MEK liquids applied directly to the gold mirror.

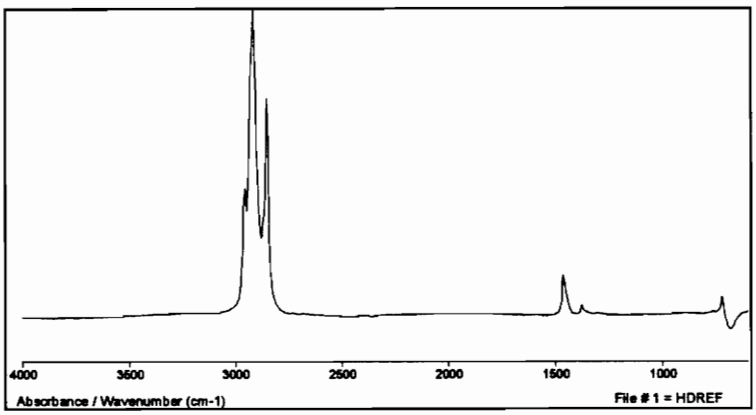

Figure 4.44 FTIR Spectrum of Hexadecane.

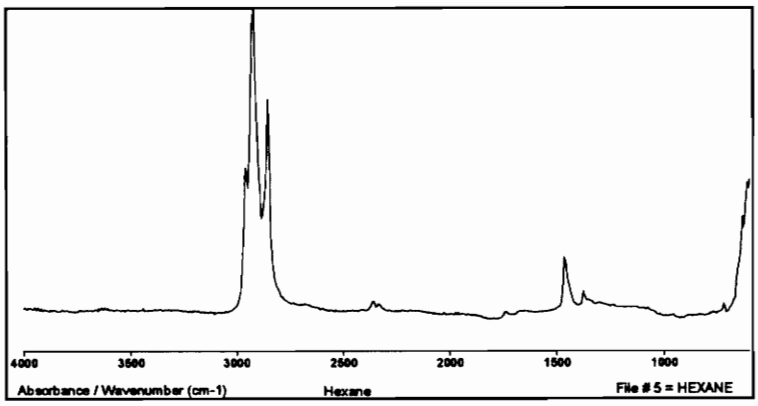

Figure 4.45 FTIR Spectrum of Hexane.

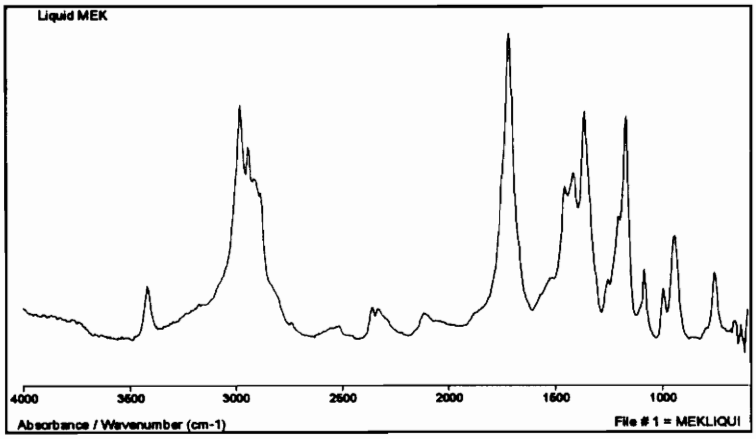

Figure 4.46 FTIR Spectrum of Liquid MEK.

The evaporation of liquid MEK on the mirror surface results in a deposit which is detected by FTIR. Figure 4.47 shows the spectra taken 10 minutes after the liquid MEK was applied to the gold mirror when the MEK was no longer visible. The spectra is significantly different from the liquid MEK spectra in Figure 4.46. A clean gold mirror used in the normal absorbance *sample scan mode* results in a spectra like that of Figure 4.48, which is clean and free of any peaks.

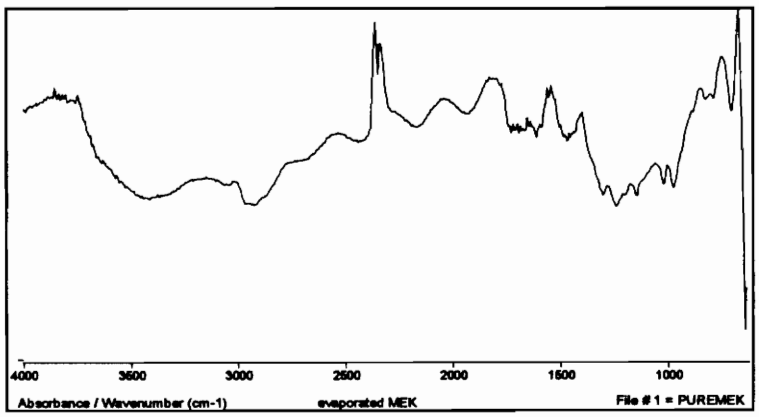

Figure 4.47 FTIR Spectrum of Film from Evaporated MEK.

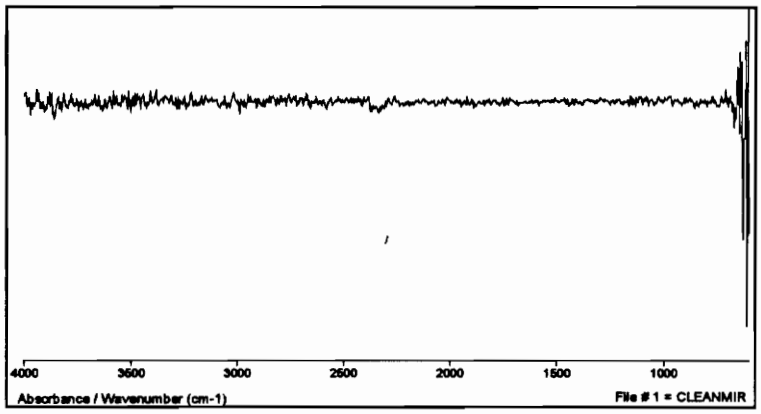

Figure 4.48 FTIR Spectrum of Clean Gold Mirror.

A very thin sample layer is needed in order to analyze monomers and wear products in the FTIR microscope. Pure monomer can be analyzed by putting liquid directly on a gold coated microscope slide. The gold coating is needed to reflect the infrared light back to the infrared detector. Disk specimens cannot be analyzed directly because infrared light does not reflect very well from the alumina surface. Scrapings taken from the disk surface can be analyzed instead. A standard glass microscope slide was used as the scraping instrument to prevent foreign matter from changing the spectra. The clarity and sharpness of the spectrum peaks are very sensitive to the film thickness on the gold slide.

FTIR spectra from disk scrapings were not useful due to weak signals, system noise and alumina particle interference. Another method of film analysis by FTIR was attempted. The organic solvent methyl ethyl ketone (MEK, $CH_3COC_2H_5$, certified grade supplied by Fisher Scientific) was applied to the disk wear track by soaking one face of the disk in about 4 ml of MEK for 15 to 20

minutes. MEK is an organic solvent that should leave only 0.001% residue after evaporation.

Selected disks were treated a second time in MEK, and lightly scraped with a glass slide to help loosen organic matter formed from the monomers and wear particles. The solution was then transferred to a glass vial and gently heated to evaporate the MEK and leave a more concentrated MEK solution. With about 0.5 ml in the vial after evaporation, the mixture was applied to the gold mirrors and allowed to evaporate.

Selected organic--MEK mixtures were also applied to clean glass microscope slides and allowed to evaporate. After a 24 hour vacuum (20 in. Hg) treatment, the films on the glass slide were transferred to the gold mirror surface. This method was chosen to ensure removal of liquids. The films on the gold mirrors were used in reflectance mode FTIR.

Although this treatment is not the same as an analysis of the original wear products, differences in FTIR spectra for monomers under different loads and speeds could be important in the understanding of tribopolymerization and other surface reactions.

Interpretation of FTIR spectra is not complete. Doctors Kajdas and Kempinski from the Warsaw Technology University, Chemical Institute at Plock will help in the continued collection and interpretation of the FTIR spectra from this study. These results will be published in a paper at a later date. Initial spectra are included here with the corresponding reference spectra of pure monomers.

The sample FTIR spectra should be compared to the pure monomer reference spectra to determine differences. Figure 4.49 shows the pure diallyl phthalate reference spectra of liquid diallyl phthalate on a clean gold mirror.

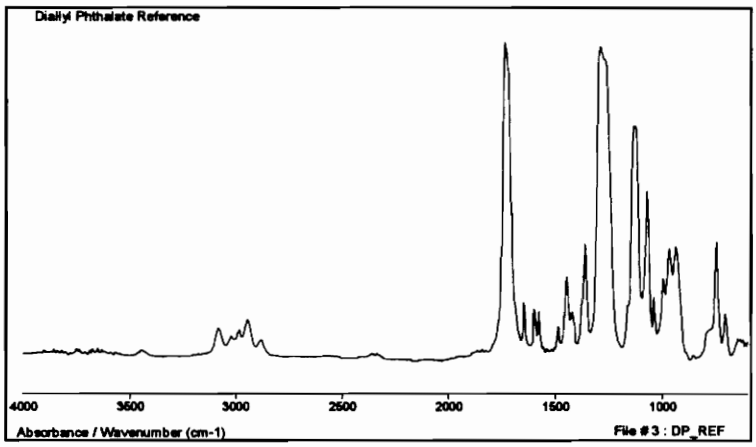

Figure 4.49 FTIR Spectrum of Diallyl Phthalate Reference.

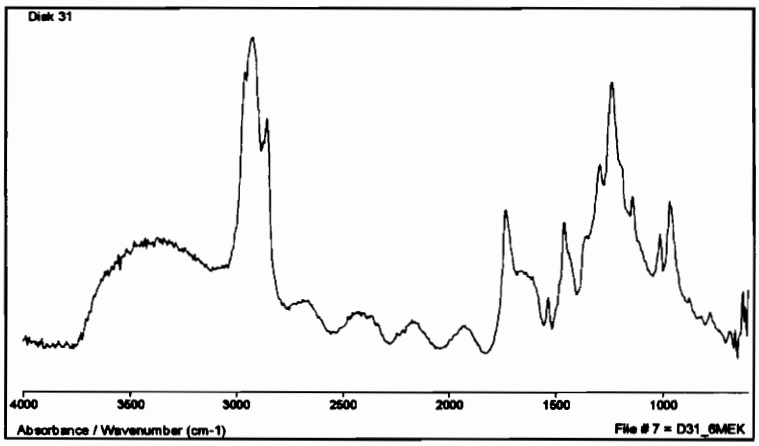

Figure 4.50 FTIR Spectrum of Low Load and Low Speed Diallyl Phthalate Disk.

Spectra from disk specimens (Figure 4.50 and 4.51) are very different from the pure monomer spectra in Figure 4.49 and the MEK film spectra in Figure 4.47. The peaks have not been identified in terms of bond types, but the difference suggests a chemical change may have occurred during the

tribological testing. The test conditions relating to Figures 4.50 and 4.51 resulted in significant alumina wear reductions.

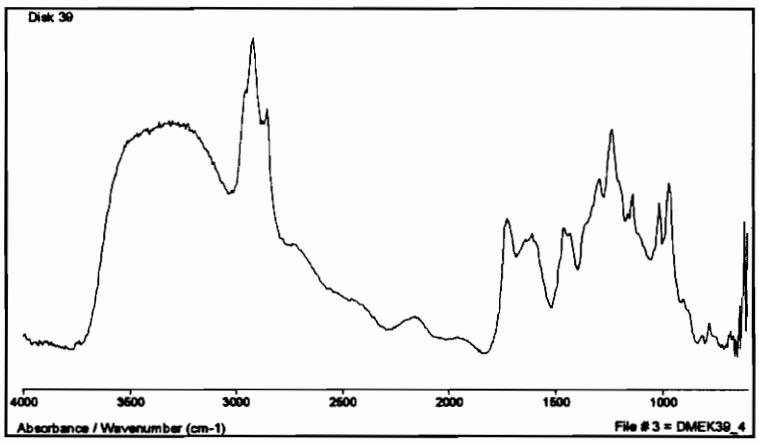

Figure 4.51 FTIR Spectrum of High Load and Low Speed Diallyl Phthalate Disk.

The spectra in Figure 4.52 is from a diallyl phthalate ball, but from a test in which wear was not reduced. The spectra is different from Figures 4.50 and 4.51, suggesting a different type of chemical reaction for different speeds.

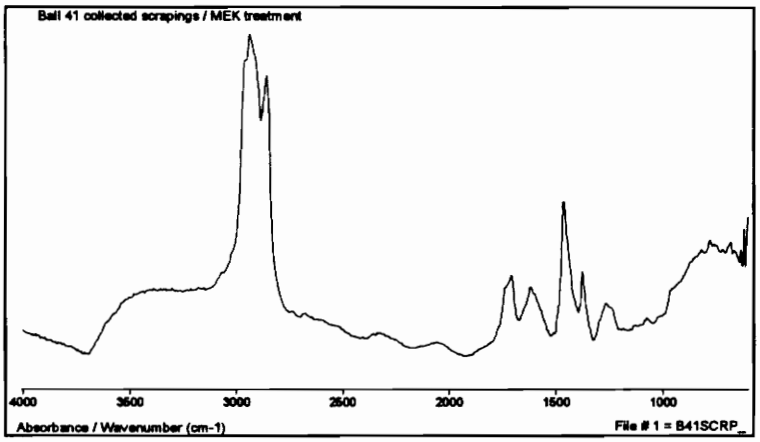

Figure 4.52 FTIR Spectrum of Low Load and High Speed Diallyl Phthalate Ball.

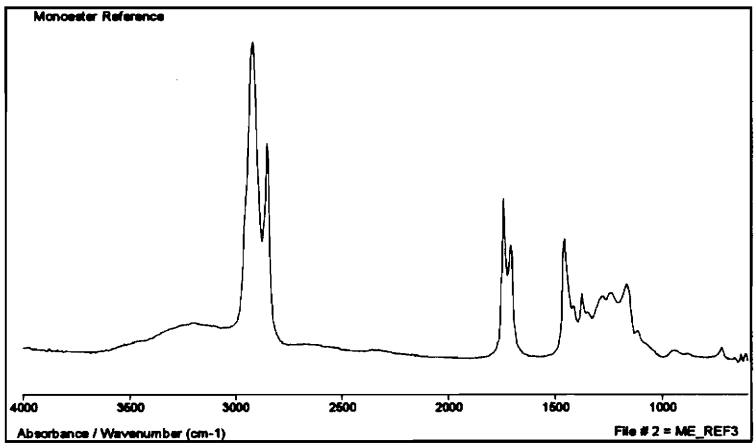

Figure 4.53 FTIR Spectrum of the Monoester Reference.

Figure 4.53 is the reference spectra for the liquid monoester. Evidence of chemical changes can be found by comparing the reference spectra with the spectra in Figure 4.54 and 4.55. Figure 4.54 is from a low load and low speed monoester test with a large wear reduction. The spectra in Figure 4.55 is from a high load and low speed test, in which alumina wear was also greatly reduced.

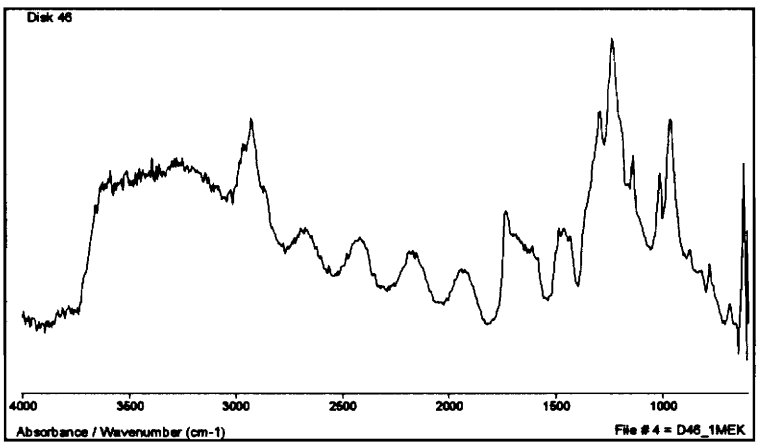

Figure 4.54 FTIR Spectrum of Low Load and Low Speed Monoester Disk.

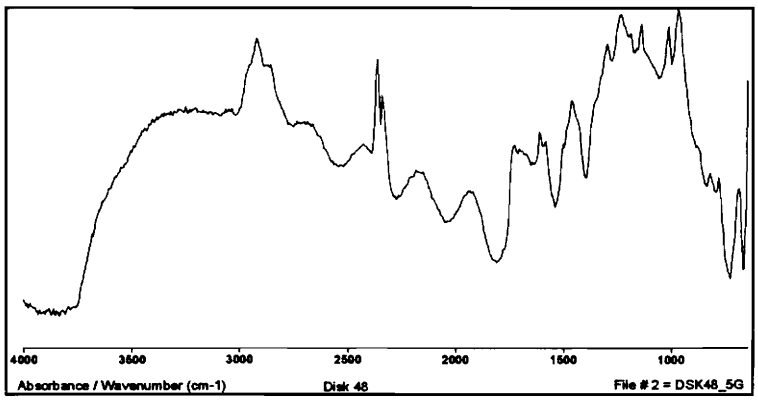

Figure 4.55 FTIR Spectrum of High Load and Low Speed Monoester Disk.

Figure 4.56 shows the reference spectra of the vinyl acetate monomer. A discussion of possible chemical changes follows Figures 4.57 and 4.58, which show spectra from selected tests with vinyl acetate.

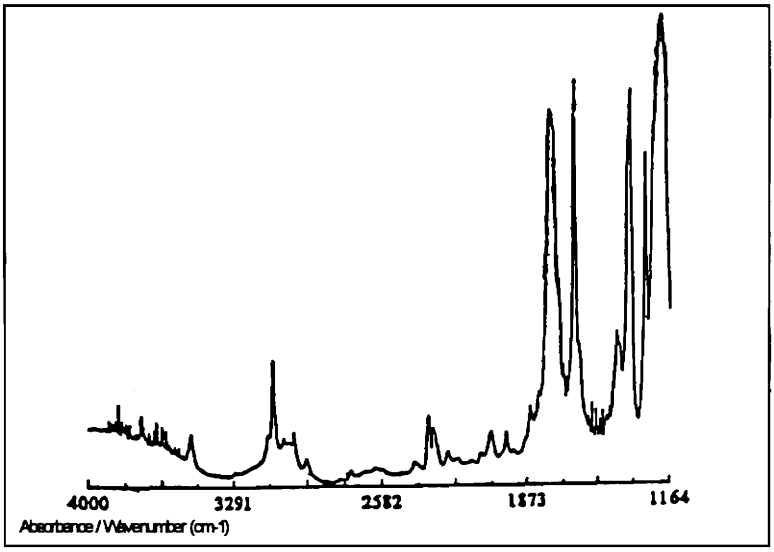

Figure 4.56 FTIR Spectrum of Vinyl Acetate Reference.

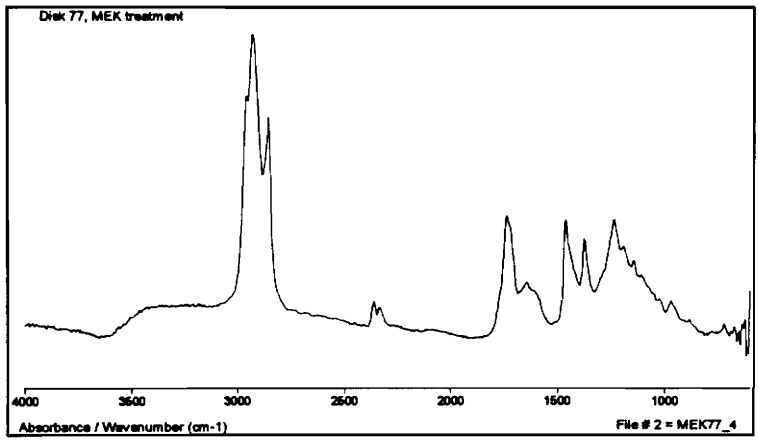

Figure 4.57 FTIR Spectrum of Low Load and Low Speed Vinyl Acetate Disk.

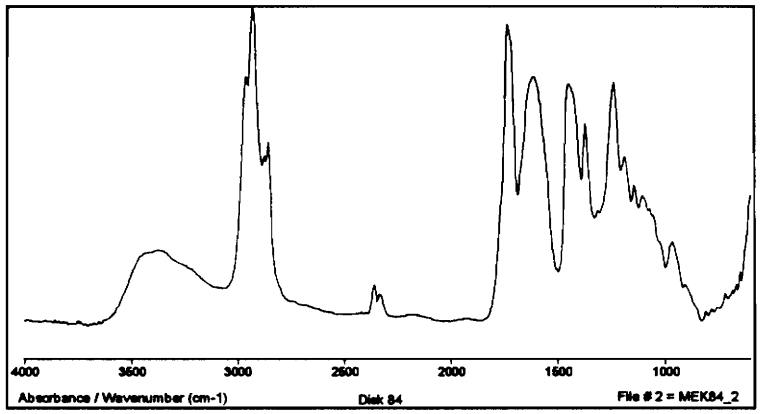

Figure 4.58 FTIR Spectrum of Low Load and High Speed Vinyl Acetate Disk.

The vinyl acetate sample spectra show very strong absorption bands associated with saturated (carbon-carbon single bonds) hydrocarbon stretching (2936 cm^{-1} and 2860 cm^{-1}). In the vinyl acetate standard spectra, the saturated HC adsorption bands (2800 - 2950 cm^{-1}) are very weak compared to the unsaturated bands (3004 - 3102 cm^{-1}). This loss of unsaturated bands in the sample spectra is possible evidence of tribopolymerization by addition polymerization. Evidence of soap formation appears in the carboxylate region (around 1600 cm^{-1}). The peak is wider in this region for the test samples than for the standard.

4.5 TEMPERATURE

4.5.1 Calculated Surface Temperature

Surface temperatures are thought to play an important role in the tribopolymerization process. Relatively low temperatures may not provide enough energy to initiate tribopolymerization for some monomers, while relatively high temperatures could cause breakdown or decomposition of the formed protective tribolayer. The pin-on-disk system generates frictional heat due to the sliding of a loaded ball on the surface of a disk.

Using a Boundary Integral Equation Method (BIEM) FORTRAN program developed by Dr. B. Vick et al [50-52], the temperature rise which occurs at the ball-disk contact area was calculated for all experimental conditions. Results of these calculations can be seen in Figure 4.59 for high speed and high load conditions. Both plastic and elastic areas of contact were assumed for area calculations. Details of all temperature work are included in Appendix C.

The assumed area of contact is based on a singular circular area. The true contact area may be several contact regions separated by a film of lubricant, with the shapes and areas of these regions being unknown. The many possible contact arrangements cause a great deal of uncertainty in heat generation and heat transfer characteristics.

Observed macroscopic wear areas at the end of each test were also used in temperature calculations. Generally, for a given load and speed, a smaller area of contact will result in higher contact temperatures.

CALCULATED TEMPERATURE RISE (KELVIN)
for Alumina-on-Alumina

SLIDING SPEED	LOAD 40 N	LOAD 160 N
0.25 m/s	P: 1526 E: 485	P: 2746 E: 1082
1.0 m/s	P: 4695 E: 1293	P: 7640 E: 2752

Coefficient of Friction = 1.0

P: plastic area E: elastic area

Figure 4.59 Calculated Temperature Rise For Elastic and Plastic Contact Areas.

Another source of uncertainty is the coefficient of friction. The previous calculations of surface temperature rise are made with an assumed value of μ = 1.0. Any actual temperature rises must be further calculated by multiplying an actual μ value by the program output of temperature rise. Previous tests of alumina on alumina with hexadecane at 0.25 m/s and 20 N load indicate μ = 0.1 [48]. For comparing frictional heat generation and temperature rises, a μ value of 0.1 will be assumed.

4.5.2 Measured Ball, Disk and Lubricant Temperatures

The bulk lubricant, disk or ball temperatures may also affect the tribopolymerization process. Temperature measurements taken at the end of each test of the disk surface, ball surface and bulk lubricant (see Appendix C) showed a definite dependence on monomer, load and speed. For the same load, speed and monomer, the measured bulk temperature rise for each experiment was found to be consistent.

A connection between measured bulk temperatures and calculated surface temperatures was not found. Appendix C shows the results of surface temperature calculations based on the macroscopic (apparent) area of contact at the end of a test. Calculated surface temperatures were higher for smaller areas of contact. However the measured bulk temperatures were generally lower for smaller areas of contact.

Measured bulk temperatures and frictional energy generation can be related. Calculations of frictional energy are shown in Figure 4.60 for all load and speed conditions, assuming μ=0.1. The current frictional heat generation values are greater than or equal to frictional heat in previous testing by Tripathy [48] and Smith [46], which resulted in 0.5 Watts and 1 Watt respectively.

The measured temperatures in Figure 4.61 show partial agreement in terms of relative increases between conditions. For example, the factor of 4 increase in energy from low load - low speed to both a) low load - high speed and b) high load - low speed, is evident in the corresponding measured temperature rises. Both the 27 °C and 29 °C temperature rises are almost four times the 8 °C temperature rise. However the high load - high speed temperature is not 16 times greater than the low load - low speed temperature.

Frictional Energy (Watts)

SLIDING SPEED	LOAD 40 N	LOAD 160 N
0.25 m/s	1	4
1.0 m/s	4	16

Figure 4.60 Frictional Energy (Watts) for the Four Load-Speed Conditions Assuming $\mu = 0.1$.

MEASURED TEMPERATURE RISE OF DISK SURFACE FOR ALUMINA-ON-ALUMINA

SLIDING SPEED	LOAD 40 N	LOAD 160 N
0.25 m/s	8 ° C	29 ° C
1.0 m/s	27 ° C	50 ° C

Temperature measurements made with type-K thermocouple immediately following test completion.

Figure 4.61 Measured Disk Temperature Rise upon Test Completion.

CHAPTER 5

DISCUSSION

5.1 WEAR OVERVIEW

The most significant and surprising result of this study is the difference in wear reduction effectiveness depending on sliding speed. Monomers were very effective in reducing wear at low speeds, for either load, and totally ineffective at high speeds, for either load. In fact, at the 1.0 m/s sliding speed, wear sometimes increased compared to the carrier fluid wear. Figure 5.1 summarizes the total wear volumes for all monomers, loads and speeds. (Note that the y-axis is scaled differently for each graph.)

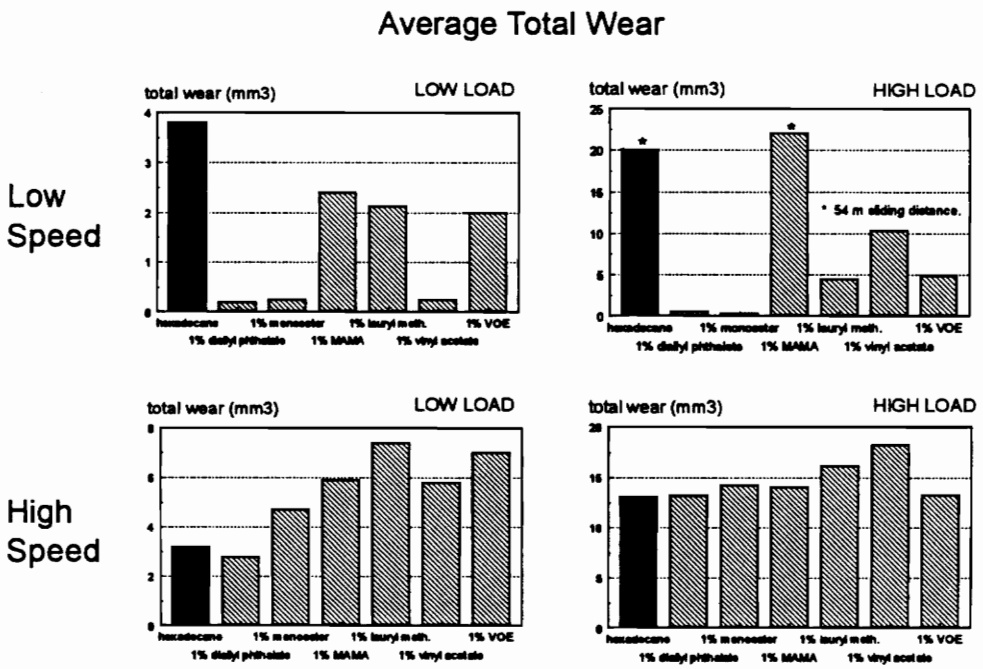

Figure 5.1 Total Wear Volume for all Monomers, Loads and Speeds.

Monomer effectiveness is discussed in terms of percentage wear reduction. Higher effectiveness refers to a larger wear reduction. Pure hexadecane (the carrier fluid) lubrication was used as the baseline for comparison of wear volumes. Of the six monomers tested, the condensation monomer (monoester) and 4 of the 5 addition monomers proved to be effective in reducing wear at the low speed operating conditions. The monomers were not effective in reducing wear at high speed conditions. Depending on the monomer and load, wear increased at high speeds compared to pure hexadecane lubrication. A summary of wear effectiveness is given in Table 5.1.

Table 5.1 Percent Total Wear Reduction for all Monomers, Loads and Speeds.

Percent Wear Reduction by Monomer

	LOAD / SPEED			
	Low / Low	**Low / High**	**High / Low**	**High / High**
Diallyl Phthalate	95	13	97	0
Monoester	93	-47	98	-8
Methyl 2-Acrylamido-2-Methoxy Acetate	37	-84	-10	-6
Lauryl Methacrylate	44	-131	78	-22
Vinyl Acetate	93	-81	49	-38
Vinyl Octadecyl Ether	48	-118	76	-1

$$\text{percent wear reduction} = \frac{\text{hexadecane wear volume} - \text{monomer wear volume}}{\text{hexadecane wear volume}} \times 100\ \%$$

Note that diallyl phthalate and the monoester are the only two monomers to have striking (greater than 90 %) wear reductions at both loads, for the lower

sliding speed. Although they polymerize by very different mechanisms, only these monomers have two functional groups per molecule. The other monomers have only one functional group per molecule. As a reminder, a functional group is the part of the compound where chemical reactions can occur during polymerization, or in this case, tribopolymerization.

Cross-sectional views of the wear scars of two disks are included as an example of the tremendous wear reduction that occurs at low speeds. One disk is from a hexadecane lubricated test and the other from an effective monoester test.

Figure 5.2 shows the profilometer trace of a hexadecane lubricated wear scar for the low load and low speed condition. Each small block on the trace is 2 mm high and 5 mm wide. The scale is a 500**X** vertical magnification and a 100**X** horizontal magnification. The addition of 1.0 wt. % monoester results in a wear scar trace like that of Figure 5.3.

Note that the two figures are not shown at the same relative scale, the pure hexadecane wear scar is a much wider wear scar. Both horizontal scales are 100**X** magnification. However the monoester vertical magnification is increased to 5000**X** due to the reduction in the depth of the wear scar. Also note the relatively smooth surface of the monoester wear scar compared to the hexadecane wear scar and to the unworn alumina surface beside the wear scar. The natural valleys in the alumina surface have been filled in, supporting the idea of a protective wear debris layer which forms during tribopolymerization. All wear effective monomers resulted in smooth wear scar surfaces for low speed conditions. The monoester wear scar shown here exemplifies the profile of an effective monomer.

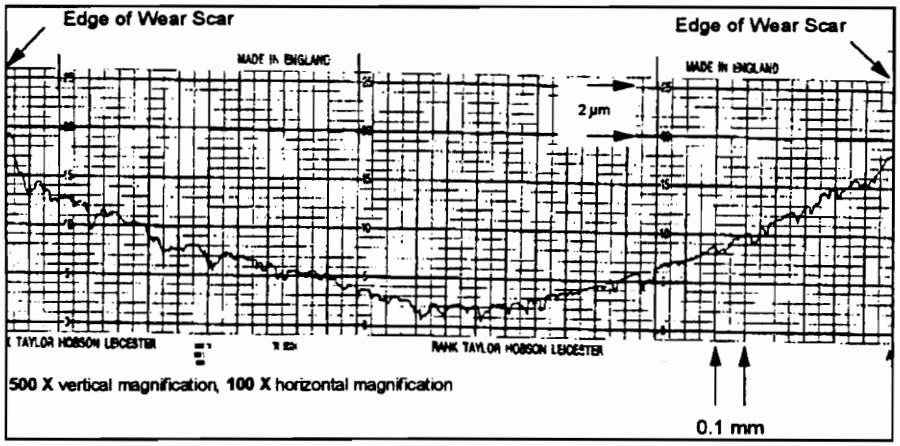

Figure 5.2 Profilometer Trace of Pure Hexadecane Wear Scar for 40 N Load and 0.25 m/s Sliding Speed. (500X vertical magnification)

In general, profilometer traces of disk wear scars show little build up on the edge of wear scars. The main wear mode is believed to be material removal, with little plowing or deformation occurring.

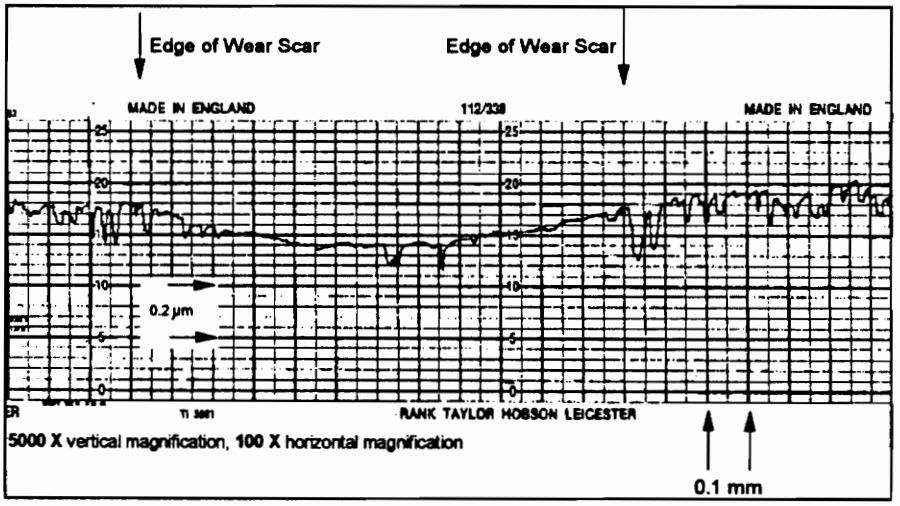

Figure 5.3 Profilometer Trace of 1.0 wt. % Monoester in Hexadecane at 40 N Load and 0.25 m/s Sliding Speed. (5000X vertical magnification)

The disk wear scar profiles appear to be concave in shape. However, ball wear is calculated assuming a flat ball wear scar. The profilometer traces in Figures 5.2 and 5.3 are shown at high vertical magnifications, compared to horizontal magnification. The image from this higher vertical magnification is misleading. The error in assuming 'flat' ball wear scars is considered to be insignificant. Most profilometer traces of disk wear scars were flat in the middle and curved mainly at the edges. Visual inspection of balls at magnifications from 16**X** to 80**X** yielded no indication of curvature.

An increase in speed tends to decrease wear with pure hexadecane lubrication. The ability to run a complete test (250 m sliding distance) at 160 N and 1.0 m/s, compared to the inability to complete a test at 160 N and 0.25 m/s is an important wear characteristic of this tribological system. The reasons for the decrease in wear at the higher speed are unknown. Possible explanations for the speed effect will be explored later.

For pure hexadecane, the change in speed at the 40 N low load does not have a statistically significant effect on wear. Total wear volumes were 3.8 and 3.2 mm^3 for 0.25 and 1.0 m/s respectively, at the 40 N load with pure hexadecane.

The relationship of current test results to previous testing by Tripathy [48] using the same monomer and alumina specimens is interesting. A summary of percent wear reductions for all monomers at 4 different loads and 0.25 m/s speed is given in Table 5.2. The wear reduction effectiveness of diallyl phthalate and the monoester increase as load is increased.

Tripathy showed MAMA to be effective (56 % ball wear reduction) in reducing wear at 20 N load and 0.25 m/s. In this testing, a marginal reduction in

wear occurred at 40 N and 0.25 m/s sliding speed. However at the 160 N load and 0.25 m/s sliding speed, no reduction in wear occurred. Wear effectiveness decreases as the normal load is increased for MAMA at 0.25 m/s sliding speed.

Table 5.2 Percent Total Wear Reductions at 0.25 m/s Sliding Speed.

	Previous Research [48]		Current Research	
Monomer	**5 N**	**20 N**	**40 N**	**160 N[1]**
Diallyl Phthalate	36	70	95	97
Monoester	10	47	93	98
MAMA	92	60	37	0[2]
Lauryl Methacrylate	3	61	44	78
Vinyl Acetate	0[2]	54	93	49
Vinyl Octadecyl Ether	4	11	48	76

[1] compared to incomplete hexadecane test
2 wear actually increased

A linear relationship between wear and load does not appear exist for lauryl methacrylate. Vinyl acetate appears to reach a maximum effectiveness between 20 N load and 160 N load.

Wear results with vinyl octadecyl ether are also interesting to compare with previous testing by Smith [46] and Tripathy [48]. The wear reduction effectiveness of vinyl octadecyl ether increases as the normal load is increased. For the vapor phase tests, with 5 N load and 0.25 m/s sliding speed by Smith, the average total wear was reduced by up to 92 % compared to dry nitrogen testing. In the case of vapor phase testing, the severe environment of higher friction and higher ambient temperature may compensate for the lower normal load. Perhaps the tribopolymerization mechanism for vinyl octadecyl ether is

initiated and proceeds more efficiently under more severe conditions of load or temperature.

5.2 PHOTOMACROGRAPHS

Although photomacrographs were not included for every monomer at all loads and speeds, the selected pictures represent the various surface features visible at 16.25**X** magnification. The difference in worn and unworn surfaces is apparent for all loads and speeds.

The appearance of hexadecane lubricated disk surfaces varies according to load and speed conditions. Unlike the powdery wear particles of low load and low speed conditions, the high load and low speed conditions result in severe surface marking, reflective areas and powdery wear particles.

At high speeds and high loads, the alumina wear track surfaces are very similar for all monomers and the carrier fluid. The mirror-like patches on the high load and high speed disk could have resulted from surface melting due to the high temperatures produced from frictional heat generation. The high load and high speed condition resulted in a wear track with two general surface features. Smooth patches, possibly due to localized surface melting under high frictional energy generation, and more powdery areas of wear were both visible.

5.3 ESEM OBSERVATIONS

The ESEM pictures suggest a trend concerning the wear debris layer and wear reduction effectiveness. The disk wear scars of all monomers (and pure hexadecane) were found to have varying degrees of a compacted wear debris layer. The area covered with a debris layer roughly indicated the wear effectiveness of the monomer. For example, the monoester wear scar at 40 N

load and 0.25 m/s sliding speed has a very smooth wear debris layer with few craters visible. A less effective monomer, e.g., vinyl octadecyl ether, disk scar also has a wear debris layer, but with more craters visible compared to the monoester surface. The least wear effective lubricants, pure hexadecane and MAMA, had only small areas of the compacted wear debris layer. This observation is in agreement with Tripathy's study of surface films by SEM examination [48,49].

The craters and pits that are visible in the monoester surface could be caused by large flakes of the wear debris layer that are worn away at times and gradually filled in with new wear debris. ESEM photographs of wear particles from monoester lubricated disks show a flake-like shape. Microcracks may propagate under repeated stressing, resulting in the formation of small flake-like particles. Similar wear characteristics were reported by Smith [46]. The cyclic stressing could result from both normal load and adhesion forces between ball and disk surfaces.

5.4 FTIR OBSERVATIONS

Several FTIRM observations deserve attention. The analysis of diallyl phthalate, monoester and vinyl acetate wear scars resulted in spectra that were different from the spectra of the film from evaporated MEK. Therefore organic matter from the disk surface is being analyzed. Also, the disk wear spectra is different from the reference spectra of the pure monomers, suggesting a chemical change due to some type of reaction. This reaction could be a reaction with the surface or the tribopolymerization reaction. Finally, the difference in diallyl phthalate spectra between an effective wear reduction test and an ineffective wear reduction test suggests that different chemical bonding is

present, dependent on sliding speed. Different sliding speeds may cause different film formations.

5.5 SPEED EFFECTS

What changes occur at high speeds that prevent monomers from decreasing wear? Each of the following sections address a factor which could play a part in the wear reduction effectiveness of monomers. The relationship between the individual factor and speed is discussed with regard to expected results and actual results.

Surface Temperature

Surface temperature could be an initiating factor for tribopolymerization. The expected wear reduction effectiveness of monomers should increase at higher temperatures, if higher temperatures initiate tribopolymerization [41]. The surface temperatures vary according to load, speed and coefficient of friction. Temperatures may increase to a point where the tribopolymerization layer decomposes or breaks down due to the thermal effects.

Higher speeds or higher loads should increase temperature, for the same coefficient of friction. The low load and low speed should produce the lowest surface temperatures while the high load and high speed should produce the highest temperatures. Based on plastic and elastic areas of contact, the calculated temperature at the ball-disk contact is higher for the 40 N load and 1.0 m/s speed condition than for the 160 N load and 0.25 m/s speed condition (see Appendix C). Figure 5.4 gives a graphic view of the possible effect of surface temperature on wear. This graph is loosely based on monoester wear volumes and calculated temperature rises for each of the load and speed combinations (assuming $\mu = 1.0$ and an elastic area of contact).

Each region (I, II, III, IV) represents one of the load-speed combinations. The range of effective tribopolymerization is limited to regions I and II, the lower surface temperature rise regimes. When the surface temperature rises are higher (III and IV), monomers may not be effective in reducing wear.

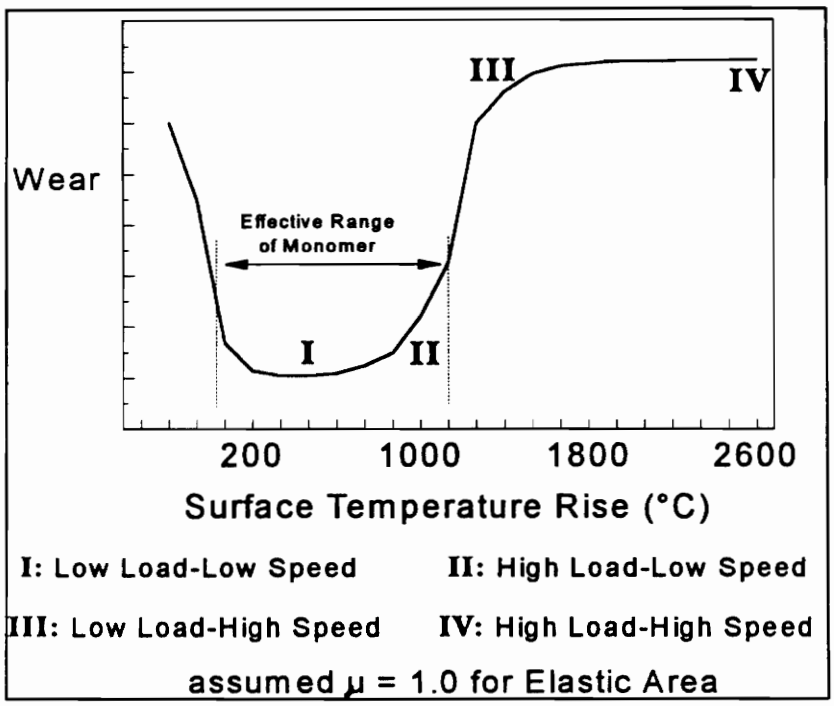

Figure 5.4 Possible Relationship between Wear Volume and Surface Temperature Rise.

This graph supports the idea that contact temperatures may be high enough to break down the formed tribolayer. Exact reasons for possible failure of the tribofilm at higher temperatures are not known. Possibilities include thermal decomposition of chemical bonds in the formed surface layer, high temperature corrosion of formed layers, or the total lack of film formation at high temperatures.

Evidence of higher surface temperatures at the high load and high speed condition is seen in 1) the measured bulk temperatures and 2) the mirror-like patches on the disk wear scar, possibly from localized melting of the alumina surface due to frictional heat.

A limiting factor in the theoretical temperature approach is the unknown and constantly changing contact area. As the test proceeds, the area of contact increases and the contact temperature decreases, if all other factors are equal.

Lubrication Transition

The increase in sliding speed from 0.25 m/s to 1.0 m/s may cause a transition from boundary lubrication to EHD (elastohydrodynamic) or partial EHD lubrication. The monomers are designed to function in the boundary lubrication regime. Perhaps a very thin separation film, a partial EHD condition, exists. Calculations of minimum oil film thickness are given in Appendix G. For pure hexadecane tests, the 1.0 m/s speed total wear volumes are lower than the 0.25 m/s speed total wear volumes, for either load (see Appendix B). The transition to total EHD is not likely as alumina wear still occurs at the high speed and higher loads still increase wear. A transition to the partial EHD condition is possible.

Exoelectron Emission

Exoelectron emission may also play an important part in initiating tribopolymerization [47]. Higher speeds and higher loads are likely to increase the rate of exoelectron emission. If exoelectron emission increases as temperature, load or speed increases, then the effectiveness of tribopolymerization should also increase. On the basis of this idea, the high load and high speed condition should be the most effective regime for wear

reduction, but it is clearly not so. Without knowing the actual change in exoelectron emission due to changes in load or speed, it is difficult to explain wear effectiveness in terms of exoelectron emission.

Pressure

Pressure at the disk-ball interface may also be an important factor in tribopolymerization. Higher pressure may increase the chance of successful tribopolymerization by influencing chemical reactions and kinetics. The theory does not support the wear data since pressure depends on normal load and the general effectiveness of monomers is dependent on speed.

Third Body Abrasion

Suspended wear particles in the lubricant fluid may act as third body abrasion particles. The higher speed would give better mixing and higher momentum to the particles causing higher abrasive wear, compared to the low speed tests. High speed tests resulted in a milky colored lubricant mixture after test completion, suggesting that more wear debris was mixed and suspended in the hexadecane solution. Third body abrasion could increase wear at the higher speed.

Mechanical Effects

The possibility of impact forces due to an imbalance in the shaft rotation or misalignment of the disk surface relative to the plane of rotation has been considered. If a rotational imbalance existed, higher speeds could increase the impact forces, causing an increase in wear. In setting up the pin-on-disk system, the surface of the disk backing piece was remachined to ensure a 90 ° angle between disk face and the rotating shaft. The fluctuation in measured normal

force was found to be very small during testing, as shown in Appendix F. The possibility of rotational imbalance is therefore ruled out as a speed factor.

Kinetics of Film Formation and Removal

High contact speeds may keep alumina wear particles from settling long enough in the wear track to react tribologically with the monomer and the ceramic surface in the formation of a protective tribolayer. The high speed tests did result in a milky colored lubricant mixture due to suspended wear debris.

Higher velocities decrease the time between ball contacts, for a given location on the disk surface. An increase by four in the sliding speed causes the time between ball contacts to decrease by a factor of four. Perhaps this shorter time is not long enough for successful wear reduction; tribopolymerization or other surface reactions cannot keep up with the wear process.

Tribochemical Reactions

Differences between high speed and low speed wear results could be caused by different reactions that occur with the contacting surfaces, wear debris particles and monomers. At the 1.0 m/s sliding speed, polymer film formation could be prevented, excessive alumina soaps could form or new reactions may be introduced which prevent wear reduction. The soap formation or new reactions could introduce a corrosive environment responsible for the *higher* levels of wear for monomers at the 1.0 m/s sliding speed. Because FTIR spectra show differences between the speeds for a given monomer, e.g., diallyl phthalate, evidence of different films is present. Different films indicate that different tribochemical reactions could be occurring depending on sliding speed.

5.6 SUMMARY

At the low sliding speed (0.25 m/s), monomers were effective in reducing alumina wear while the high speed (1.0 m/s) condition resulted in no change or an increase in wear. Support for tribopolymerization is found at the low speed condition by wear volume analysis and ESEM analysis. The wear debris layer is more consistent in appearance and is believed to be more firmly attached for wear reduction effective monomers. This wear debris layer may be the result of chemical bonds with the surface and/or bonds between wear particles and monomers. Although FTIRM did not prove that tribopolymerization had occurred, no evidence was found to disprove the mechanism at low speeds. A strong argument exists for different film formation processes under different speeds. The films formed at low speed are effective in reducing alumina wear while films formed at high speeds are ineffective.

Although each of the preceding theories on the interaction of speed and wear was examined individually, the effect of high speed on wear reduction is likely not due to one factor. The factors with the strongest arguments for the ineffectiveness of monomers at high speed are: transition of lubrication regime (boundary lubrication to partial EHD) at the high speed, higher surface temperatures at the high speed, and tribochemical reactions that are dependent on sliding speed.

CHAPTER 6

CONCLUSIONS

1) A designed experiment on the tribopolymerization mechanism was performed at loads and speeds higher than previously tested. The effects on alumina wear of load and speed variation was tested for six potential polymer forming compounds (monomers).

2) C_{36} dimer acid/ethylene glycol monoester, diallyl phthalate, lauryl methacrylate, vinyl acetate and vinyl octadecyl ether were effective in reducing alumina wear at 0.25 m/s sliding speed for both the 40 N and 160 N load.

3) At 1.0 m/s sliding speed and 40 N load, monomers either increased or had no effect on alumina wear.

4) Monomers effective in reducing wear at 40 N were also effective in reducing wear at 160 N.

5) At the 40 N low load and the 0.25 m/s low speed, diallyl phthalate, the monoester and vinyl acetate resulted in large reductions in wear (greater than 90 %). Lauryl methacrylate and vinyl octadecyl ether resulted in marginal reductions in wear (40 to 50 %). MAMA caused a marginal reduction (46 %) in disk wear but an insignificant reduction (18 %) in ball wear.

6) At the 160 N high load and the 0.25 m/s low speed, the 1 wt. % mixtures of diallyl phthalate and monoester resulted in large wear reductions (greater than 97 %). Lauryl methacrylate and vinyl octadecyl ether were also very effective in reducing wear (at least 73 to 83 %). Vinyl Acetate was only marginally effective in reducing wear (at least 50 %). MAMA had no effect on wear.

7) Vinyl octadecyl ether and lauryl methacrylate were more effective in reducing wear at the high load (160 N) than at the low load (40 N) condition, for the 0.25 m/s sliding speed.

8) Vinyl acetate and MAMA were more effective in reducing wear at the low load (40 N) than at the high load (160 N) condition, for the 0.25 m/s siding speed.

9) ESEM surface studies show a more consistent and compacted wear debris layer on the alumina surface corresponds to a higher level of wear reduction effectiveness, for the low speed disk specimens.

10) FTIRM analysis of disk surfaces supports the idea that different speeds result in the formation of different surface films, for the same monomer and normal load.

11) The 160 N load and 1.0 m/s sliding speed is a limiting test condition for the current alumina specimens due to disk cracking.

CHAPTER 7

RECOMMENDATIONS

SLIDING SPEED

In order to understand the effect of speed on alumina wear, experiments should be performed at a controlled (160 N) load while varying the sliding speed. Start tests at 0.15 m/s and increase by 0.1 m/s up to 0.95 m/s. Pure hexadecane lubricant tests should be completed first, followed by tests with selected monomers. The objective of these experiments should be to understand the kinetics of film formation and film removal as related to sliding speed. Also the lubrication regime (boundary lubrication, partial EHD or EHD) should be determined.

TEMPERATURE

Surface temperature is considered to have an important effect on wear reduction effectiveness. The high speed and high load tests performed in this study extended the range of frictional heat generation studied under lubricated conditions. However more information is needed on how surface temperature affects the tribochemical processes. Does surface temperature control the formation and breakdown of surface layers?

MONOMERS

The use of other monomers which may polymerize at higher temperatures or have a wider temperature range for effective wear reduction should be explored. Monomers soluble in carrier fluids other than hexadecane should also

be considered. The use of another carrier fluid will determine if hexadecane reacts with alumina to form soaps that increase wear at high speeds. Other possible monomers are those which form polymers with high temperature stability.

LOAD

Further tests should be performed to determine the effect of load on wear because the wear effectiveness of lauryl methacrylate and vinyl octadecyl ether increased with higher loads. For lauryl methacrylate and vinyl octadecyl ether, determine the optimum load for effective wear reduction by varying the load with a constant 0.25 m/s sliding speed.

MOLECULAR ARRANGEMENT

The 3-D molecular arrangement of MAMA, vinyl acetate, vinyl octadecyl ether and lauryl methacrylate should be examined with regard to how changes in normal load may inhibit or induce chemical reactions with the surface, wear particles and other monomer molecules. Wear reduction effectiveness of MAMA and vinyl acetate decreased as load increased, while the effectiveness of vinyl octadecyl ether and lauryl methacrylate increased as the load increased. Molecular computer modeling by Tripathy [48] showed that vinyl octadecyl ether and lauryl methacrylate are relatively simple and linear arrangements of atoms, while the atoms of MAMA and vinyl acetate are in a compact arrangement without long chains.

PIN-ON-DISK MACHINE

Research on tribopolymerization would benefit greatly by a new pin-on-disk testing device. The loading system used in this research proved to be very effective at the high loads and high speeds. A smaller milling machine or a new

method of providing rotation would be acceptable. The design should include vapor phase capability, atmospheric control and a heated chamber. A torque transducer should be included in order to determine the friction force. Actual wear rates could be measured by including a Linear Voltage Differential Transformer (LVDT) attached to the linear motion ball spline. If LVDT and torque transducers are used, the real time data acquisition of sensor voltages should be recorded using an A-D computer acquisition system.

BALL HOLDER

The ball holder design needs improvement. Tests that failed due to ball rolling were a major waste of time and materials. The current design is difficult to machine and may allow ball rolling if not tightened properly.

Instead of the screw-on ball holder described by Smith [46], a gripping device similar to a pin-vise finger chuck should be explored. Figure 6.1 shows a schematic of the proposed ball holding device. As the outer ball holder is screwed on the threaded rod, the tapered inner diameter squeezes the 4 prong chuck together, providing a griping force on the ball. A support underneath the ball to counter the normal force is also recommended but not shown in the schematic.

LUBRICANT

At high speeds, the steady state distribution of liquid is questionable. The centrifugal force of the spinning disk may cause lubricant starvation conditions at the ball - disk contact area. If a design change could recirculate or alter the lubricant location, the lubricant condition at the contact area could be ensured.

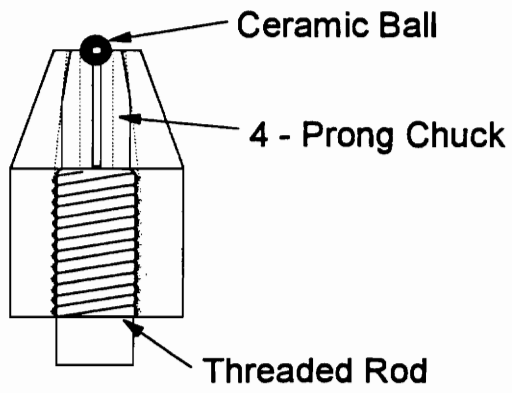

Figure 7.1 Schematic Diagram of Recommended Ball Holder.

EXOELECTRON EMISSION

The effects of exoelectron emission should be explored by conducting tests that measure the change in exoelectron emission for alumina on alumina sliding as load and sliding velocity change.

FTIRM

Examination of surface layers on wear scars should continue with the use of Fourier Transform Infrared Microspectroscopy (FTIRM).

REFERENCES

1. M. J. Furey and C. Kajdas, "Tribopolymerization as a Novel Approach to Ceramic Lubrication," *Proc. of the 4th Int'l Symp. on Ceramic Materials and Components for Engines*, R. Carlsson, T Johansson and L. Kahlman, eds., Elsevier Applied Science, London, pp. 1211-1218 (1992).

2. R. N. Katz, "Opportunities and Prospects for the Application of Structural Ceramics," Structural Ceramics, *Treatise on Materials Science and Technology*, Vol. **29**, J. B. Watchman, Jr., ed., Academic Press Inc., Boston, pp. 1-26 (1989).

3. M. J. Furey, "The Formation of Polymeric Films Directly on Rubbing Surfaces to Reduce Wear", *Wear*, **26,** pp. 369-392 (1973).

4. M. J. Furey and C. Kajdas, "Models of Tribopolymerization as an Anti-Wear Mechanism," *Proc. of the Japan Int'l Tribology Conf.*, Nagoya, Oct. 29 - Nov. 1, **II**, pp. 1089-1094 (1990).

5. K. Kato, "Tribology of Ceramics," *Wear,* **136**, pp. 117-133, (1990).

6. P. Studt, "Influence of Lubricating Oil Additives on Friction of Ceramics under Conditions of Boundary Lubrication," *Wear*, **115**, pp. 185-191 (1987).

7. S. Sasaki, "The Effect of Surrounding Atmosphere on the Friction and Wear of Alumina, Zirconia, Silicon Carbide, and Silicon Nitride," Wear of Materials 1989, K. C. Ludema, ed., ASME, New York (1989) pp 409-417; Wear, 134, pp. 185-200 (1989).

8. Y. Tsunai and Y. Enomoto, "Tribochemistry of Silicon Based Ceramics in Alcohols," Proc. 8th Int'l Symp. on Alcohol Fuels, Tokyo pp. 715-721 (1988).

9. S. Jahanmir and T. E. Fischer, "Friction and Wear of Silicon Nitride Lubricated by Humid Air, Water, Hexadecane and Hexadecane + 0.5 Percent Stearic Acid," Tribology Trans., 31, pp. 32-43 (1988).

10. T. E. Fischer, M. P. Anderson, S. Jahanmir and R Salher, "Friction and Wear of Tough and Brittle Zirconia in Nitrogen, Air, Water, Hexadecane, and Hexadecane Containing Stearic Acid," Wear, 124, pp. 133-148 (1988).

11. Y. Tsunai and Y. Enomoto, "Tribochemical Wear of Silicon Nitride in Water, n-Alcohol and Their Mixtures," Wear of Materials 1989, K. C. Ludema, Ed., ASME, New York, pp. 369-374 (1989).

12. E. E. Klaus, Y. Phillips, S. C. Lin, N. L. Wu and Y. L. Duda, "Structure of Films Formed During the Deposition of Lubrication Molecules on Iron and Silicon Carbide," Tribology Trans., 33, pp. 25-32 (1990).

13. W. T. Wu, Y. L. Duda and E. E. Klaus, "Lubrication Studies with Alumina-on-Alumina, Steel-on-Steel, and Steel-on-Alumina Bearing Systems," J. Am. Ceram. Soc., 73, pp. 2247-2254 (1990).

14. K. H. Zum Gahr, "Sliding Wear of Ceramic-Ceramic, Ceramic-Steel, and Steel-Steel Pairs in Lubricated and Unlubricated Contact," Wear, 133, pp. 1-22 (1989).

15. J. J. Habeeb, A. G. Blahey and W. N. Rogers, "Wear and Lubrication of Ceramics," Tribology -- Friction, Lubrication and Wear: Fifty Years On, Proc. of the Institution of Mechanical Engineers, IMech, C132/87, London, pp. 555-564 (1987).

16. P. Adam, "Super-Hot Engine Lubricants Sought", Lubricants World, September, pp. 14-17, 43 (1992).

17. J. F. Braza, H. S. Cheng, M. E. Fine, A. K. Gangopadhyay, L. M. Keer, and R. E. Worden, "Mechanical Failure Mechanisms in Ceramic Sliding and Rolling Contacts", Tribology Transactions, Vol. 32, No. 1, pp. 1-8 (1989).

18. R. D. Arnell, P. B. Davies, J. Halling, and T. L. Wholmes, Tribology: Principles and Design Applications, MacMillan Press Ltd., London, (1993).

19. Y. L. Lauer and R. S. Dwyer, "Tribochemical Lubrication of Ceramics by Carbonaceous Vapors," Tribology Transactions, **34**, 4, pp. 521-528 (1991).

20. J. Lepage, A. Mezin, R. Ramboarina, "On a Mechanism of Lubrication by Adsorbed Gases," *Wear*, **140**, pp. 149-163, (1990).

21. J. F. Makki and E. E. Graham, "Vapor Phase Deposition on High Temperature Surfaces," *Tribology Transactions*, **33**, 4, pp. 595-603 (1990).

22. E. E. Graham, E. E. Klaus, "Lubrication from the Vapor Phase at High Temperatures," *ASLE Transactions*, **29**, 1, pp. 229-234, (1986).

23. J. Makki and E. Graham, "Formation of Solid Films from the Vapor Phase on High Temperature Surfaces," *Lubrication Engineering*, **47**, 3, pp. 199-206, (1991).

24. B. Hanyaloglu and E.E. Graham, "Effect of Surface Temperature on Vapor Phase Lubrication," *Lubrication Engineering*, **49**, pp. 227-232, (1993).

25. T. E. Fischer and H. Tomizawa, "Interaction of Tribochemistry and Microstructure in the Friction and Wear of Silicon Nitride," Wear, 105, pp. 29-45 (1985).

26. H. G. Scott, "Friction and Wear of Zirconia at Very Low Sliding Speeds," Wear of Materials 1985, K. C. Ludema, ed., ASME, New York, pp. 8-12 (1985).

27. H. Ishigaki, I. Kawaguchi, M. Iwasa and Y Toibana, "Friction and Wear of Hot Pressed Silicon Nitride and Other Ceramics," Wear of Materials 1985, K. C. Ludema, ed., ASME, New York, pp. 13-21 (1985).

28. M. G. Gee, "The Formation of Aluminum Hydroxide in the Sliding Wear of Alumina," Wear, 153, pp. 201-227 (1992).

29. C. C. Cheng, R. A. Erck, A. Erdemir, G. R. Fenske, "Ion-Assisted Deposition of Silver Films on Ceramics for Friction and Wear Control," *Lubrication Engineering*, **46**,1, pp. 23-30 (1990).

30. A. Erdemir, O. O. Ajayi, G. R. Fenske, R. A. Erck, R. A. Erck, and J. H. Hsieh, "The Synergistic Effects of Solid and Liquid Lubrication on the Tribological Behavior of Transformation-Toughened ZrO_2 Ceramics," *Tribology Transactions*, 35, 2, pp 287-297, (1992).

31. K. Hokkirigawa, "Wear Mode Map of Ceramics," *Wear*, **136**, pp. 117-133 (1990).

32. D. E. Deckman, S. Jahanmir, S. M. Hsu, "Wear Mechanisms of α-Alumina Lubricated with a Paraffin Oil," Wear, 149, pp. 155-168 (1991).

33. D. H. Buckley, and K. Miyoshi, "Tribological Properties of Strucutral Ceramics," in *Treatise on Materials Science and Technology*, Academic Press Inc., Boston, Vol. 29, pp. 293-365 (1989).

34. Hogmark, S., Olsson, M., and Blomberg, A., "Wear Mechanisms of Advanced Ceramic Materials," *Journal of Hard Materials*, **3**, 2, pp. 153-167 (1992).

35. G. W. Stachowiak and G. B. Stachowiak, "Enviromental Effects on Wear and Friction of Toughened Zirconia Ceramics," *Wear*, **160**, pp. 153-162 (1993).

36. M. J. Furey, Tribology. In Encyclopedia of Materials Science and Engineering, Editor-in Chief M. B. Bever, Pergamon Press, Oxford, 1986, pp. 5145-5157.

37. M. J. Furey and C. Kajdas, "Tribopolymerization," 4th Int'l Tribology Conf., Budapest, Hungary, Sept. 22-24 (1987).

38. M. J. Furey and C. Kajdas, "Tribopolymerization as a Lubrication Mechanism for High-Energetic Contacts of Solids," 6th Int'l Tribology Colloq., Technische Akademie Esslingen, Esslingen, Germany, Jan. 12-14 (1988).

39. M. J. Furey and C. Kajdas, "The Planned Formation of Polymeric Films on Rubbing Surfaces to Reduce Wear," *61st Colloid Surface Science Symposium*, Americal Chemical Society, The University of Michigan, Ann Arbor, June 21-24 (1987).

40. M. J. Furey, C. Kajdas, and R. Kempinski, "Tribopolymerization as an Anti-Wear Mechanism: Surface Interactions with Dimer Acid/Glycol Derivatives," *200th Amer. Chem. Soc. National Meeting*, Div. of Colloid and Surface Chemistry, Paper COLL 26, Washington DC, August 26-31 (1989).

41. M. J. Furey, C. Kajdas, T. C. Ward and J. W. Hellgeth, "Thermal and Catalytic Effects on Tribopolymerization as a New Boundary Lubrication Mechanism," Wear, 136, pp. 85-97 (1990).

42. M. J. Furey and J. F. Kunc, "A Radio Tracer Approach to the Study of Engine Valve Train Lubrication," *Lubrication Engineering*, July, pp. 302-309 (1958).

43. P. Marin-LaFleche, C. Kajdas, M. J. Furey, T. C. Ward and J. W. Hellgeth, "A Study of Tribopolymerization Under Fretting Contact Conditions," Proc. of the 8th Int'l Colloq. Tribology -- "Tribology 2000", Esslingen, Germany, Jan 14-16 Vol I (1992).

44. P.Marin-LaFleche, "A Study of Tribopolymerization Under Fretting Conditions," MS Thesis, Mechanical Engineering, Virginia Polytechnic Institute and State University, Blacksburg, VA, May 1990.

45. M. J. Furey, C. Kajdas, R. Kempinski and B. S. Tripathy, "Tribopolymerization and the Behavior of Oxygen-Containing Monomers in Reducing Ceramic Wear," EUROTRIB'93 Congress, Budapest, Hungary, Aug. 30 - Sept. 2 (1993).

46. J. C. Smith, "Ceramic Lubrication: Vapor Phase Tribopolymerization and A New High Speed, High Load Pin-on-Disk Machine," MS Thesis, Mechanical Engineering, Virginia Polytechnic Institute and State University, Blacksburg, VA, February 1994.

47. M. J. Furey, C. Kajdas, R. Kempinski and B. S. Tripathy, "Tribology of Ceramics: Antiwear Action of Vinyl Monomers," 1994 Annual Meeting of the Society of Tribologists and Lubrication Engineers, Pittsburgh, PA, May 2-5 (1994).

48. B. S. Tripathy, "A New Approach to Ceramic Lubrication: Tribopolymerization," Ph.D. Dissertation, Mechanical Engineering, Virginia Polytechnic Institute and State University, Blacksburg, VA, August 1994.

49. B. S. Tripathy, M. J. Furey, C. Kajdas, "Mechanism of Wear Reduction of Alumina by Tribopolymerization," *Wear* Preprint, WEASTD7013 (1994).

50. B. Vick, M. J. Furey and S. J. Foo, "An Analysis of Frictional Heating in Sliding Contact Using a Boundary Integral Equation Method," Numerical Heat Transfer, Part A, Vol. 20, pp. 19-40 (1990).

51. S.J. Foo, "Theoretical Study of Heat Distribution and Surface Temperature Generated in Oscillating Contact," MS Thesis, Mechanical Engineering, Virginia Polytechnic Institue and State University, Blacksburg, VA, Jan. 1990.

52. B. Vick, L.P. Golan II, and M.J. Furey, "Thermal Effects Due to Surface Film in Sliding Contact," *Journal of Tribology*, Paper No. 93-Trib-25, 1993.

53. G. R. Moore, D. E. Kline, Properties and Processing of Polymers for Engineers, Prentice-Hall, Inc. Englewood Cliffs, NJ, 1984.

54. Ronald H. Walpole, Raymond H. Myers, Probability and Statistics for Engineers and Scientists, Fifth Edition, MacMillan Publishing Company, New York, 1993.

55. M. Schwartz, Editor-in-Chief, Handbook of Structural Ceramics, McGraw-Hill Incorporated, New York, 1992.

56. B. J. Hamrock and D. Dawson, Ball Bearing Lubrication: Elastohydrodynamics of Elliptical Contacts, John Wiley and Sons, New York, (1981).

57. D. Ducoulombier, H. Zhou, C. Boned, J. Peyrelasse, H. Saint-Guirons, and P. Xans, "Pressure (1-1000 bars) and Temperature (20-100°C) Dependence of Viscosity of Liquid Hydrocarbons," *Journal of Physical Chemistry*, Vol. **90**, No. 8, (1986).

APPENDIX A

MODIFICATIONS TO HIGH-SPEED HIGH-LOAD TEST MACHINE

Improvements have been made to the existing high-speed high-load pin-on-disk machine. This device was designed and built by Smith [46], but was not used for tribological tests. In order to accurately run pin-on-disk tests, changes were made to certain components of the machine.

First, the rotational speed of the milling machine was calibrated using a strobotach at all machine speeds. The horizontal positioning system of the milling machine was calibrated to provide accurate placement of the ball on the disk at the desired radius. The combination of radius and rotational speed resulted in two speeds and two radii to result in two speeds, the high-speed of 1.0 m/s and the low speed of 0.25 m/s.

The normal load transducer was re-calibrated for more accuracy at low loads. Smith had a calibration up to 500 N, however the load range of interest for these tests is 160 N and below. Figure A1 shows the calibration for the load cell. Data points of indicated load in microstrain and known weights were recorded for each actual mass placed on top of the ball spline shaft. The top of the ball spline loaded the strain gage such that the weight of the mass was also the normal load. Test loads were controlled by adjusting the cylinder pressure to obtain the desired normal load.

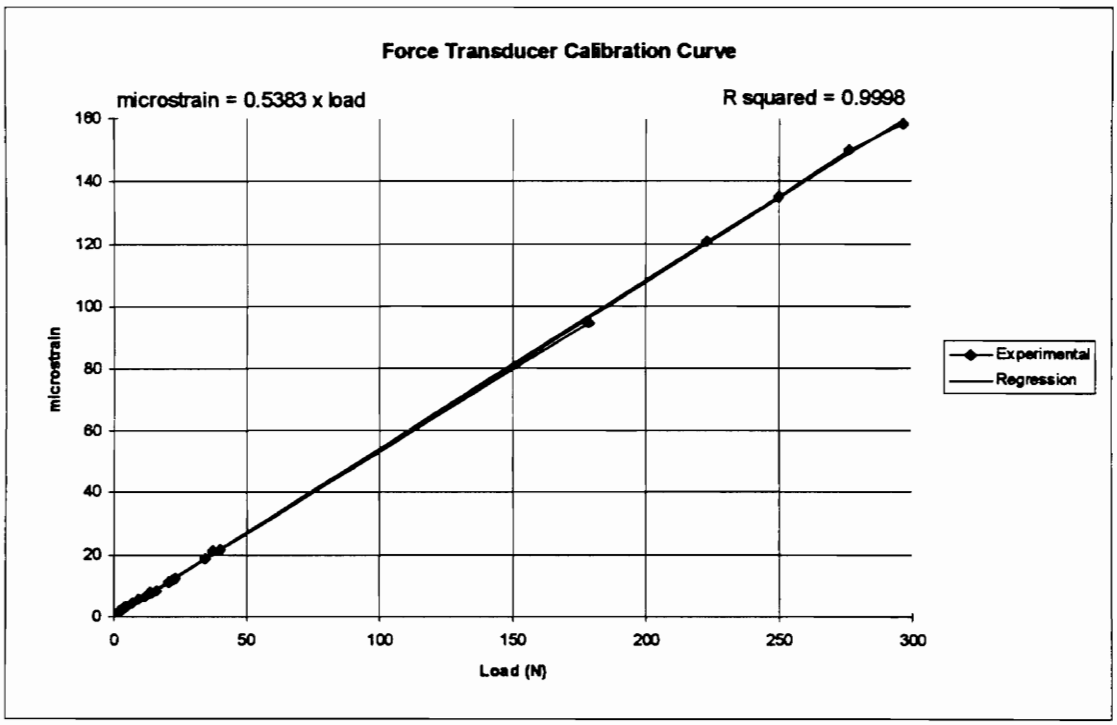

Figure A1. Calibration Curve For Normal Load Transducer.

The disk holder which fits into a standard milling machine chuck was found to be slightly warped and caused a non-parallel rotation relative to the ball. This wobble effect caused a oscillating load. The disk holder was re-machined to reduce rotational disk wobble by making the shaft exactly perpendicular to the face.

Each pin-on-disk test required a fresh supply of a carrier fluid and a monomer additive. Hexadecane was used as the carrier fluid in order to compare results with previous testing by Tripathy [48]. As originally designed, the lubricant cup required a volume of 31 ml per test in order to completely cover the ball. A Teflon insert piece was designed and machined to fit in the cup holder without affecting operation. Figures A1 and A2 show the front, side, top,

and isometric views of the insert. The insert reduced the volume of lubricant required from 31 ml to 18 ml per test, a 42 percent reduction.

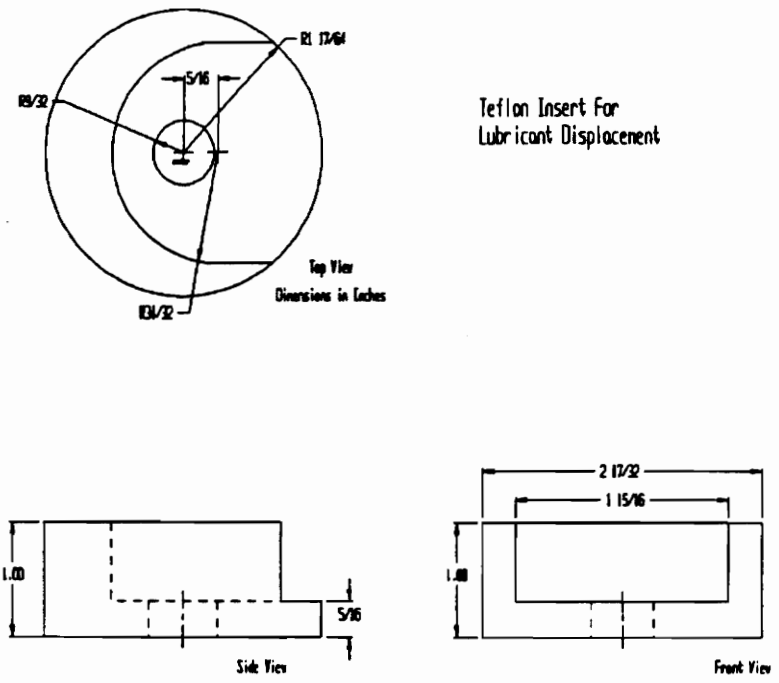

Figure A2. Views and Dimensions of Lubricant Displacement Piece.

The 1 m/s sliding speed demands the highest machine rotational speed, 1435 RPM. At this speed, the lubricant splashed out of the cup holder. A splash guard which fits in the cup holder was designed and built from aluminum. This addition eliminated the splash problem.

In order to use both sides of a disk, a nylon spacer piece was placed between the disk and the steel disk holder. At the 160 N load and 1.0 m/s sliding speed, the nylon disk spacer partially melted during a test. The material for this piece was changed to Teflon, which has a higher glass transition temperature and crystal melt temperature than the nylon [53]. The Teflon insert shown in Figure A3. did not melt during the high-speed, high-load tests.

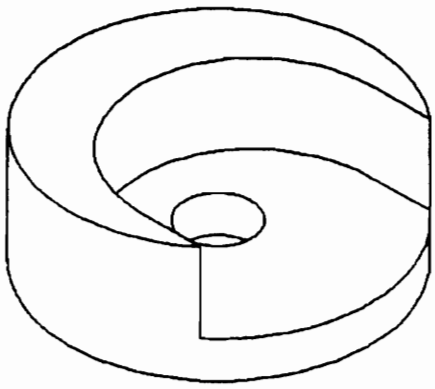

Figure A3. Isometric View of Lubricant Displacement Piece.

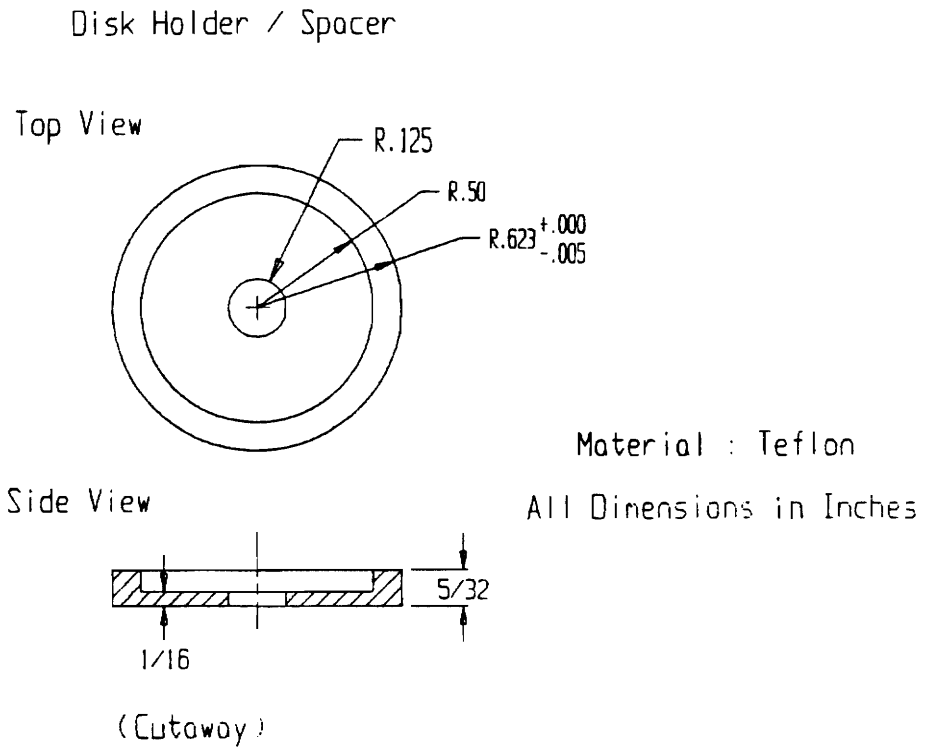

Figure A4. Views and Dimensions of Disk Backing Piece.

APPPENDIX B

WEAR RESULTS SUMMARY TABLES

Table B1. Ball Wear Volumes (1).

(1)

BALL WEAR	alumina ball on alumina disk 250 m sliding distance, wear in mm3			
	LOAD			
	40 N		160 N	
additive in hexadecane ↓	SPEED			
	0.25 m/s	1.0 m/s	0.25 m/s	1.0 m/s
none	1.2 1.26 1.15	2.2 1.6	8.6 *1 12. *2 7.4 *3	3.47 3.5
average	**1.2**	**1.9**	**9.4 *4**	**3.48**
1% diallyl phthalate	0.095 0.085	2.0 1.7	0.2 0.28	3.8 3.5
average	**0.09**	**1.865**	**0.24**	**3.65**
1% monoester	0.027 0.066	2.8 2.7	0.12 0.28	6.1 4.9
average	**0.047**	**2.76**	**0.20**	**5.52**
1% MAMA	0.77 1.18	2.54 4.23	10.5 *5 9.6 *6	5.11 4.02
average	**0.98**	**3.37**	**10.0 *7**	**4.6**

* tests not completed due to excessive ball wear
sliding distances as shown : 1 - 50 m 2 - 62.5 m 3 - 51.25 m 4 - 54 m 5 - 52.8 m 6 - 54.5 m 7 - 54 m

Table B2. Ball Wear Volumes (2).

(2)

BALL WEAR	alumina ball on alumina disk 250 m sliding distance, wear in mm3			
	LOAD			
	40 N		160 N	
additive in hexadecane ↓	SPEED			
	0.25 m/s	1.0 m/s	0.25 m/s	1.0 m/s
none	1.2	2.2	8.6 *1	3.47
	1.26	1.6	12.3 *2	3.5
	1.15		7.4 *3	
average	**1.2**	**1.9**	**9.4 *4**	**3.48**
1% lauryl methacrylate	0.47	5.61	1.56	5.61
	0.74	3.83	1.64	4.88
average	**0.6**	**4.72**	**1.6**	**5.25**
1% vinyl acetate	0.11	3.5	3.1	5.9
	0.12	4.0	5.1	5.9
average	**0.12**	**3.7**	**4.1**	**5.9**
1% VOE	1.0	4.0	1.8	4.2
	0.5	3.8	2.4	4.7
average	**0.75**	**3.93**	**2.1**	**4.4**

* tests not completed due to excessive ball wear
sliding distances as shown : 1 - 50 m 2 - 62.5 m 3 - 51.25 m 4 - 54 m

Table B3. Disk Wear Volumes (1).

DISK WEAR	alumina ball on alumina disk 250 m sliding distance, wear in mm3			(1)
	LOAD			
	40 N		160 N	
additive in hexadecane	SPEED			
↓	0.25 m/s	1.0 m/s	0.25 m/s	1.0 m/s
none	2.6	1.0	13.6 *1	9.67
	3.0	1.5	8.9 *2	9.66
	2.1		10 *3	
average	**2.6**	**1.3**	**10.8 *4**	**9.67**
1% diallyl phthalate	0.12	1.1	0.019	9.95
	0.095	0.8	0.68	9.1
average	**0.11**	**0.91**	**0.35**	**9.5**
1% monoester	0.058	2.1	0.17	9.6
	0.36	1.7	0.27	7.74
average	**0.21**	**1.9**	**0.22**	**8.7**
1% MAMA	1.2	2	13.2 *5	10.1
	1.6	2.9	11.1 *6	8.8
average	**1.4**	**2.5**	**12.1 *7**	**9.5**

* tests not completed due to excessive ball wear
sliding distances as shown : 1 - 50 m 2 - 62.5 m 3 - 51.25 m 4 - 54 m 5 - 52.8 m 6 - 54.5 m 7 - 54 m

Table B4. Disk Wear Volumes (2).

DISK WEAR	alumina ball on alumina disk 250 m sliding distance, wear in mm3				(2)
	LOAD				
	40 N		160 N		
additive in hexadecane	SPEED				
↓	0.25 m/s	1.0 m/s	0.25 m/s	1.0 m/s	
none	2.6 3.0 2.1	1.0 1.5	13.6 *1 8.9 *2 10 *3	9.67 9.66	
average	**2.6**	**1.3**	**10.8 *4**	**9.67**	
1% lauryl methacrylate	1.8 1.26	2.69 2.68	3.13 2.62	12.1 9.6	
average	**1.53**	**2.69**	**2.88**	**10.9**	
1% vinyl acetate	0.11 0.16	2.04 2.08	4.6 7.8	12.7 11.9	
average	**0.13**	**2.06**	**6.2**	**12.3**	
1% VOE	1.95 0.54	2.76 3.3	2.19 3.25	7.9 9.9	
average	**1.24**	**3.03***	**2.7**	**8.9**	

* tests not completed due to excessive ball wear
sliding distances as shown : 1 - 50 m 2 - 62.5 m 3 - 51.25 m 4 - 54 m

The symbols in Tables B5 and B6 illustrate the relative change in total wear volume for the test (monomer, load and speed) compared to hexadecane wear volumes. Arrows pointing up indicate an increase in wear, arrows pointing down indicate a decrease in wear, and an **X** indicates no significant change.

Table B5. Total Wear Volumes (1).

(1)

TOTAL WEAR — alumina ball on alumina disk, 250 m sliding distance, wear in mm3

additive in hexadecane	LOAD 40 N, SPEED 0.25 m/s	LOAD 40 N, SPEED 1.0 m/s	LOAD 160 N, SPEED 0.25 m/s	LOAD 160 N, SPEED 1.0 m/s
none	3.8 4.3 3.2	3.3 3.2	21.7 *1 21.2 *2 17.5 *3	13.14 13.16
average	**3.8**	**3.2**	**20.1 *4**	**13.15**
1% diallyl phthalate	0.21 0.18	3.1 2.5	0.22 0.96	13.8 12.6
average	**0.2** ↓	**2.8** ↓	**0.59** ↓	**13.2** X
monoester	0.085 0.43	4.9 4.4	0.17 0.56	15.7 12.6
average	**0.25** ↓	**4.7** ↑	**0.36** ↓	**14.2** X
MAMA	2 2.8	4.5 7.2	23.6 *5 20.6 *6	15.2 12.9
average	**2.4** ↓	**5.9** ↑	**22.1 *7** X	**14.0** X

* tests not completed due to excessive ball wear
sliding distances as shown : 1 - 50 m 2 - 62.5 m 3 - 51.25 m 4 - 54 m 5 - 52.8 m 6 - 54.5 m 7 - 54 m

Table B6. Total Wear Volumes (2).

TOTAL WEAR	alumina ball on alumina disk 250 m sliding distance, wear in mm3				(2)
	LOAD				
	40 N		160 N		
additive in hexadecane ↓	SPEED				
	0.25 m/s	1.0 m/s	0.25 m/s	1.0 m/s	
none	3.8 4.3 3.2	3.3 3.2	21.7 *1 21.2 *2 17.5 *3	13.14 13.16	
average	**3.8**	**3.2**	**20.1 *4**	**13.15**	
1% lauryl methacrylate	2.27 2.0	8.3 6.5	4.69 4.26	17.7 14.5	
average	**2.13** ↓	**7.4** ↑	**4.5** ↓	**16.1** ↑	
1% vinyl acetate	0.22 0.28	5.5 6.1	7.8 12.9	18.5 17.8	
average	**0.25** ↓	**6.8** ↑	**10.3** ↓	**18.2** ↑	
1% VOE	2.96 1.02	6.8 7.1	4.0 5.65	12.1 14.5	
average	**2.0** ↓	**7.0** ↑	**4.84** ↓	**13.3** X	

* tests not completed due to excessive ball wear
sliding distances as shown : 1 - 50 m 2 - 62.5 m 3 - 51.25 m 4 - 54 m

APPENDIX C

TEMPERATURE RISE CALCULATIONS AND OBSERVATIONS

THEORETICAL CALCULATIONS

Assumptions in the modeling of the ball-disk thermal system include a single circular area of contact between ball and disk and a constant sliding velocity. The thermal conductivity, thermal diffusivity, hardness of the ball and the disk, applied load, velocity, theoretical area of contact, and assumed coefficient of friction are all required for temperature calculations and are shown in Table C1.

Table C1. Alumina Properties And Test Conditions For Temperature Calculations.

Material (Ball and Disk) :	99.5% pure Alumina (Al_2O_3)
Sliding Speed (V) :	0.25 m/s and 1.0 m/s
Normal Load (W) :	40 N and 160 N
Thermal Conductivity (k) :	25.9 Watts per meter per Kelvin
Thermal Diffusivity (α) :	7.57 E-6 m^2 per second
Hardness :	1.47 E10 N per m^2
Coefficient of Friction (μ) :	1.0
Modulus of Elasticity (E) :	3.72 E 11 N per m^2
Poissons Ratio (ν) :	0.22
Area Of Contact :	Elastic, Plastic and Apparent

Example calculation of plastic and elastic areas of contact are shown below. The BIEM temperature calculation program requires the input of a *half-length in the direction of sliding*, and a *half length perpendicular to the direction of sliding*. Contact areas are assumed to be circular for the sphere on flat geometry of the pin-on disks experiments. The circular area can then be used as the square area.

$$A_{circle} = A_{square}$$

The half lengths of contact (L) are one half of the length of one side of the square.

$$L = \frac{(A_{square})^{1/2}}{2}$$

Elastic and plastic areas of contact can be calculated as follows. For plastic area the half length is found by :

$$\text{Load} = \text{Area} \times \text{Hardness}$$

$$L = \frac{(\text{Load} / \text{Hardness})^{1/2}}{2}$$

For elastic area, the radius of contact (a) for a circular contact area is given by :

$$a = \left[\frac{3 \times \text{load} \times \text{radius}}{4 \times E'} \right]^{1/3}$$

where E′ is the modified modulus of elasticity,

$$\frac{1}{E'} = \frac{(1 - \nu^2)}{E1} + \frac{(1 - \nu^2)}{E2}$$

and the half length is given by :

$$L = \frac{1}{2} \times [\pi \times a^2]^{\frac{1}{2}}$$

Temperature rises at sliding surfaces are calculated using the half lengths, sliding speed, normal load, thermal conductivity, coefficient of friction and thermal diffusivity.

CALCULATED TEMPERATURE RISE*
(KELVIN)

SLIDING SPEED:	LOAD 40 N	LOAD 160 N
0.25 m/s	P: 1526 E: 485	P: 2746 E: 1082
1.0 m/s	P: 4695 E: 1293	P: 7640 E: 2752

Coefficient of Friction = 1.0
P: plastic area E: elastic area

* Calculated with Dr. B. Vick's Temperature Program, Temperature Based on a Single Circular Area of Contact

Figure C1. Calculated Temperature Rises.

Temperature rises for the basic 4 load speed combinations are shown in Figure C1. An increase by a factor of 4 in the speed resulted in a higher temperature than an increase by a factor of 4 in the load for both plastic and

elastic area calculations. This is due in large part to the increase in area when load increases. The assumed area of contact does not change when the velocity changes. However in both cases the frictional heat generation increases by the same amount.

The ball wear scar area at the end of a test was used as the apparent area of contact, as an additional source of temperature comparisons based on the area of contact. The ball wear scar represents the maximum possible area of contact. Due to the actual contact at asperities and the lack of contact between asperities the actual contact area at the end of a test is less than the ball wear scar area. This results in an underestimate of the temperature throughout the test when the apparent (macroscopic) area is smaller. By plotting temperature rise versus area on a log-log scale, an approximately straight line relationship is seen for the increasing area determined by plastic, elastic and apparent areas. Figures C2 through C15 show calculated temperature rises for hexadecane and all monomer mixtures for all testing conditions. Assumed contact areas are based on plastic, elastic and apparent areas of contact. Apparent areas of contact are based on the average of all tests at a given load and speed.

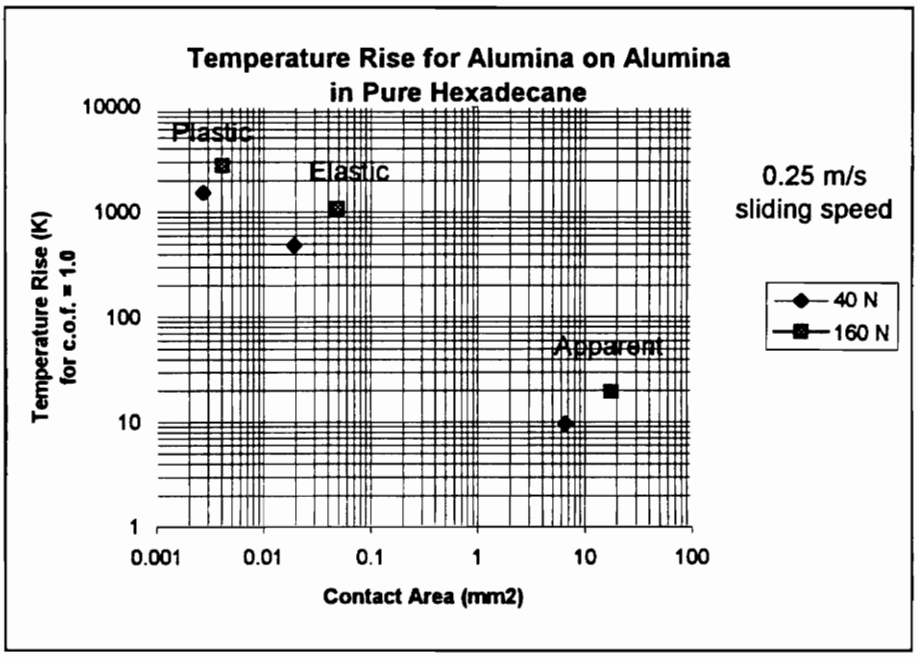

Figure C2. Calculated Temperature Rises for Plastic, Elastic and Apparent Areas of Contact with μ = 1.0 (0.25 m/s, Pure Hexadecane).

Plastic and elastic areas result in calculated temperatures which are probably higher than actual temperatures. For example, the temperatures in Figure C3. for a plastic area, 160 N load and 1.0 m/s sliding speed result in close to a 10000 °C temperature rise for μ = 1.0, or 1000 ° C for μ = 0.1. At the same time temperature rise calculations based on the apparent post-test area of contact are lower than actual temperature rises at the rubbing surfaces. For example in Figure C2, the 40 N load and 0.25 m/s sliding speed result in a temperature rise of 10 ° C for μ = 1.0, or 1 ° C for μ = 0.1. The 1 ° C temperature rise is less than the measured disk temperature at the end of a test. Actual temperatures are probably in between the calculated temperatures from apparent and elastic areas of contact. The next section describes the technique for measuring ball, disk and lubricant temperatures and the results.

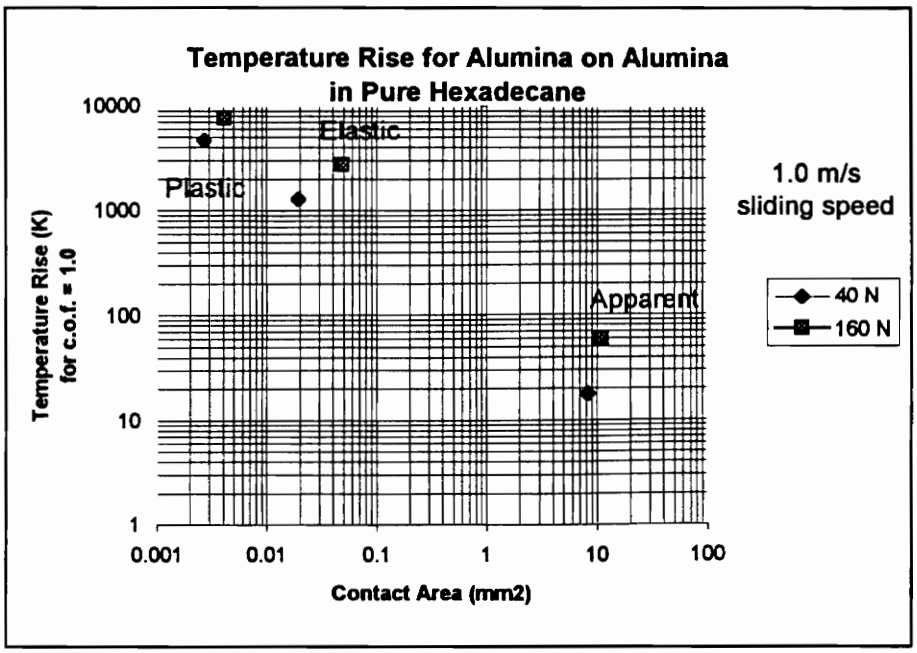

Figure C3. Calculated Temperature Rises for Plastic, Elastic and Apparent Areas of Contact with μ = 1.0 (1.0 m/s, Pure Hexadecane).

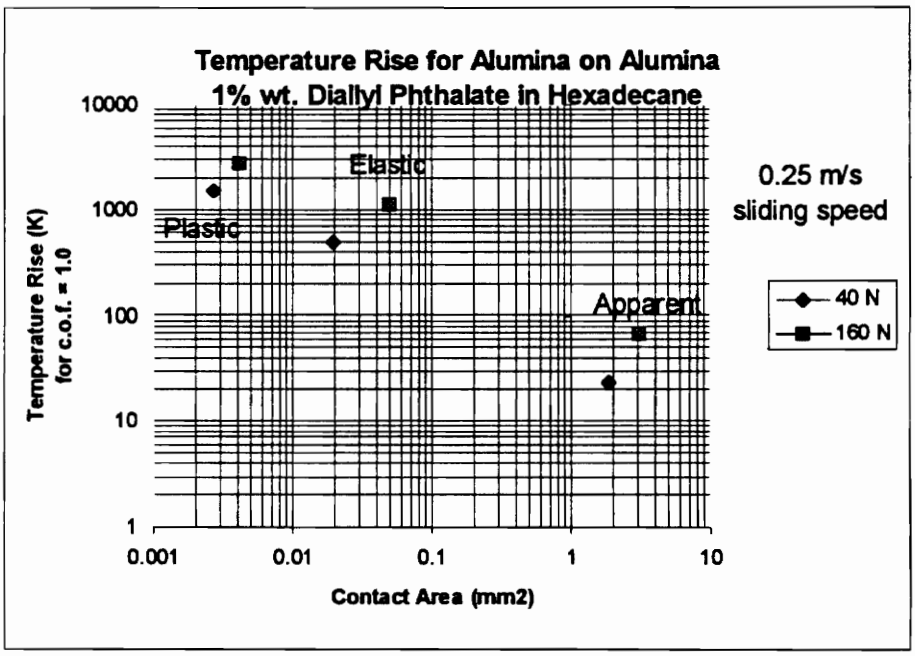

Figure C4. Calculated Temperature Rises for Plastic, Elastic and Apparent Areas of Contact with μ = 1.0 (0.25 m/s, Diallyl Phthalate).

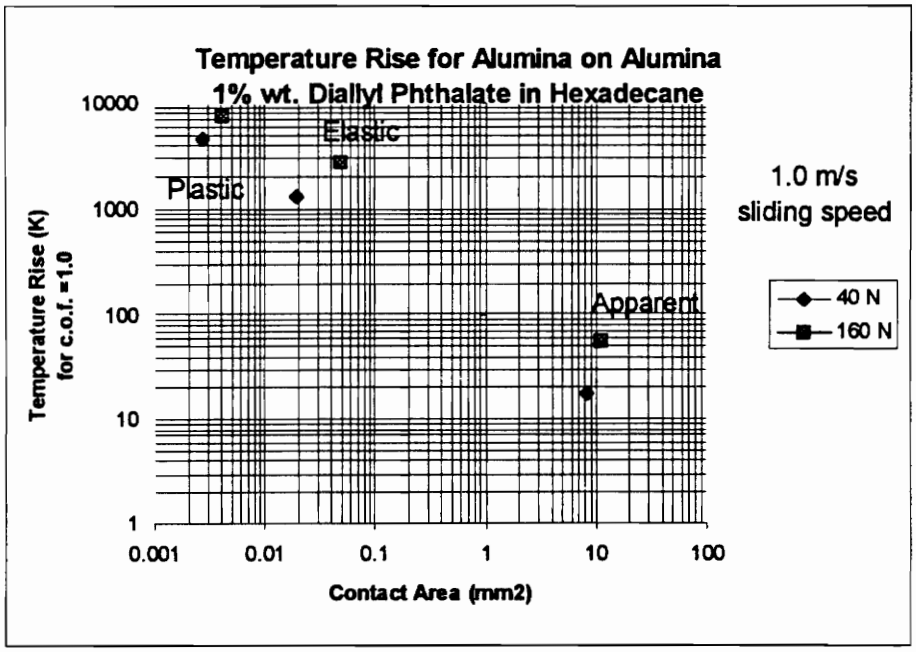

Figure C5. Calculated Temperature Rises for Plastic, Elastic and Apparent Areas of Contact with μ = 1.0 (1.0 m/s, Diallyl Phthalate).

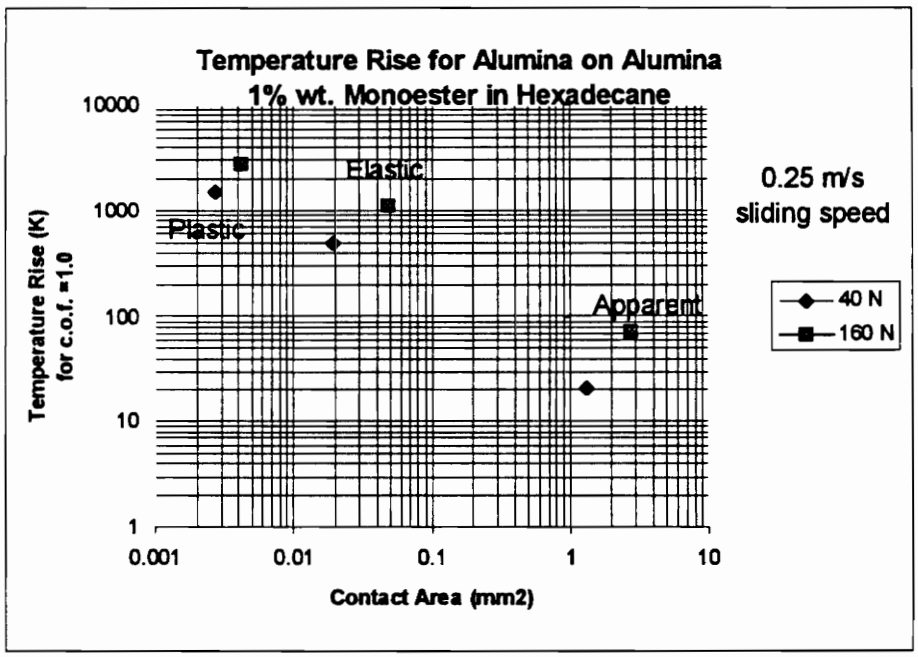

Figure C6. Calculated Temperature Rises for Plastic, Elastic and Apparent Areas of Contact with μ = 1.0 (0.25 m/s, Monoester).

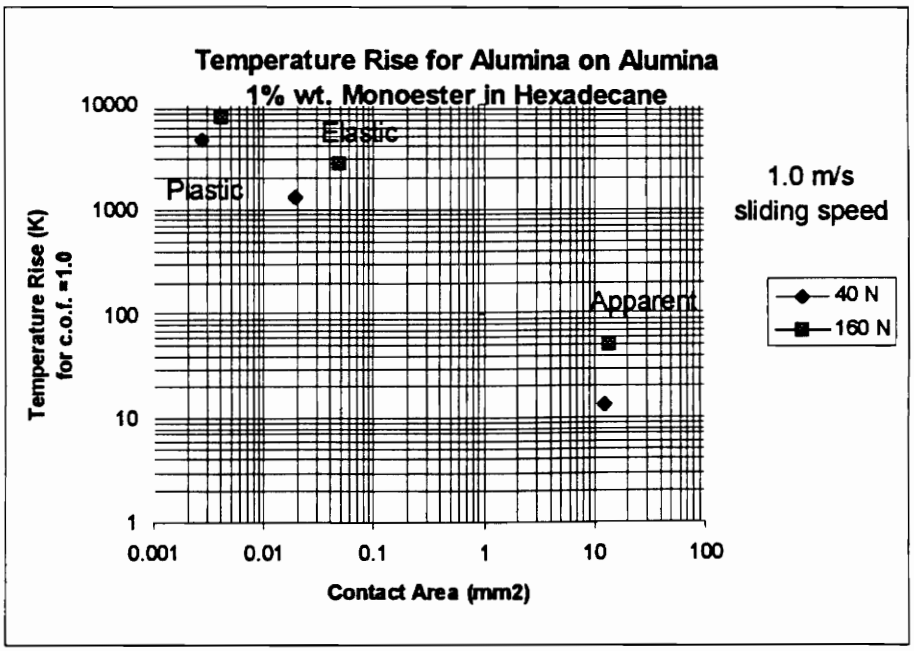

Figure C7. Calculated Temperature Rises for Plastic, Elastic and Apparent Areas of Contact with $\mu = 1.0$ (1.0 m/s, Monoester).

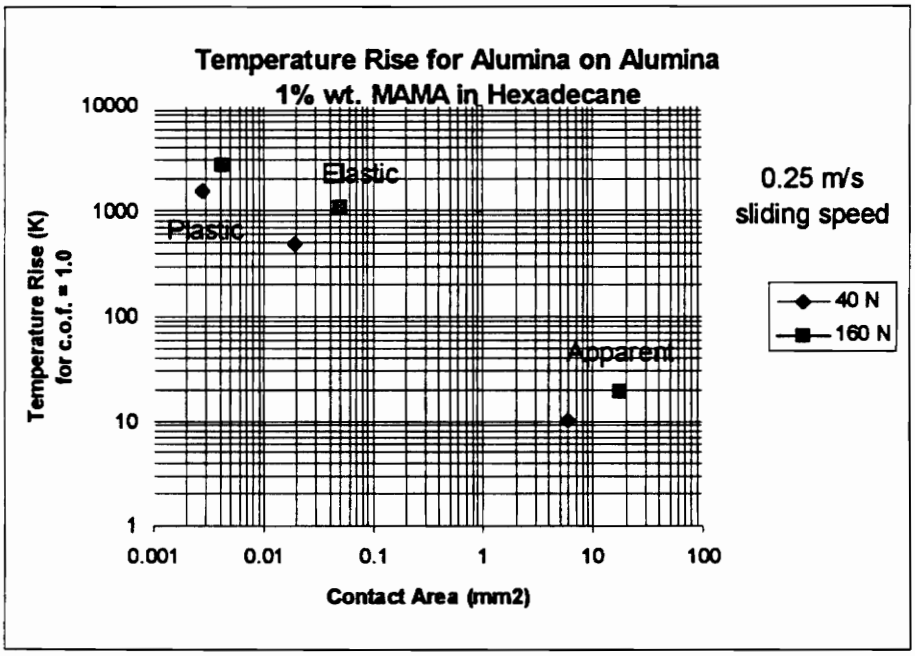

Figure C8. Calculated Temperature Rises for Plastic, Elastic and Apparent Areas of Contact with $\mu = 1.0$ (0.25 m/s, MAMA).

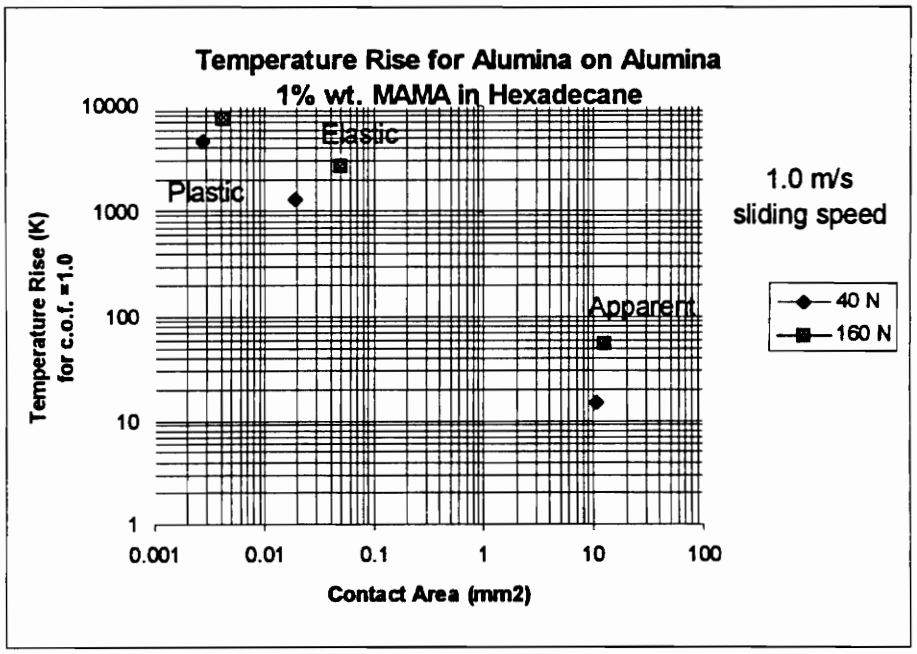

Figure C9. Calculated Temperature Rises for Plastic, Elastic and Apparent Areas of Contact with μ = 1.0 (1.0 m/s, MAMA).

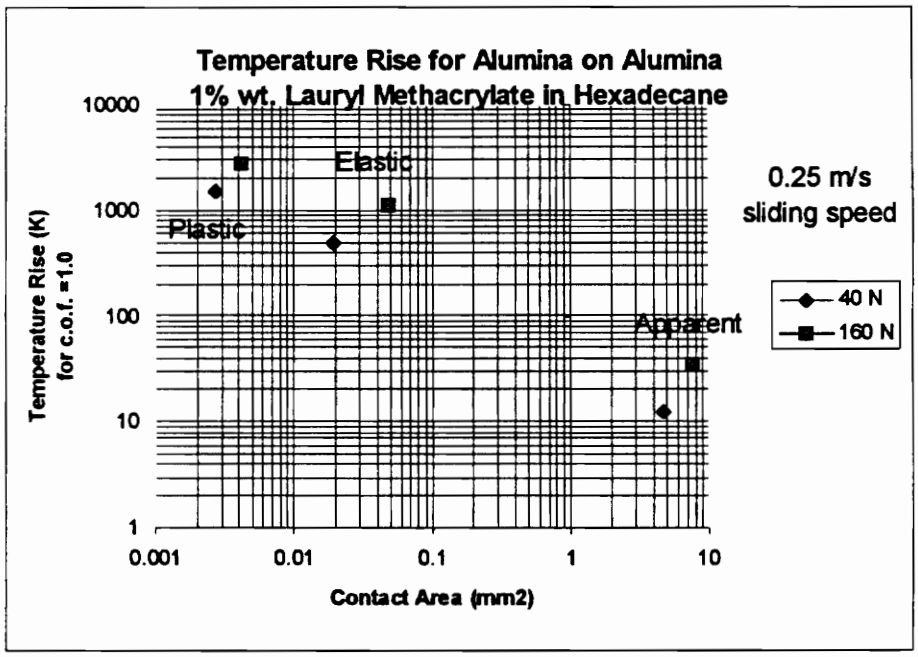

Figure C10. Calculated Temperature Rises for Plastic, Elastic and Apparent Areas of Contact with μ = 1.0 (0.25 m/s, Lauryl Methacrylate).

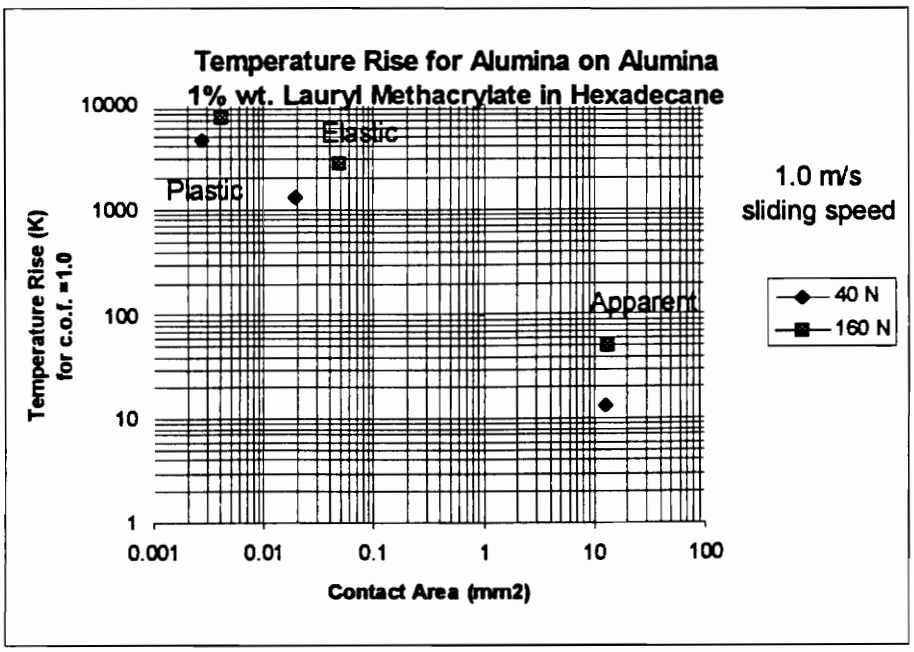

Figure C11. Calculated Temperature Rises for Plastic, Elastic and Apparent Areas of Contact with μ = 1.0 (1.0 m/s, Lauryl Methacrylate).

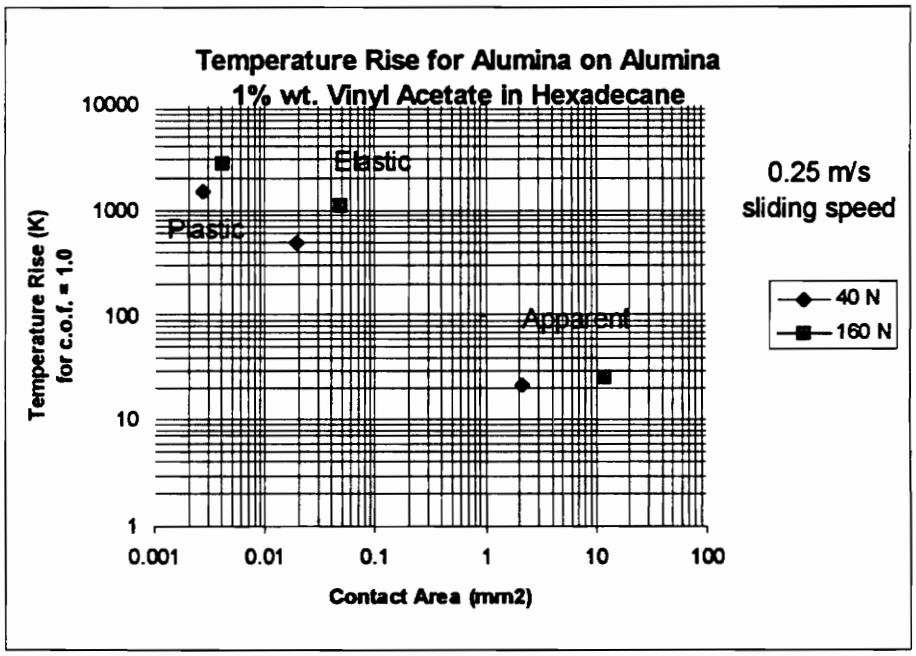

Figure C12. Calculated Temperature Rises for Plastic, Elastic and Apparent Areas of Contact with μ = 1.0 (0.25 m/s, Vinyl Acetate).

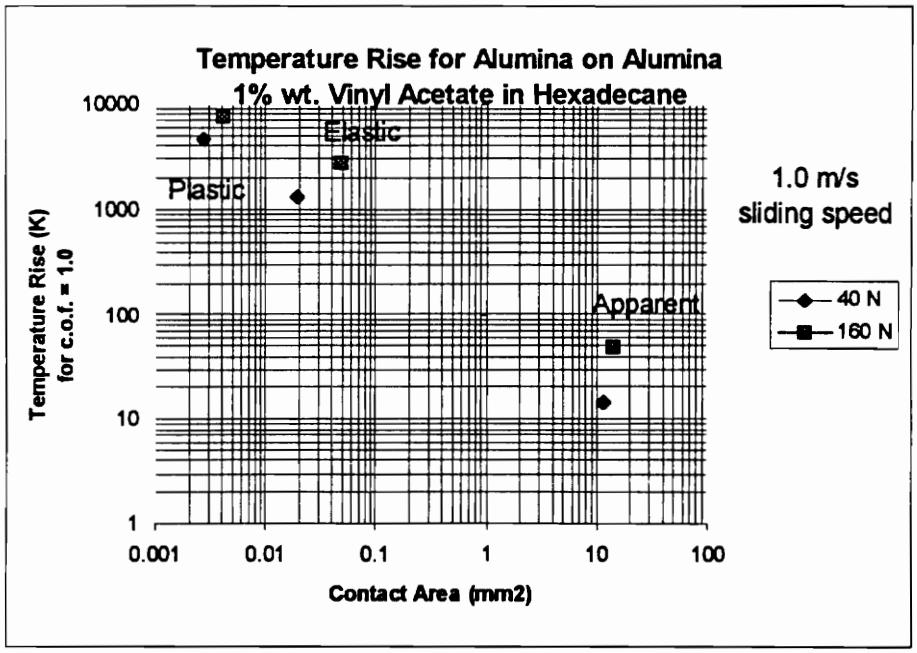

Figure C13. Calculated Temperature Rises for Plastic, Elastic and Apparent Areas of Contact with μ = 1.0 (1.0 m/s, Vinyl Acetate).

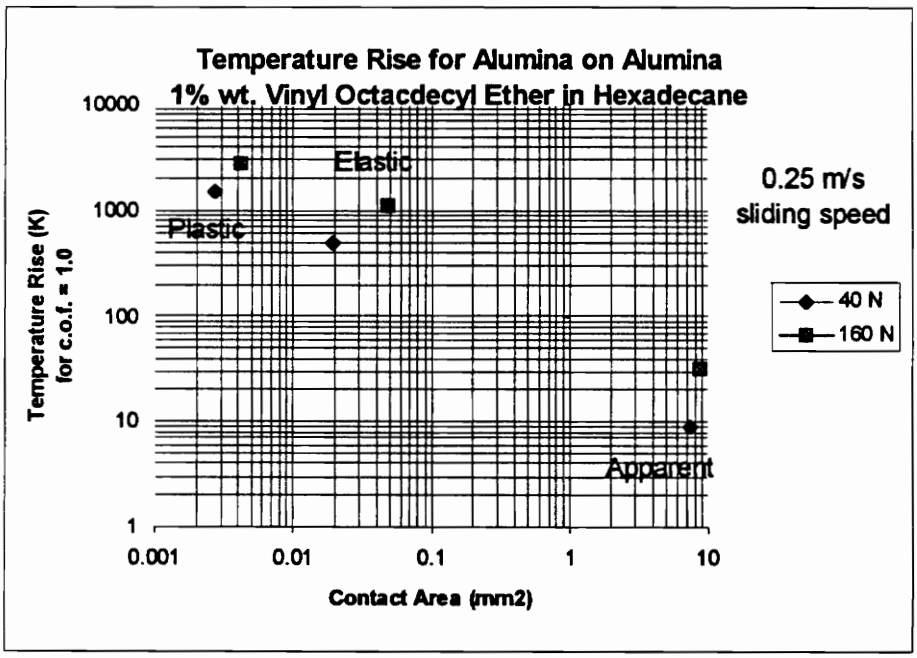

Figure C14. Calculated Temperature Rises for Plastic, Elastic and Apparent Areas of Contact with μ = 1.0 (0.25 m/s, Vinyl Octadecyl Ether).

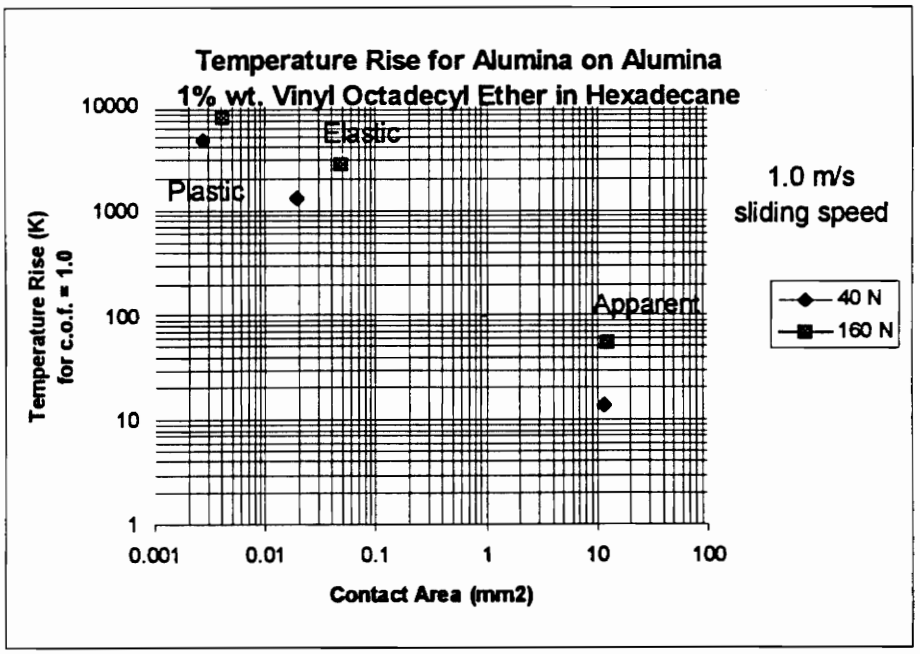

Figure C15. Calculated Temperature Rises for Plastic, Elastic and Apparent Areas of Contact with μ = 1.0 (1.0 m/s, Vinyl Octadecyl Ether).

OBSERVED TEMPERATURE RISES

Immediately after the end of each test, when the load was removed and the rotation stopped, a type K thermocouple was inserted into the test region to record temperatures on the ball surface, on the disk surface, and in the bulk lubricant. Although placement of the thermocouple could vary for any of the three locations, the temperature variation did not exceed 2 °C for the ball and lubricant temperatures, and 10 ° C for the disk temperatures. The thermocouple tip physically touched the ball and disk on the wear scars. The actual temperature rises were calculated by subtracting the ambient temperature (usually 21 °C) from the recorded temperatures. Figures C16 - C19 show the average recorded temperature rises for each of the four load-speed regimes and for all lubricants.

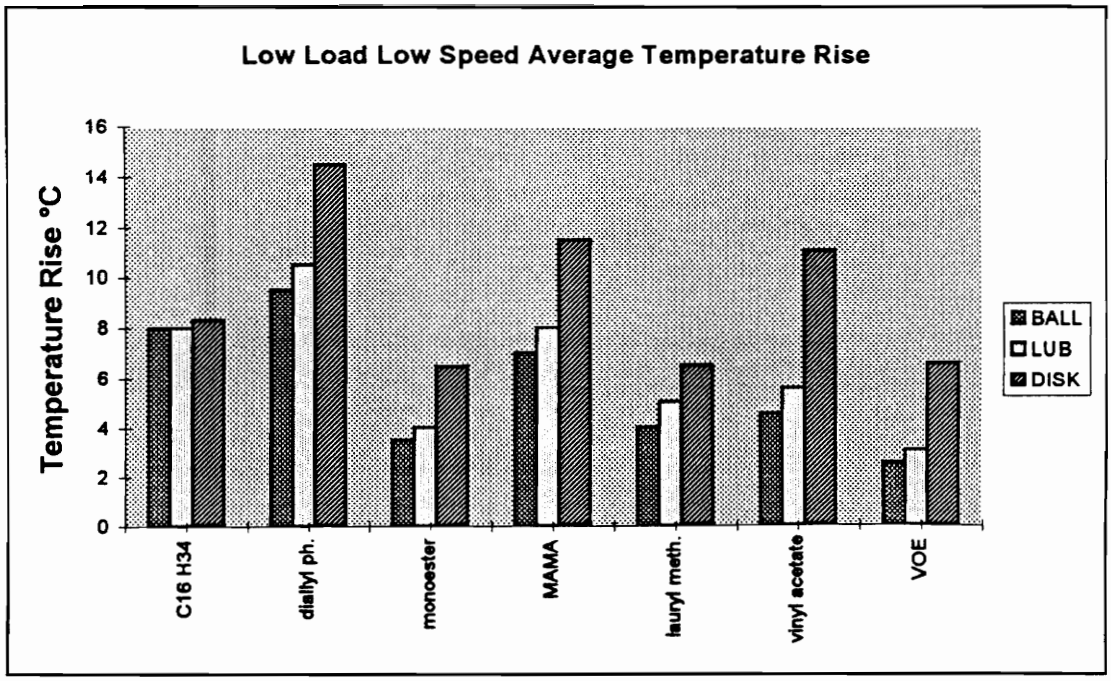

Figure C16. Average Measured Temperature Rises for Low Load and Low Speed Testing Conditions.

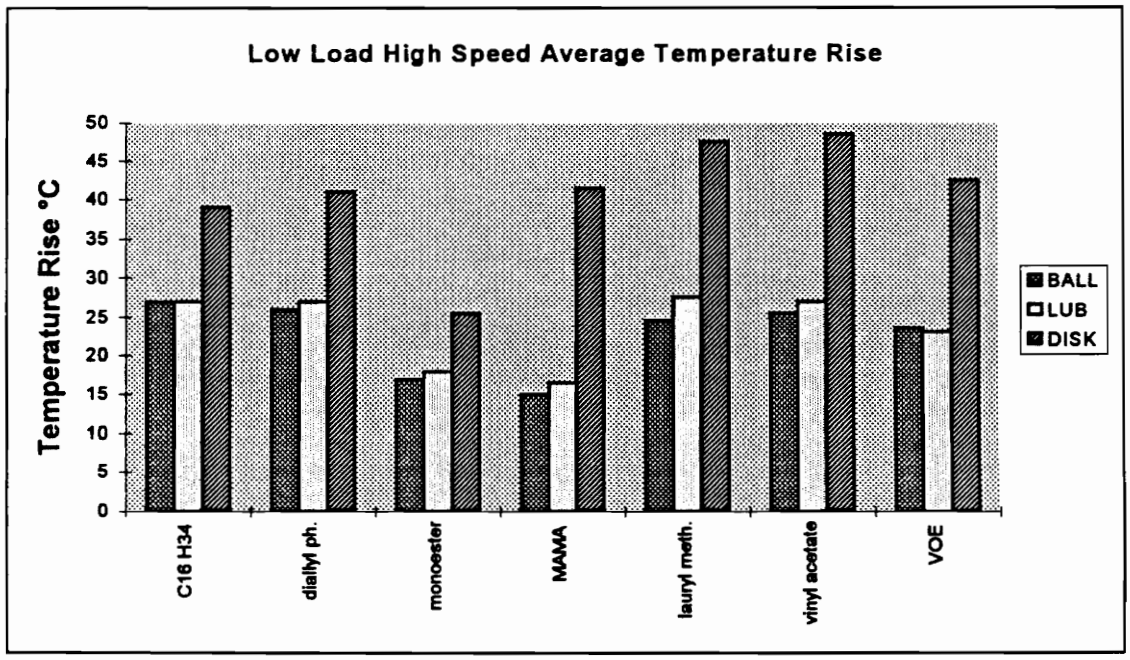

Figure C17. Average Measured Temperature Rises for Low Load and High Speed Testing Conditions.

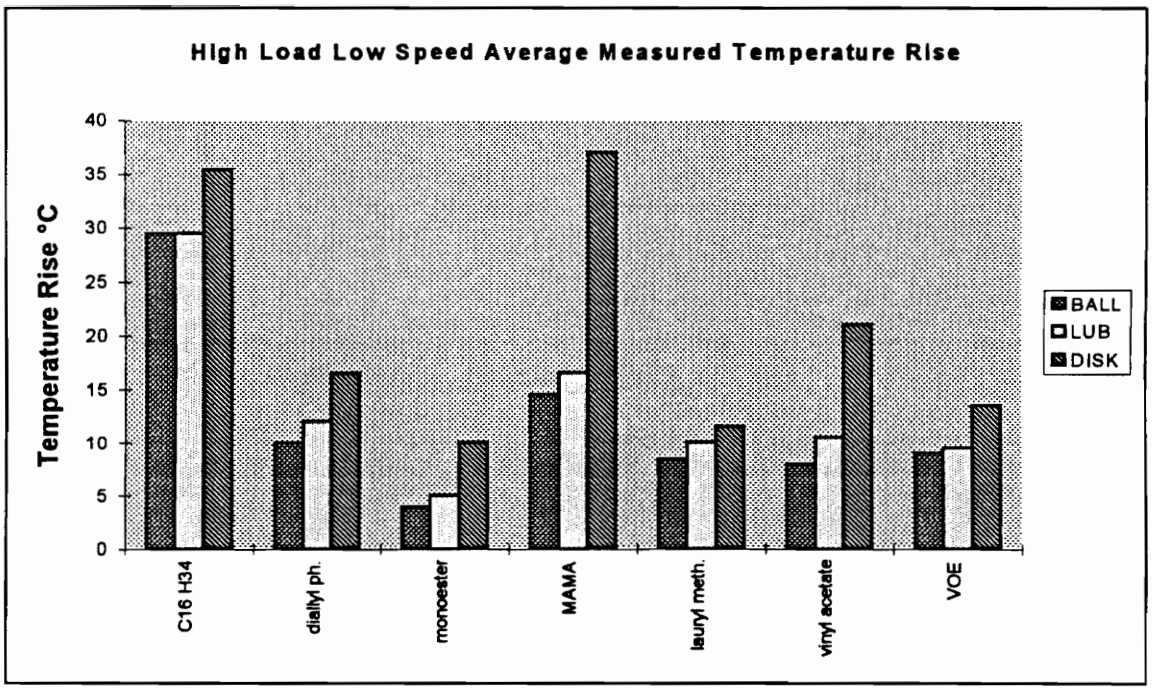

Figure C18. Average Measured Temperature Rises for High Load and Low Speed Testing Conditions.

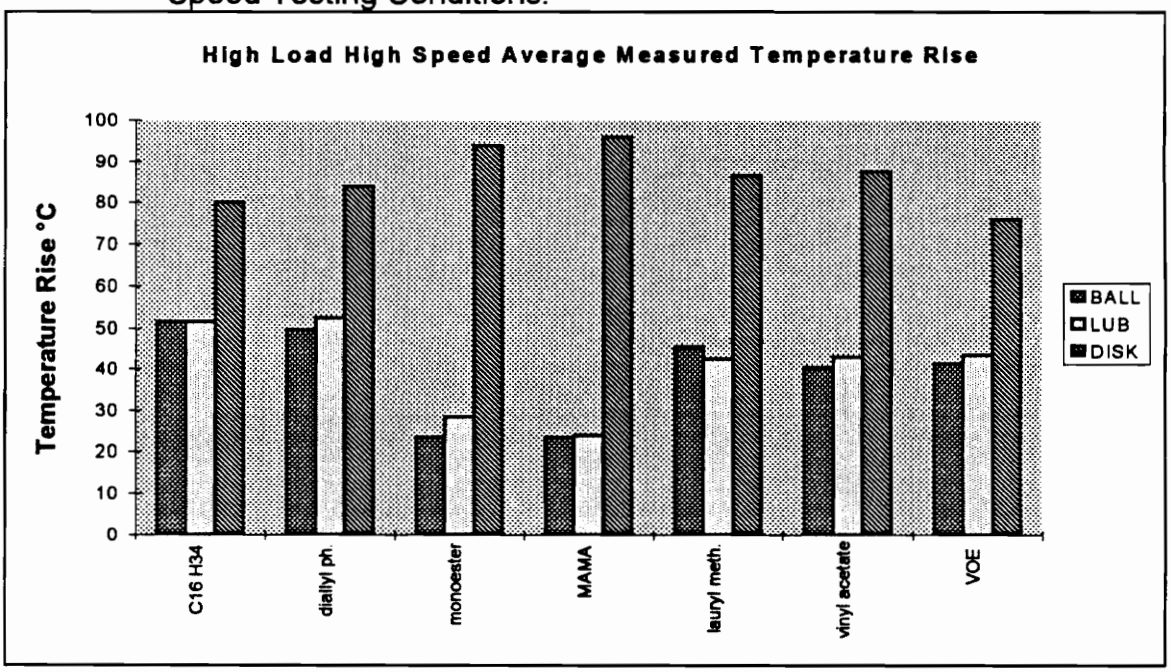

Figure C19. Average Measured Temperature Rises for High Load and High Speed Testing Conditions.

The noticeable difference in measured temperatures based on monomers raises an important question. If load and speed are kept constant, what changes in the system to cause different temperature rises? The frictional heat generation is dependent on the speed, the normal load and the coefficient of friction, μ. Assuming steady state conditions, temperature in a system is dependent on frictional heat generation, heat storage, and the heat transfer due to conduction, radiation, and convection.

The heat conduction in the different monomer systems could change due to changes in the thermal conductivity of the liquids. However a 1 wt. % addition of monomer to hexadecane should not cause a noticeable change. Heat storage capabilities and the mass of the systems should also be fairly constant. For a given rotational speed, changes in heat convection to the surroundings should be minimal. A more significant change could be the variation in μ. Previous testing by Tripathy [48] showed small changes in μ for different monomers. In vapor phase tribological testing by Smith [46], the coefficient of friction did change significantly depending on the monomer system.

The most noticeable and significant changes in measured temperature occur when wear is noticeably reduced, perhaps indicating friction is also reduced. In Figure C18, the disk temperatures are reduced compared to pure hexadecane for all the wear effective monomers, while the MAMA compound (which did not reduce wear) disk temperature was not reduced. However MAMA did reduce the ball and lubricant temperatures. All effective monomers at the 160 N load and 0.25 m/s sliding speed had lower temperature rises compared to pure hexadecane. An unexpected temperature observation is the diallyl phthalate at low speed and low load. Figure C16 shows that the temperature

rises are 1 ° C to 5 ° C higher for the diallyl phthalate monomer compared to pure hexadecane, even though wear is reduced. This temperature difference is low and within the observed variation for any set of temperature measurements.

At high speeds, MAMA and monoester result in lower temperature rises for ball and lubricant temperature while disk temperature remains consistent for all lubricants. The ball and lubricant temperature rises are consistent for all other monomers and hexadecane.

An analysis of calculated temperature rises and observed temperature rises yields the following conclusions.

- For the same coefficient of friction, calculated temperature rises based on apparent area for effective monomers are higher than pure hexadecane calculated temperatures because the effective monomers have a smaller area of contact at the end of tests compared to hexadecane. However wear effective monomers' measured temperature rises are generally lower than temperture rises for pure hexadecane.

- 1 wt. % monomer additions to hexadecane result in lower measured temperature rises for high load and low speed conditions.

- The high load and high speed test conditions did not show significant temperature rise reductions compared to hexadecane except for MAMA and monoester.

- The ineffective wear reduction monomer (MAMA) did not reduce disk temperature rise for high load and low speed conditions, nor did it significantly reduce temperature rises for low load and low speed.

APPENDIX D

STATISTICAL ANALYSIS OF WEAR RESULTS

All wear data required for statistical calculations is presented with an explanation of the analysis of variance (ANOVA) technique. The statistical software used in the analysis is Minitab™ Version 8.0. Tables D1, D2 and D3 show data used in the ANOVA calculations for ball wear, disk wear and total wear respectively. Any given test condition (load, speed and lubricant) was performed two times to demonstrate repeatability and for statistical significance. Pure hexadecane tests at low speeds were repeated 3 times.

Table D1. Ball Wear Data (mm^3).

Load	Speed	Hexa-decane	Diallyl Phthalate	Monoester	MAMA	Lauryl Meth.	Vinyl Acetate	VOE
1	1	1.2	0.095	0.027	0.77	0.47	0.11	1.0
1	1	1.26	0.085	0.066	1.18	0.74	0.12	0.5
1	1	1.15						
1	2	2.2	2.0	2.8	2.54	5.61	3.5	4.0
1	2	1.6	1.70	2.7	4.23	3.83	4.0	3.8
2	1	8.6	0.2	0.12	10.45	1.56	3.1	1.8
2	1	12.3	0.28	0.28	9.59	1.64	5.1	2.4
2	1	7.4						
2	2	3.47	3.8	6.1	5.11	5.61	5.9	4.2
2	2	3.5	3.5	4.9	4.02	4.88	5.9	4.7

Loads: 1 = 40 N 2 = 160 N Speeds: 1 = 0.25 m/s 2 = 1.0 m/s

Table D2. Disk Wear Data (mm^3).

Load	Speed	Hexa-decane	Diallyl Phthalate	Monoester	MAMA	Lauryl Meth.	Vinyl Acetate	VOE
1	1	2.6	0.12	0.058	1.2	1.80	0.11	1.95
1	1	3.0	0.095	0.36	1.6	1.26	0.16	0.54
1	1	2.1						
1	2	1.0	1.1	2.1	2.0	2.69	2.04	2.76
1	2	1.5	0.8	1.7	2.9	2.68	2.08	3.3
2	1	13.6	0.019	0.17	13.2	3.13	4.6	2.19
2	1	8.9	0.68	0.27	11.05	2.62	7.8	3.25
2	1	10.0						
2	2	9.67	9.95	9.6	10.1	12.1	12.7	7.9
2	2	9.66	9.1	7.74	8.8	9.6	11.9	9.9

Loads: 1 = 40 N 2 = 160 N Speeds: 1 = 0.25 m/s 2 = 1.0 m/s

Table D3. Total Wear Data (mm^3).

Load	Speed	Hexa-decane	Diallyl Phthalate	Monoester	MAMA	Lauryl Meth.	Vinyl Acetate	VOE
1	1	3.8	0.21	0.085	2.0	2.27	0.22	2.96
1	1	4.3	0.18	0.43	2.8	2.0	0.28	1.02
1	1	3.2						
1	2	3.3	3.1	4.9	4.5	8.3	5.5	6.8
1	2	3.2	2.5	4.4	7.2	6.5	6.1	7.1
2	1	21.7	0.22	0.17	23.6	4.69	7.8	4.0
2	1	21.2	0.96	0.56	20.6	4.26	12.9	5.65
2	1	17.5						
2	2	13.14	13.8	15.7	15.2	17.7	18.5	12.1
2	2	13.16	12.6	12.6	12.9	14.5	17.8	14.5

Loads: 1 = 40 N 2 = 160 N Speeds: 1 = 0.25 m/s 2 = 1.0 m/s

The tests at 160 N load and 0.25 m/s speed which did not complete the desired 250 m are included in the analysis of variance. Since the wear volume under these conditions was the highest, any results at 160 N and 0.25 m/s can be considered conservative. Both pure hexadecane and MAMA resulted in the same sliding distance, indicating that the two lubricants behaved similarly.

Factorial experiments are designed to give information about the effects of certain selected factors on some event. In these experiments, the three factors were load, speed and monomer additive. A factor is defined as a feature of the experiment which can be varied from trial to trial [54]. Levels of a particular factor are those actual values used in the experiments. For example the 2 levels of load are 40 and 160 N.

ANOVA (Analysis Of Variance) is a very common method for comparing the means of a population. For the pin-on-disk experiments, the wear volumes represent sample averages of wear, with the number of samples (n) usually being two, which is assumed to represent a larger population of wear volumes. In the ANOVA method, the total variance of the mean values is divided into meaningful components, representing the factors and factor interactions. The null hypothesis (H_o) for a general analysis of variance states that the means (μ) are all equal :

$$H_o : \mu_1 = \mu_2 = \mu_3 = \ldots = \mu_n .$$

The alternative hypothesis (H_1) states that at least 2 of the means are not equal.

For the 3 factor, 2 level experiment on wear volumes, the null hypothesis changes such that specific effects of factors and interactions are examined. The first null hypothesis states that the main effects of factor A (load) are all equal, or in other words, the factor A has no significance on the wear volumes. If this hypothesis can be rejected, then factor A shows a significant effect on wear. A confidence level is associated with rejecting or accepting a null hypothesis. The wear volume experiments have 7 null hypotheses, one for each factor and each interaction. For each population of disk wear, ball wear, total wear and

monomer, wear volumes are analyzed and factored according to load, speed and hexadecane versus monomer condition.

Each statistical analysis compared one monomer solution versus the pure hexadecane tests for either ball wear, disk wear, or total wear. This results in 18 different analyses of variance. For each ANOVA, there were 3 main factors with 2 levels per factor. The factors being load (40 and 160 N), speed (0.25 and 1.0 m/s), and additive (none and 1% monomer). The output gave the level of significance for the 3 main effects, 3 first order interactions (load × speed, load × additive, speed × additive), and 1 second order interaction (load × speed × additive). The Minitab command for each case was :

MTB > glm 'wear'='load'|'speed'|'additive'

For each source of variance, the Minitab output for Analysis of Variance lists the following: , the degrees of freedom, the sum of squares (SS) values, the mean square (MS) value, the F-ratio and the P-value. Only the F-ratio and P-value are necessary for the analysis. The F-ratio and P-value are related and determine whether to reject or fail to reject the null hypotheses. The F-ratio is simply the ratio of the source mean square value (MS) divided by the Error mean-square value (MS). The P-value determines the confidence level in rejecting Ho and stating that a particular source of variance is significant. Rejecting the null hypothesis is the same as accepting the alternative hypothesis.

The confidence level in rejecting Ho is equal to 1 minus the P-value. For example, for the diallyl phthalate ball wear in Table D4 the confidence level in rejecting the null hypothesis that *load*speed* is not a significant effect is: 1 - 0.047 = 0.953, or 95.3 percent. The summary statement would be, "We are 95

% confident that *load*speed* is a significant effect." P-values of 0.000 would be interpreted as a 99% confidence level that Ho can be rejected. Larger F-ratios result in lower P-values, which tend to cause a rejection of Ho.

Due to the masking effect, a main factor cannot be considered insignificant if any interaction effect is significant. For example, if the *load*speed* effect was significant, then the load effect cannot be considered insignificant regardless of the F-ratio or P-value. Significant results (ones which reject Ho) always apply.

The first iteration of analysis of variance results in a significance level for all main effects and interactions. Interactions which have a F-ratio less than 1 are insignificant and can be eliminated from the analysis. The F-ratios for all other effects and interactions will change due to the change in the Error terms. The eliminated interaction values add to the number of degrees of freedom and the sum of squares values (SS) for Error, which causes the mean-square value (MS) to also change.

Tables D4 - D21 gives the original analysis of variance output. Changes made by the elimination of insignificant interactions are also shown in the 'D#-B' tables. The Significant ? column was added to clearly show the effect of a main factor or an interaction. P-values less than 0.001 are indicated with < 0.001. The Adj term in front of SS and MS refers to a statistical adjustment made for the unbalance in the number of samples per condition. This refers to the 3 tests made for hexadecane at low speeds. Other test conditions each had 2 tests. Significant first-order interactions, e.g., Load x Speed, indicate that the effect of one factor is dependent on the other factor.

Table D4. Diallyl Phthalate Ball Wear Statistics

Analysis of Variance for Wear

Source	DF	Adj SS	Adj MS	F	P	Significant ?
Load	1	37.750	37.750	28.33	<0.001	Yes (99%)
Speed	1	0.002	0.002	0.00	0.971	-----
Additive	1	28.328	28.328	21.26	<0.001	Yes (99%)
Load*Speed	1	6.805	6.805	5.11	0.047	Yes (95%)
Load*Additive	1	16.870	16.870	12.66	0.005	Yes (99%)
Speed*Additive	1	29.621	29.621	22.23	<0.001	Yes (99%)
Load*Speed*Additive	1	18.766	18.766	14.08	0.004	Yes (99%)
Error	10	13.326	1.333			
Total	17	185.719				

Table D5. Diallyl Phthalate Disk Wear Statistics

Analysis of Variance for Wear

Source	DF	Adj SS	Adj MS	F	P	Significant ?
Load	1	177.32	177.322	133.89	<0.001	Yes (99%)
Speed	1	15.476	15.476	11.69	0.007	Yes (99%)
Additive	1	48.847	48.847	36.88	<0.001	Yes (99%)
Load*Speed	1	19.618	19.618	14.81	0.003	Yes (99%)
Load*Additive	1	16.869	16.869	12.74	0.005	Yes (99%)
Speed*Additive	1	42.634	42.634	32.19	<0.001	Yes (99%)
Load*Speed*Additive	1	18.270	18.270	13.80	0.004	Yes (99%)
Error	10	13.243	1.324			
Total	17	367.552				

Table D6. Diallyl Phthalate Total Wear Statistics

Analysis of Variance for Wear

Source	DF	Adj SS	Adj MS	F	P	Significant ?
Load	1	374.6	374.61	304.24	<0.001	Yes (99%)
Speed	1	16.23	16.23	13.18	0.005	Yes (99%)
Additive	1	150.8	150.81	122.48	<0.001	Yes (99%)
Load*Speed	1	3.41	3.41	2.77	0.127	No
Load*Additive	1	65.28	65.28	53.02	<0.001	Yes (99%)
Speed*Additive	1	140.7	140.72	114.29	<0.001	Yes (99%)
Load*Speed*Additive	1	74.00	74.00	60.10	<0.001	Yes (99%)
Error	10	12.31	1.23			
Total	17	943.76				

Table D7. Monoester Ball Wear Statistics

Analysis of Variance for Wear

Source	DF	Adj SS	Adj MS	F	P	Significant ?
Load	1	44.116	44.116	31.58	<0.001	Yes (99%)
Speed	1	2.065	2.065	1.48	0.252	------
Additive	1	15.44	15.444	11.05	0.008	Yes (99%)
Load*Speed	1	4.470	4.470	3.20	0.104	No
Load*Additive	1	13.02	13.028	9.32	0.012	Yes (95%)
Speed*Additive	1	47.918	47.918	34.30	<0.001	Yes (99%)
Load*Speed*Additive	1	23.292	23.292	16.67	0.002	Yes (99%)
Error	10	13.972	1.397			
Total	17	194.673				

Table D7-B. Monoester Ball Wear Statistics

Analysis of Variance for Wear

Source	DF	Adj SS	Adj MS	F	P	Significant ?
Load	1	44.116	44.116	21.2	0.001	Yes (99%)
Speed	1	2.065	2.065	0.99	0.341	------
Additive	1	15.44	15.444	7.42	0.019	Yes (95%)
Load*Additive	1	13.02	13.028	6.26	0.029	Yes (95%)
Speed*Additive	1	47.918	47.918	23.0	<0.001	Yes (99%)
Load*Speed*Additive	1	23.292	23.292	11.19	0.006	Yes (99%)
Error	11	22.883	2.08			
Total	17	194.673				

Table D8. Monoester Disk Wear Statistics

Analysis of Variance for Wear

Source	DF	Adj SS	Adj MS	F	P	Significant ?
Load	1	150.135	150.135	103.7	<0.001	Yes (99%)
Speed	1	15.986	15.986	11.04	0.008	Yes (99%)
Additive	1	48.359	48.359	33.40	<0.001	Yes (99%)
Load*Speed	1	13.012	13.012	8.99	0.013	Yes (95%)
Load*Additive	1	26.734	26.734	18.46	0.002	Yes (99%)
Speed*Additive	1	43.477	43.477	30.03	<0.001	Yes (99%)
Load*Speed*Additive	1	11.918	11.918	8.23	0.017	Yes (95%)
Error	10	14.479	1.448			
Total	17	341.755				

Table D9. Monoester Total Wear Statistics

Analysis of Variance for Wear

Source	DF	Adj SS	Adj MS	F	P	Significant ?
Load	1	350.99	350.99	216.60	<0.001	Yes (99%)
Speed	1	31.09	31.09	19.19	0.001	Yes (99%)
Additive	1	118.87	118.87	73.36	<0.001	Yes (99%)
Load*Speed	1	2.33	2.33	1.44	0.258	No
Load*Additive	1	75.69	75.69	46.71	<0.001	Yes (99%)
Speed*Additive	1	179.82	179.82	110.97	<0.001	Yes (99%)
Load*Speed*Additive	1	68.59	68.59	42.33	<0.001	Yes (99%)
Error	10	16.20	1.62			
Total	17	944.34				

Table D10. MAMA Ball Wear Statistics

Analysis of Variance for Wear

Source	DF	Adj SS	Adj MS	F	P	Significant ?
Load	1	109.528	109.52	69.72	<0.001	Yes (99%)
Speed	1	18.773	18.77	11.95	0.006	Yes (99%)
Additive	1	2.331	2.331	1.48	0.251	No
Load*Speed	1	57.420	57.42	36.55	<0.001	Yes (99%)
Load*Additive	1	0.046	0.046	0.03	0.868	No
Speed*Additive	1	1.328	1.328	0.85	0.380	No
Load*Speed*Additive	1	0.406	0.406	0.26	0.622	No
Error	10	15.709	1.571			
Total	17	225.184				

Table D10-B. MAMA Ball Wear Statistics

Analysis of Variance for Wear

Source	DF	Adj SS	Adj MS	F	P	Significant ?
Load	1	109.528	109.52	81.27	<0.001	Yes (99%)
Speed	1	18.773	18.77	13.93	0.003	Yes (99%)
Additive	1	2.331	2.331	1.73	0.211	No
Load*Speed	1	57.420	57.42	42.6	<0.001	Yes (99%)
Error	13	17.518	1.348			
Total	17	225.184				

Table D11. MAMA Disk Wear Statistics

Analysis of Variance for Wear

Source	DF	Adj SS	Adj MS	F	P	Significant ?
Load	1	322.860	322.86	198.5	<0.001	Yes (99%)
Speed	1	4.607	4.607	2.83	0.123	No
Additive	1	0.336	0.336	0.21	0.659	No
Load*Speed	1	3.489	3.489	2.15	0.174	No
Load*Additive	1	0.297	0.297	0.18	0.678	No
Speed*Additive	1	0.202	0.202	0.12	0.732	No
Load*Speed*Additive	1	4.092	4.092	2.52	0.144	No
Error	10	16.260	1.626			
Total	17	358.734				

Table D11-B. MAMA Disk Wear Statistics

Analysis of Variance for Wear

Source	DF	Adj SS	Adj MS	F	P	Significant ?
Load	1	322.860	322.86	242.7	<0.001	Yes (99%)
Speed	1	4.607	4.607	3.46	0.086	Yes (90%)
Load*Speed	1	3.489	3.489	2.62	0.129	No
Load*Speed*Additive	1	4.092	4.092	3.07	0.102	No
Error	13	17.291	1.33			
Total	17	358.734				

Table D12. MAMA Total Wear Statistics

Analysis of Variance for Wear

Source	DF	Adj SS	Adj MS	F	P	Significant ?
Load	1	800.19	800.19	359.66	<0.001	Yes (99%)
Speed	1	39.93	39.93	17.95	0.002	Yes (99%)
Additive	1	4.58	4.58	2.06	0.182	No
Load*Speed	1	88.04	88.04	39.57	<0.001	Yes (99%)
Load*Additive	1	0.73	0.73	0.33	0.580	No
Speed*Additive	1	2.29	2.29	1.03	0.334	No
Load*Speed*Additive	1	6.91	6.91	3.11	0.109	No
Error	10	22.25	2.22			
Total	17	1023.60				

Table D12-B. MAMA Total Wear Statistics

Analysis of Variance for Wear

Source	DF	Adj SS	Adj MS	F	P	Significant ?
Load	1	800.19	800.19	383.0	<0.001	Yes (99%)
Speed	1	39.93	39.93	19.11	0.001	Yes (99%)
Additive	1	4.58	4.58	2.19	0.166	No
Load*Speed	1	88.04	88.04	42.1	<0.001	Yes (99%)
Speed*Additive	1	2.29	2.29	1.10	0.318	No
Load*Speed*Additive	1	6.91	6.91	3.31	0.096	Yes (90%)
Error	11	22.98	2.09			
Total	17	1023.60				

Table D13. Lauryl Methacrylate Ball Wear Statistics

Analysis of Variance for Wear

Source	DF	Adj SS	Adj MS	F	P	Significant ?
Load	1	35.041	35.041	23.17	<0.001	Yes (99%)
Speed	1	1.716	1.716	1.13	0.312	-------
Additive	1	4.046	4.046	2.68	0.133	-------
Load*Speed	1	13.806	13.806	9.13	0.013	Yes (95%)
Load*Additive	1	18.766	18.766	12.41	0.006	Yes (99%)
Speed*Additive	1	46.174	46.174	30.53	<0.001	Yes (99%)
Load*Speed*Additive	1	10.399	10.399	6.88	0.025	Yes (95%)
Error	10	15.123	1.512			
Total	17	173.832				

Table D14. Lauryl Methacrylate Disk Wear Statistics

Analysis of Variance for Wear

Source	DF	Adj SS	Adj MS	F	P	Significant ?
Load	1	187.092	187.092	116.8	<0.001	Yes (99%)
Speed	1	12.043	12.043	7.52	0.021	Yes (95%)
Additive	1	11.084	11.084	6.92	0.025	Yes (95%)
Load*Speed	1	13.243	13.243	8.27	0.017	Yes (95%)
Load*Additive	1	14.027	14.027	8.76	0.014	Yes (95%)
Speed*Additive	1	36.793	36.793	22.97	<0.001	Yes (99%)
Load*Speed*Additive	1	12.139	12.139	7.58	0.020	Yes (95%)
Error	10	16.019	1.602			
Total	17	316.316				

Table D15. Lauryl Methacrylate Total Wear Statistics

Analysis of Variance for Wear

Source	DF	Adj SS	Adj MS	F	P	Significant ?
Load	1	379.58	379.58	210.79	<0.001	Yes (99%)
Speed	1	24.05	24.05	13.35	0.004	Yes (99%)
Additive	1	28.32	28.32	15.73	0.003	Yes (99%)
Load*Speed	1	0.00	0.00	0.00	0.968	No
Load*Additive	1	63.23	63.23	35.11	<0.001	Yes (99%)
Speed*Additive	1	162.24	162.24	90.09	<0.001	Yes (99%)
Load*Speed*Additive	1	44.87	44.87	24.92	<0.001	Yes (99%)
Error	10	18.01	1.80			
Total		17 813.33				

Table D15-B. Lauryl Methacrylate Total Wear Statistics

Analysis of Variance for Wear

Source	DF	Adj SS	Adj MS	F	P	Significant ?
Load	1	379.5	379.5	204.9	<0.001	Yes (99%)
Speed	1	24.05	24.05	12.98	0.004	Yes (99%)
Additive	1	28.32	28.32	15.29	0.002	Yes (99%)
Load*Additive	1	63.23	63.23	34.14	<0.001	Yes (99%)
Speed*Additive	1	162.2	162.2	87.61	<0.001	Yes (99%)
Load*Speed*Additive	1	44.87	44.87	24.23	<0.001	Yes (99%)
Error	11	20.37	1.85			
Total	17	813.33				

Table D16. Vinyl Acetate Ball Wear Statistics

Analysis of Variance for Wear

Source	DF	Adj SS	Adj MS	F	P	Significant ?
Load	1	69.382	69.382	45.18	<0.001	Yes (99%)
Speed	1	0.009	0.009	0.01	0.940	------
Additive	1	1.269	1.269	0.83	0.385	-------
Load*Speed	1	19.612	19.612	12.77	0.005	Yes (99%)
Load*Additive	1	3.693	3.693	2.40	0.152	No
Speed*Additive	1	31.147	31.147	20.28	<0.001	Yes (99%)
Load*Speed*Additive	1	6.310	6.310	4.11	0.070	Yes (90%)
Error	10	15.358	1.536			
Total	17	174.147				

Table D16-B. Vinyl Acetate Ball Wear Statistics

Analysis of Variance for Wear

Source	DF	Adj SS	Adj MS	F	P	Significant ?
Load	1	69.382	69.382	38.12	<0.001	Yes (99%)
Speed	1	0.009	0.009	0.005	0.945	-------
Additive	1	1.269	1.269	0.697	0.422	--------
Load*Speed	1	19.612	19.612	10.27	0.007	Yes (99%)
Speed*Additive	1	31.147	31.147	17.11	0.002	Yes (99%)
Load*Speed*Additive	1	6.310	6.310	3.47	0.090	Yes (90%)
Error	11	20.02	1.82			
Total	17	174.147				

Table D17. Vinyl Acetate Disk Wear Statistics

Analysis of Variance for Wear

Source	DF	Adj SS	Adj MS	F	P	Significant ?
Load	1	296.760	296.76	164	<0.001	Yes (99%)
Speed	1	8.370	8.370	4.63	0.057	Yes (90%)
Additive	1	3.574	3.574	1.98	0.190	-------
Load*Speed	1	5.098	5.098	2.82	0.124	No
Load*Additive	1	0.039	0.039	0.02	0.887	No
Speed*Additive	1	30.125	30.125	16.68	0.002	Yes (99%)
Load*Speed*Additive	1	4.422	4.422	2.45	0.149	No
Error	10	18.060	1.806			
Total	17	373.635				

Table D17-B. Vinyl Acetate Disk Wear Statistics

Analysis of Variance for Wear

Source	DF	Adj SS	Adj MS	F	P	Significant ?
Load	1	296.7	296.7	179	<0.001	Yes (99%)
Speed	1	8.370	8.370	5.06	0.046	Yes (95%)
Additive	1	3.574	3.574	2.16	0.170	-------
Load*Speed	1	5.098	5.098	3.08	0.107	No
Speed*Additive	1	30.12	30.12	18.2	0.001	Yes (99%)
Load*Speed*Additive	1	4.422	4.422	2.67	0.13	No
Error	11	18.21	1.66			
Total	17	373.635				

Table D18. Vinyl Acetate Total Wear Statistics

Analysis of Variance for Wear

Source	DF	Adj SS	Adj MS	F	P	Significant ?
Load	1	647.27	647.27	263.43	<0.001	Yes (99%)
Speed	1	9.33	9.33	3.80	0.080	Yes (90%)
Additive	1	9.02	9.02	3.67	0.084	Yes (90%)
Load*Speed	1	4.85	4.85	1.97	0.190	No
Load*Additive	1	3.97	3.97	1.62	0.232	No
Speed*Additive	1	118.56	118.56	48.25	<0.001	Yes (99%)
Load*Speed*Additive	1	20.72	20.72	8.43	0.016	Yes (95%)
Error	10	24.57	2.46			
Total	17	916.38				

Table D19. Vinyl Octadecyl Ether Ball Wear Statistics

Analysis of Variance for Wear

Source	DF	Adj SS	Adj MS	F	P	Significant ?
Load	1	37.429	37.429	27.35	<0.001	Yes (99%)
Speed	1	0.017	0.017	0.01	0.914	-----
Additive	1	6.340	6.340	4.63	0.057	Yes (90%)
Load*Speed	1	15.117	15.117	11.05	0.008	Yes (99%)
Load*Additive	1	17.086	17.086	12.49	0.005	Yes (99%)
Speed*Additive	1	31.527	31.527	23.04	<0.001	Yes (99%)
Load*Speed*Additive	1	9.317	9.317	6.81	0.026	Yes (95%)
Error	10	13.683	1.368			
Total	17	161.171				

Table D20. Vinyl Octadecyl Ether Disk Wear Statistics

Analysis of Variance for Wear

Source	DF	Adj SS	Adj MS	F	P	Significant ?
Load	1	157.440	157.440	96.47	<0.001	Yes (99%)
Speed	1	8.190	8.190	5.02	0.049	Yes (95%)
Additive	1	19.335	19.335	11.85	0.006	Yes (99%)
Load*Speed	1	5.630	5.630	3.45	0.093	Yes (90%)
Load*Additive	1	23.775	23.775	14.57	0.003	Yes (90%)
Speed*Additive	1	29.782	29.782	18.25	0.002	Yes (99%)
Load*Speed*Additive	1	4.918	4.918	3.01	0.113	No
Error	10	16.320	1.632			
Total	17	283.784				

Table D21. Vinyl Octadecyl Ether Total Wear Statistics

Analysis of Variance for Wear

Source	DF	Adj SS	Adj MS	F	P	Significant ?
Load	1	342.77	342.77	198.06	<0.001	Yes (99%)
Speed	1	9.61	9.61	5.55	0.040	Yes (95%)
Additive	1	47.77	47.77	27.60	<0.001	Yes (99%)
Load*Speed	1	2.38	2.38	1.37	0.268	No
Load*Additive	1	79.58	79.58	45.98	<0.001	Yes (99%)
Speed*Additive	1	119.53	119.53	69.07	<0.001	Yes (99%)
Load*Speed*Additive	1	27.17	27.17	15.70	0.003	Yes (99%)
Error	10	17.31	1.73			
Total	17	749.79				

VARIANCE

The mean square of the error term (Adj MS for Error) in the preceding analysis of variance can be used as an estimator of the variance term (σ^2). Table D22 lists the estimate of variance from Tables D4 - D21. If insignificant factors were eliminated from the analysis, then values from the second iteration were used (Tables D#-B).

Table D22. Estimate of the Variance Term from Analysis of Variance.

Monomer / Hexadecane	Ball Wear	Disk Wear	Total Wear
Diallyl Phthalate	1.333	1.324	1.23
Monoester	2.08	1.448	1.62
MAMA	1.348	1.33	2.09
Lauryl Methacrylate	1.512	1.602	1.85
Vinyl Acetate	1.82	1.66	2.46
Vinyl Octadecyl Ether	1.368	1.632	1.73

VARIABILITY

Many sources exist which are beyond the experimental control when working with ceramics. Variation in properties of balls and disks is possible, not only batch to batch, but also from ball to ball and disk to disk. The mechanism of wear is very complicated and small changes in the micro-structure of the ceramic could cause significant changes in wear and friction.

A common problem in the manufacture of ceramics is the variability of properties in the final product [55]. Structural flaws and differences in porosities are common to ceramics due to difficulties in processing. Density or porosity of ceramics is perhaps the greatest variable. Ceramic strength is largely dependent on the crystal grain size and spacing. Larger crystals cause larger space between crystals, resulting in a weaker ceramic. Smaller and more uniform crystals result in higher density and offer greater strength. All balls and disks used in high speed - high load tests were taken from the same batch.

APPENDIX E

NORMAL LOAD ANALYSIS

The strain indicator voltage output was recorded using Global Lab data acquisition software with an IBM PC based system to demonstrate the loading which occurs during a typical test,. All data was sampled and recorded at 100 Hertz, which is fast enough to avoid any signal aliasing due to the rotational cycling. The highest sliding speed (1.0 m/s) has a corresponding rotational speed of 1432 RPM, which is about 24 Hertz. Figures E1 and E2 show the normal load increase at the beginning of the pin-on-disk experiments.

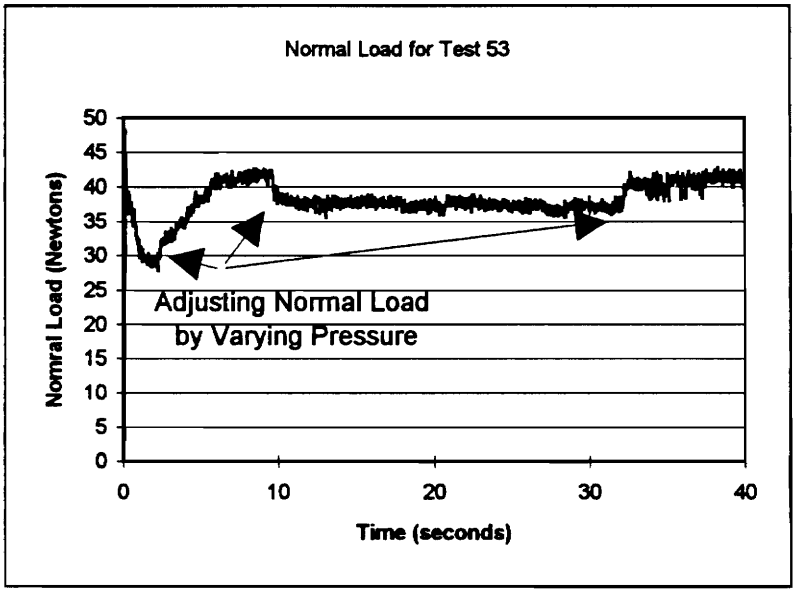

Figure E1. Normal Load Versus Time for Test with Low Load and High Speed Conditions (First 40 Seconds).

Test conditions of Figure E1 were 40 N load and 1.0 m/s sliding speed. The beginning of any test requires the pressure to be increased to the desired load, with some fine adjustments to stabilize exactly at the desired load.

Figure E2 shows the vibrations caused by disk cracking. The oscillations in normal load at the audible disk crack points were similar to a logarithmic decay and had a frequency of about 12.5 Hertz. This particular test was aborted at 18.5 seconds. The purpose of including this graph is to show the steady load level, even at 160 N and 1.0 m/s.

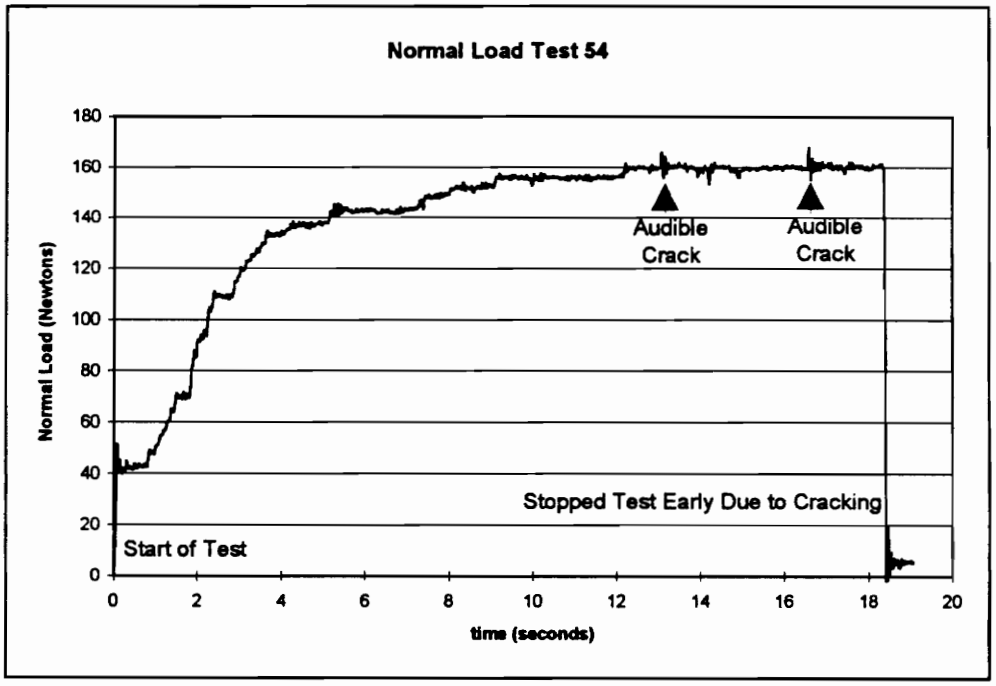

Figure E2. Normal Load Versus Time for High Load and High Speed Conditions.

The normal load in Figure E3 is taken from the middle of a 40 N load and 1.0 m/s sliding speed test. The consistent and low fluctuation of normal load is representative of all experiments in this study.

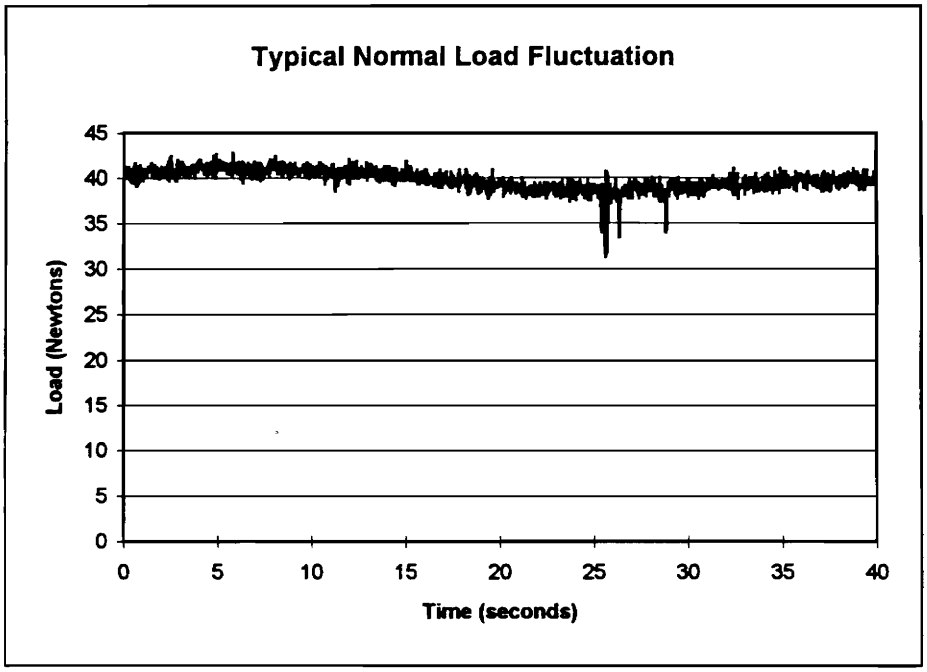

Figure E3. Typical Normal Load Fluctuation for 40 N Load, 1.0 m/s Speed.

APPENDIX F

TEST CONDITIONS AND PROBLEMS

HIGH SPEED - HIGH LOAD TEST CONDITIONS

Initial tests in the high speed high load machine with hexadecane as the only lubricant were used as baseline measurements of wear. A test matrix of varying loads and speeds was planned to determine the relative effects of changes in loads and speeds. The loads were 40 N and 160 N and the speeds 0.25 m/s and 1.0 m/s. However the 160 N load in pure hexadecane resulted in excessive ball wear such that the mechanical safety catch on the pin-on-disk machine engaged in much less than the planned 500 m. The sliding distance was changed to 250 m, however the 160 N load and 0.25 m/s speed still resulted in excessive wear and the test could only proceed to about 50 to 60 m sliding distance.

Five of the six monomer solutions allowed tests at 160 N and 0.25 m/s to continue for the desired 250 m distance, therefore the 160 N load and 0.25 m/s speed is considered to be a severe wear condition for pure hexadecane tests. Because pure hexadecane only allowed for an average of 54 sliding meters to occur before ball wear was at the maximum, a monomer which allows a complete test at the high load and the low speed can be considered very effective in reducing wear.

TESTING PROBLEMS

Several problems arose during early testing which were fixed or compensated for by changes in procedure or equipment in later tests. For

example, the alumina ball could easily roll in the holder if not properly tightened. By fully tightening the ball holder on the threaded shaft before screwing the ball and lubricant holder into the spline shaft, ball roll was eliminated.

Excessive ball wear at the high load and high speed condition caused the length of tests to be changed from 500 m sliding distance to 250 m of sliding distance. At the 160 N and 1.0 m/s test conditions, the surface of the nylon disk spacer melted on the alumina disk. The problem was resolved by changing from nylon to Teflon for the disk spacer. At 160 N load and 1.0 m/s, disks tended to crack at about 50 to 60 seconds into the four minute test. This cracking did not stop the test operation, as the disk remained in the holder and no large ceramic pieces contaminated the disk ball contact zone. The cracks in the disk were audible during the test and visible after the test.

APPENDIX G

CALCULATION OF OIL FILM THICKNESS

This section shows the method and results of calculations of oil film thickness for the four load-speed conditions tested. The equations are derived from the Navier-Stokes equations developed for elastohydrodynamic contact between two ellipsoids [56]. Tripathy previously [48] calculated the oil film thickness for alumina ball-on-disk contact for 20 N load and 0.25 m/s sliding speed, however the ball was 1/8 inch diameter. The sliding regime was boundary lubrication since the calculated minimum film thickness was 0.44 μm, less than the average surface roughness of 0.55-0.65 μm.

The following calculations are for a 1/4 inch alumina ball under two loads and two speeds. The minimum oil film thickness, h_{min}, between two sliding ellipsoids is given by:

$$h_{min} = H R_x$$

where

$$H = 3.63 U^{0.68} G^{0.49} W^{-0.073} (1 - e^{-0.68k})$$

H, R_x, U, G W and k are non-dimensional minimum oil film thickness, radius, velocity, pressure, load and geometry factors, respectively. The parameters are given by:

$$\frac{1}{R_x} = \frac{1}{r_a} + \frac{1}{r_b}$$

where r_a and r_b are radii of contact

$$U = \frac{\eta\, u}{E'\, R_x}$$ where η is the viscosity at zero pressure

and $$u = \frac{u_a + u_b}{2}$$ where u_a and u_b are velocities of body a and b

and $$E' = \frac{2}{\frac{1 - \nu_a^2}{E_a} + \frac{1 - \nu_b^2}{E_b}}$$ where ν is Poisson's ratio and E is the elastic modulus

$$G = \frac{E'}{P_{iv,as}} \qquad \text{where } P_{iv,as} \cong \frac{1}{\alpha}$$

$$W = \frac{F}{E'\, R_x^2}$$ where F is the normal load

k is the ratio of the radii of contact along x and y directions, and is equal to 1 for two spheres in contact.

$$k = \frac{a}{b} = 1$$

For alumina on alumina in hexadecane, the following values can be used:

$R_x = r_a = 1.5875$ E-03 m ($r_b = \infty$ for a flat disk)

$\eta = 2.31$ cP $= 2.31$ E-03 Pa·sec (for hexadecane at 40 °C)

$\alpha = 11.1$ E-04

$u = 0.125$ m/s and 0.5 m/s

$F = 40$ N and 160 N

The values of viscosity and the pressure-viscosity coefficient for hexadecane come from reference [57]. The substitution of the values into the equations results in minimum oil film thicknesses shown in Table G1.

Table G1. Calculated Minimum Oil film Thicknesses.

Normal Load	Sliding Speed	h_{min} (calculated film thickness)
40 N	0.25 m/s	0.84 μm
160 N	0.25 m/s	0.76 μm
40 N	1.0 m/s	2.1 μm
160 N	1.0 m/s	1.9 μm

The results show that the low speed tests, at the beginning of a test for a fresh ball and disk, are only slightly above the average surface roughness of alumina. (0.55-0.65 μm). Boundary lubrication is still very possible and expected. The film thicknesses at the high speed is almost four times the average surface roughness. This large difference may indicate that a transition has occurred to the partial EHD condition. These calculated values are expected to change as soon as wear occurs and the ball on disk contact geometry changes.

VITA

The author was born on January 15, 1970 in Frederick Maryland to Mr. Robert Tritt and Mrs. Alice Tritt of Myersville, Maryland. He received his Bachelor of Science degree with highest honors in Mechanical Engineering from Virginia Polytechnic Institute and State University in May of 1993. He began working towards a Master of Science degree in Mechanical Engineering at Virginia Polytechnic Institute and State University in August 1993. Upon completion of the MS degree, he will work for Progressive Design Corporation in Richmond, Virginia.

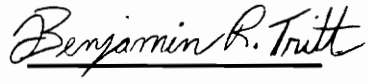

Benjamin R. Tritt